OPTIMIZATION OF TYROSINE-DERIVED POLYCARBONATE TERPOLYMERS

FOR BONE REGENERATION SCAFFOLDS

by

MARIA HANSHELLA C. RESURRECCION-MAGNO

A Dissertation submitted to the

Graduate School-New Brunswick

Rutgers, The State University of New Jersey

in partial fulfillment of the requirements

for the degree of

Doctor of Philosophy

Graduate Program in Chemistry and Chemical Biology

written under the direction of

Joachim Kohn, Ph.D.

and approved by

_____

_____

_____

_____

New Brunswick, New Jersey

January 2012

ABSTRACT OF THE DISSERTATION

OPTIMIZATION OF TYROSINE-DERIVED POLYCARBONATE TERPOLYMERS

FOR BONE REGENERATION SCAFFOLDS

By MARIA HANSHELLA C. RESURRECCION-MAGNO

Dissertation Director:
Joachim Kohn, Ph.D.

Tyrosine-derived polycarbonates (TyrPC) are a versatile class of polymers highly suitable for bone tissue engineering. Among the tyrosine-derived polycarbonates, poly(DTE carbonate) has an FDA masterfile that documents its biocompatibility and non-toxicity and has shown potential utility in orthopedics due to its osteoconductive properties and strength. DTE stands for desaminotyrosyl-tyrosine ethyl ester and is the most commonly used tyrosine-derived monomer. However, *in vitro* degradation studies showed that poly(DTE carbonate) did not completely resorb even after four years of incubation in phosphate buffered saline. Thus for bone regeneration, which only requires a temporary implant until the bone heals, poly(DTE carbonate) would not be the best choice.

The goal of the present research was to optimize a scaffold composition for bone regeneration that is based on desaminotyrosyl-tyrosine alkyl ester (DTR), desaminotyrosyl-tyrosine (DT) and poly(ethylene glycol) (PEG). Five areas of research

were presented: (1) synthesis and characterization of a focused library of TyrPC terpolymers; (2) evaluation of the effects of how small changes on the composition affected the mechanism and kinetics of polymer degradation and erosion; (3) fabrication of bioactive three-dimensional porous scaffold constructs for bone regeneration; (4) assessment of osteogenic properties *in vitro* using pre-osteoblasts; and (5) evaluation of bone regeneration potential, with or without recombinant human bone morphogenetic protein-2 (rhBMP-2), *in vivo* using a critical sized defect (CSD) rabbit calvaria (cranium) model.

Small changes in the composition, such as changing the R group of DTR from ethyl to methyl, varying the mole percentages of DT and PEG, and using a different PEG block length, affected the overall properties of these polymers. Porous scaffolds were prepared by a combination of solvent casting, porogen leaching and phase separation techniques. Calcium phosphate was coated on the surface post-fabrication. The scaffolds displayed (i) a bimodal pore architecture with micropores (< 20 μm) and macropores (200 – 400 μm), (ii) a highly interconnected and open pore structure, and (iii) a highly organized microstructure. These scaffolds supported robust cell attachment and promoted osteogenic differentiation of pre-osteoblasts. This is the first report that a synthetic polymeric scaffold either without a biological supplement or with a minimal dose of rhBMP-2 induced comparable bone regeneration to a commercially available bone substitute in a non-rodent CSD animal model.

I thank my friends, Priti Tiwari, Bahar Demirdirek, Melissa Aranzamendez, Andrew Nato, Cherry Santos, Leilani Del Rosario, Jim Minglana, and Ophir Ortiz for all the good times and laughter we shared, which eased the burdens of graduate school;

And my family, my sister, Honeylyn, and my brother-in-law, Eric, my nephews, Eric Joshua and Jerome, and niece, Jianna, for generously sharing their home and everything they own; My Papa and Inay, Pablo and Luisita Resurreccion, my sister, Hasmin; Romy and Rajan; and brother, Harris; Pam and Ryan Miguel for encouraging me to work harder, for their love and untiring support;

Tito Joven Catilo for firmly believing in me;

Tito Er and Tita Fe Fernandez; Nanay Zoila; Our Lady of Fatima;

My Sweetie, Eduardo, and son, Johnnuel, for the selfless way you have supported me in this pursuit, for the constant emotional support, patience and understanding and for just being there when I needed you the most.

You are the reasons why I have accomplished what I have accomplished thus far.

Dedication

To Eduardo

To Johnnuel,

for all the times when Mommy wasn't there to share your laughter or your pain when you

scraped your knees, to celebrate milestones and to embrace you

To Papa and Inay

Table of Contents

List of Tables

List of Figures

List of Abbreviations

<u>Polymer notation:</u>
To simplify the naming of the tyrosine-derived terpolymers, the notation RXXYY(M_w) is used to name poly(DTR-*co*-XX%-DT-*co*-YY%-PEGMW carbonate) where R is the alkyl pendent chain, XX is the mole percent of DT, YY is the mole percent of PEG and M_w is the weight average molecular weight of PEG. As an example, poly(DTE carbonate) will be designated as E0000 where E stands for ethyl while poly(DTE-*co*-25%-DT-*co*-02%-PEG$_{2K}$ carbonate) will have a notation of E2502(2K).

3D	three-dimensional
ACN	acetonitrile
ANOVA	analysis of variance
AFIRM	Armed Forces Institute of Regenerative Medicine
AUC	area under curve
CaCl$_2$	calcium chloride
CMU	Carnegie Mellon University
CP	calcium phosphate
CSD	critical-sized defect
DCM	dichloromethane, or methylene chloride
DI H$_2$O	deionized water
DMF	dimethyl formamide
DSC	differential scanning calorimetry
DT	desaminotyrosyl-tyrosine
DTE	desaminotyrosyl-tyrosine ethyl ester
DTM	desaminotyrosyl-tyrosine methyl ester
DTR	desaminotyrosyl-tyrosine alkyl ester
DT*t*Bu	desaminotyrosyl-tyrosine *ter*t-butyl ester
EtO	ethylene oxide
FDA	Food and Drug Administration
GPC	gel permeation chromatography
HCl	hydrochloric acid

HPLC	high performance liquid chromatography
IPA	isopropyl alcohol
k or k'	rate constant
M*n*	number average molecular weight
M*w*	weight average molecular weight
MeOH	methanol
MW	molecular weight
n	sample size
NaCl	sodium chloride
NaOH	sodium hydroxide
^{1}H NMR	proton nuclear magnetic resonance
NJCBM	New Jersey Center for Biomaterials
PBS	phosphate buffered saline
PDI	polydispersity index (M*w*/M*n*)
PEG	poly(ethylene glycol)
PEG1K	poly(ethylene glycol), molecular weight 1,000 Da
PGA	poly(glycolic acid)
PLGA	poly(lactic acid-*co*-glycolic acid)
PLA	poly(lactic acid)
PLLA	poly(L-lactic acid)
PVA	poly(vinyl alcohol)
R^2	Pearson correlation coefficient
SD	standard deviation
SEM	scanning electron microscopy
t	time
T*g*	glass transition temperature (units: $^\circ$C)
T*m*	melting point (units: $^\circ$C)
TGA	thermogravimetric analysis
TFA	trifluoroacetic acid
TyrPC	tyrosine-derived polycarbonate
TyrPC+CP	tyrosine-derived polycarbonate with calcium phosphate

Units

º	degree
μ l	microliters
μ m	micrometers
M	Molar
MHz	megahertz
mg	milligrams
ml	milliliters
N	Normality

CHAPTER 1

Introduction

Approximately 500,000 bone grafting procedures are performed in the United States annually and the cost of such procedures in order to repair bone defects is a staggering $2.5 billion per year.[1] Currently, autologous (from the patient) bone grafting remains the "gold standard" for the treatment of bone-related injuries. Another option is allogeneic (from another individual) bone grafts. Both autogenous and allogeneic bone grafts contain the intrinsic properties needed to regenerate bone, namely, "osteogenic progenitor cells, osteoinductive growth factors and osteoconductive matrices". [2, 3] Osteoconduction is the ability of grafts to support cell attachment, growth, and migration of cells through an interconnected and porous structure. Osteoinduction is the ability of grafts to initiate differentiation of stem cells to osteoblasts. Osteogenicity is the ability of grafts to enhance the bone-implant interface such that better bone apposition occurs. However, the utility of autologous grafts is limited by scarcity and donor-site morbidity and that of allogeneic grafts is limited by the risk of disease and infection[4-6]. Metals and ceramics are also used as bone substitutes. While metal generally provides the appropriate mechanical strength, metal implants are non-resorbable and do not integrate well with the surrounding tissue. The utility of ceramics such as calcium phosphates in bone tissue engineering is understandable as calcium phosphate, specifically hyrdoxyapatite, is naturally present in bone which enhances osteoconduction and

osteointegration (bone-implant apposition).[7, 8] However, ceramics are brittle, exhibit low

mechanical strength and have shown unpredictable degradation *in vivo.* [5, 9]

The limitations of these remedies have compelled scientists to look for other

alternatives to bone grafts by developing bone graft substitutes using a variety of

materials that include natural and synthetic polymers, and ceramics such as calcium

phosphates. One of the desirable characteristics of synthetic degradable polymers for

tissue engineering is the tunability of their properties which can be tailored readily by

modifying their composition, structure and architecture in order for these materials to

degrade and resorb in a time-frame that is parallel to tissue regeneration. Thus, synthetic

degradable polymers can be particularly good candidates to meet the specific

requirements of various tissue engineering applications.

1.1   Fracture healing and bone repair [10]

When bone is injured the normal physiologic response to injury follows a

sequence of events: inflammation, soft callus formation, hard callus formation and

remodeling. [11] (Figure 1.1)

Inflammation is characterized by a cellular process. Hematoma occurs at the

injury site and platelets, macrophages, and monocytes begin the clean-up and repair

process. When the elevated cellular activity has subsided, usually occurs within a few

days after injury, mesenchymal stem cells, osteoprogenitor cells, fibroblasts, and

endothelial cells arrive at the injury site and start the rebuilding process.

When the inflammation subsides, a fibrous tissue layer, called a callus, forms

around the fracture. This stage occurs over the course of several weeks and what is

formed is a cartilaginous/bony tissue, which is then eventually mineralized to form the hard callus.
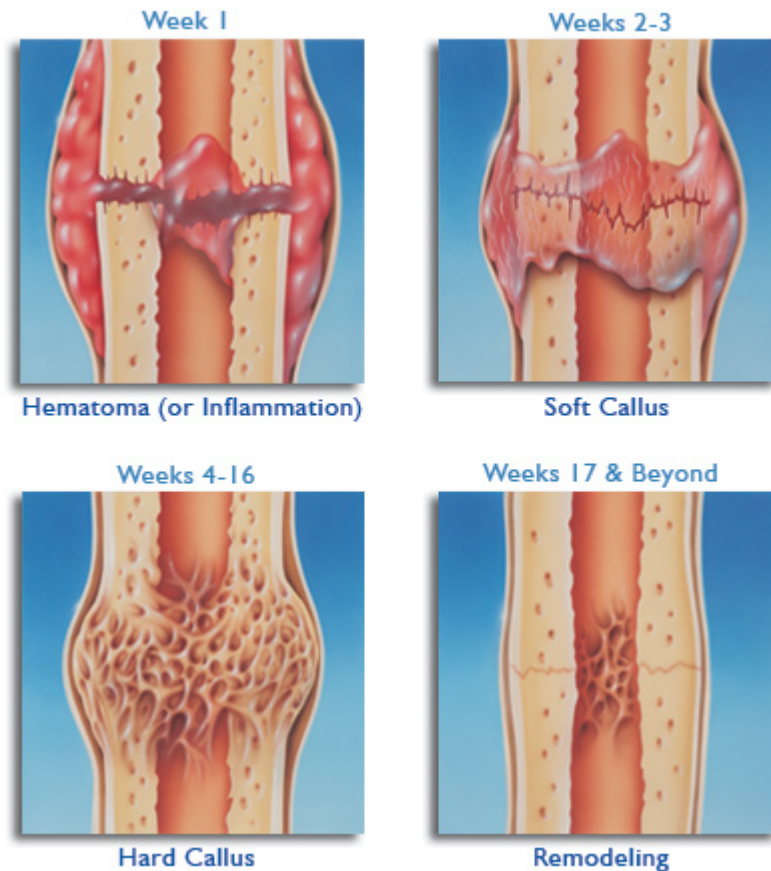
Figure 1.1 The sequence of events during fracture healing, (1) inflammatory stage, (2) soft callus formation, (3) hard callus formation, and (4) bone remodeling. (image from http://medical-definitions.com/fracture/bone-fracture-healing.htm)

In the final stage of healing, the woven bone formed within the callus is slowly remodeled as lamellar bone which may take years to complete.

However, there are instances when this process does not occur and nonunion between ends of a fracture results. This occurrence is especially true in bone defects that are caused by trauma, such as blasts injuries experienced by soldiers at war that result in

significant bone loss. These types of defects are classified as critical sized defects which are characterized as the size of defect that the normal healing process cannot heal on its own. In these cases, the use of bone grafts or bone graft substitutes may be necessary.

1.2   Bone grafts and bone graft substitutes

Autogenous grafts remain as the "gold standard" for the treatment of non-unions because it possesses all the characteristics required for bone growth, namely, osteogenicity, osteoconductivity, and osteoinductivity.[2, 3] An autograft is a tissue harvested from the patient, usually from the iliac crest. However, the use of autografts is severely limited by supply and requirement for an additional surgery to obtain the graft that may result in donor site morbidity and other complications.

An alternative to autografts are allografts which are taken from donors or cadavers. The use of allografts eliminates donor site morbidity but there is a risk of disease transmission from donor to recipient.

Despite the benefits of autografts and allografts, their limitations have necessitated the development of new alternatives.

Laurencin, et al, [12] has provided a scheme for classifying bone grafts according to the primary material that the graft is made of: allograft-, cell-, factor-, polymer- or ceramic-based, and an extensive list of materials that are currently available. These bone graft substitutes may be used alone or in combination with other materials. Allograft-based substitutes are made of demineralized bone matrix prepared in proprietary methods in order to preserve the osteoinductive agents intrinsically present in bone. Factor-based bone graft substitutes are materials that have growth factors such as BMP-2 (Infuse™

Bone Graft, Medtronic Sofamor Danek, Inc.) and BMP-7 (Stryker Biotech, Inc.). These growth factors have been shown to induce new bone formation. Cell-based bone graft substitutes are materials with mesenchymal stem cells (Osiris, Inc.) cultured on different materials. In the polymer-based category, bone grafts can be further classified into natural or synthetic polymer. Healos® (Orquest, Inc.) is a fully resorbable product that is made of collagen fibers coated with hydroxyapatite. It is intended for spinal fusion. Of the synthetic polymers, there are those that are classified as non-resorbable and those that are resorbable: Cortoss ® and Rhakoss ® (Orthovita, Inc.) fall under the first category, while Bone Tec Inc.'s porous poly(lactic-co-glycolic acid) foam and Immix Extenders ® (Osteobiologics, Inc.) fall under the second category. A large percentage of bone graft substitutes are based on ceramics. Ceramics include calcium phosphate, bioactive glass, and calcium sulfate.

1.3   Tissue Engineering

Bone tissue engineering (bone TE) is an alternative that offers options for regenerating defective bones by the use of cells, biologically active substances and a scaffold or combinations thereof. The scaffold provides support to cellular processes and acts as a three-dimensional framework for new bones to attach, proliferate and migrate[13], which leads to formation of new tissues over time, with the scaffold degrading and eventually replaced by new bone. In the choice of scaffolds for bone repair, the nature and structure of bone are considered. The best scaffolds are the autografts because of their biocompatibility (lack of immunogenic response), osteoconductivity, osteoinductivity, osteogenicity, osteointegration and mechanical match.[9, 14] These are the

same characteristics that a synthetic scaffold should possess in order to successfully regenerate new bones.

1.4   Material considerations

The choice of material depends on the application, such as for structural support, or delivery of drugs or active agents. [11] Materials for bone tissue engineering include natural or synthetic polymers, ceramics, and composites. These materials differ in their modes of degradation, degradation time, and mechanical properties. These are just some properties that can be adjusted in order for the material to fit an intended application.

Among the natural polymers, type-1 collagen, hyaluronic acid and chitosan have been used as bone tissue engineering materials.

Most of these synthetic polymers generally degrade by hydrolysis of labile bonds. Among these are: (1) polyanhydrides have been developed for high strength applications [15]; (2) poly(propylene fumarate)[16, 17]; (3) polycaprolactone [18]; (4) polyphosphazenes[19]; (5) polylactide, polyglycolide and co-polymers thereof. [20, 21] Aliphatic polyesters based on poly(lactic acid) or PLA, poly(glycolic acid) or PGA and co-polymers thereof have been widely used in tissue engineering. These polymers degrade over a period of 0.5 to 15 months and erode between 3 to 48 months depending on the polymer composition and the molecular weight (MW). The acidic degradation products, lactic acid for PLA and glycolic acid for PGA, are natural metabolites. However, a burst release of these acidic byproducts to the implant site may cause inflammation. [22, 23] Pins, screws, mesh, nails, etc. are just some of the orthopedic products with regulatory approval that are made from these polyesters. [9, 24, 25].

Ceramics have also been widely investigated because they mimic the inorganic composition of bone and will enhance osteointegration by stimulating the precipitation and deposition of calcium phosphate from body fluids. Ceramics have high compressive modulus, often exceeding that of trabecular bone (20 MPa to 2 GPa), which can result in stress shielding and they tend to be very brittle.[11]

In order to minimize the limitations of polymers and ceramics and to combine the advantages of both materials, polymer/ceramic scaffolds are being investigated as scaffold materials for bone regeneration. [25-28]

Other bone regeneration approaches include the use of implantable or injectable natural, synthetic-based or bioactive ceramic composite scaffolds as carriers of mesenchymal stem cells[29] and growth factors.[30, 31] Gene therapy is also being considered as a potential solution for bone regeneration in the CMF.[32] These unproven approaches are in the early stages of evaluation and seek to overcome the challenges encountered with clinically available materials.

1.5   Scaffold fabrication techniques

In order to mimic the pore architecture of bone, scaffolds have been fabricated using conventional techniques like solvent casting, particulate leaching, thermally induced phase separation, melt molding, gas foaming, or combinations thereof or new methods like rapid prototyping (RP), also known as solid free form fabrication. [2, 24]. Readers are directed to a review by Rezwan et al.[25]

All of these current treatment options are inadequate in restoring anatomical form and function in the defect where bone is being regenerated. A biomaterial platform that may provide a compelling therapeutic solution to regenerate bone is tyrosine-derived polycarbonates (Tyr-PC).

1.6   Tyrosine-derived polycarbonates

Tyrosine-derived polycarbonates, referred to as TyrPC, are a class of degradable polymers that belong to a family of versatile "pseudo"-poly(amino acids) that were first introduced by the Kohn lab in 1984. These polymers, specifically, poly(DTE carbonate), are known for their biocompatibility, [33] and tunable mechanical, thermal, degradation and osteoconductive properties. [34-37]. TyrPC polycarbonates are synthesized from tyrosine-derived monomers, desaminotyrosyl-tyrosine alkyl ester (DTR), which has an alkyl pendent chain, and desaminotyrosyl-tyrosine (DT), which has a free carboxylic acid group.

In order to tailor the properties of these polymers for a specific application, a number of modifications on the polymer composition have been explored, such as (1) variations on the alkyl pendent chain[34, 36]; (2) incorporation of DT [38]; and (3) co-polymerization with PEG [39-41]. Variations in the alkyl pendent chain result in polymers that have different properties. For example, decreasing the alkyl chain length resulted in an increase in the glass transition temperature, faster degradation and increased apposition with the native bone[36]. In addition, incorporation of DT results in faster polymer degradation and erosion, while incorporation of PEG into the polymer backbone allows for modification of bulk and surface properties. In poly(DTR-co-x%-PEG$_{MW}$

carbonate), the PEG content, the length of the pendent chain R, and the length of PEG block affected the properties of the copolymers. Increasing the PEG content in these copolymers, while keeping the length of the R group and PEG block length constant, resulted in a decrease in the glass transition temperature, increase in water uptake, faster degradation of the polymer backbone and very little or no rat lung fibroblast and osteoblast attachment on the surfaces of these copolymers [39, 41].

1.7   Tyrosine-derived polycarbonate scaffold design

A scaffold should approximate the features of the tissue it is replacing.[42] Trabecular bone has a porosity of approximately 90% and a high degree of pore interconnectivity (Figure 1.2). Therefore, materials designed to replace trabecular bone are designed to reflect the same high degree of porosity and interconnectivity. A method that combines solvent casting, porogen leaching and phase separation techniques was used to fabricate TyrPC scaffolds.[43, 44] These scaffolds showed a bimodal pore distribution of macropores (200 – 400 μm) and micropores (< 20 μm), a highly interconnected porous network, and an organized microarchitecture surrounding the macropores.
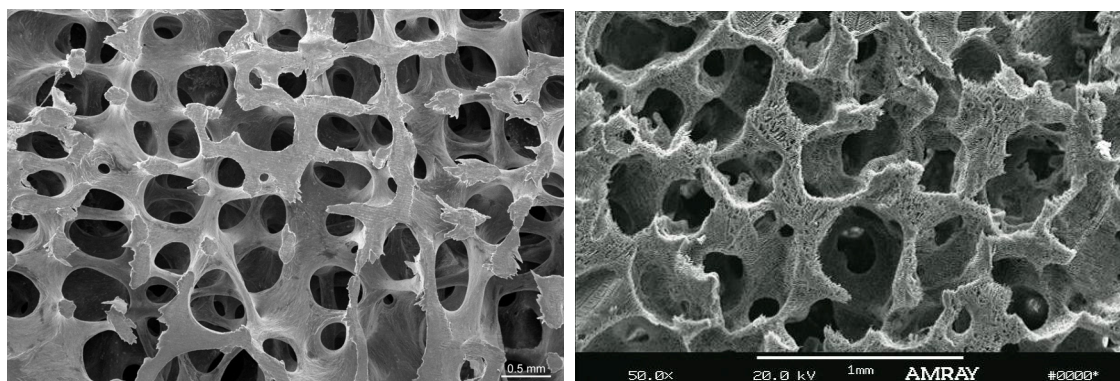
Figure 1.2. SEM image of the 3rd lumbar vertebra of a 30 year old woman. (image from http://www.brsoc.org.uk/gallery/images/12lg.jpg) (scale bar 500 μm) showing the highly interconnected pores of bone (left) and SEM image of TyrPC scaffolds showing a pore architecture that is similar to bone (scale bar 1 mm).

1.8   Hypothesis

There are a lot of biomaterials for bone tissue engineering that are either currently available in the market or under investigation but none has shown adequate restoration of form and function.

Through incorporation of DTM or DTE for better bone apposition and mechanical stiffness, DT for controlling the degradation rate and PEG blocks for better bulk and surface properties, two new libraries of polymers can be synthesized that will have a more desirable range of resorbability and osteoconductivity than can be achieved in currently used synthetic degradable biomaterials for tissue engineering scaffolds.

The addition of bioactive enchancements (mineralized coatings and/or biologics) to 3D porous Tyr-PC (tyrosine-derived polycarbonate) terpolymer scaffolds will result in increased osteoconductivity and new bone formation.

1.9   Specific Aims

The central objective of this study was to optimize a scaffold for bone regeneration that is based on tyrosine-derived polycarbonate terpolymers. The specific aims of this dissertation are:

1. To synthesize and characterize two new libraries of linear tyrosine-derived polycarbonates composed of DTR (desaminotyrosyl-tyrosine alky ester), where R = M or E, DT (desaminotyrosyl-tyrosine) and PEG (poly(ethylene glycol)) with different compositions.

2. To fabricate and characterize porous scaffolds with or without bioactive enhancements for bone tissue engineering from these polymers, and to investigate *in vitro* degradation and resorption profiles.

3. To evaluate the *in vitro* osteogenic potentials in pre-osteoblasts and human-derived mesenchymal stem cells, and *in vivo* bone regeneration capability of these scaffolds, with or without bioactive enhancement through surgical implantation in a critical-sized defect (CSD) rabbit calvaria (cranium) model.

The *in vitro* cell studies and *in vivo* rabbit calvaria studies were done in collaboration with Dr. Jeffrey O. Hollinger's group at the Carnegie Mellon University (CMU).

1.10   Thesis Organization

The current chapter provides an overview of current technologies used in the field of bone tissue engineering, namely, commercially available products and alternative therapies that are being investigated, and the limitations associated with these therapies. All experimental methods are described in Chapter 2 except for the methods for *in vitro* cell studies, micro-CT analysis, and histology/histomorphometric analysis. The methods for these studies are described in full in the Appendix because these studies were done by our collaborators from Carnegie Mellon University and the Cleveland Clinic. Following chapter 2, each chapter begins with a short introduction that talks about pertinent issues that are covered in that section, followed by results and discussion, and finally a short conclusion/summary.

Chapter 3 will discuss the synthesis and characterization of a focused library of the tyrosine-derived polycarbonate terpolymers that was designed for potential application in bone regeneration. Chapter 4 will discuss the in vitro degradation and erosion profiles of this library of polymer. Chapter 5 will discuss the optimization of the scaffold fabrication method. Chapter 6 is the summary of results from the in vitro cell work done at CMU. Chapter 7 will discuss the results of the *in vivo* rabbit calvarial critical sized defect. The results of these experiments will be presented as a concluding remark in the final chapter.

CHAPTER 2

Materials and methods

This chapter describes the materials and methods used throughout this work, namely, (1) reagents and chemicals used; (2) synthesis of desaminotyrosyl-tyrosine methyl ester (DTM) and a focused library of tyrosine-derived polycarbonate (TyrPC) terpolymers including characterization methods like proton nuclear magnetic resonance spectroscopy (^{1}H-NMR) for confirmation of chemical structure, gel permeation chromatography (GPC) for determination of polymer molecular weight relative to polystyrene standards, thermogravimetric analysis (TGA) for determination of polymer decomposition temperature and amount of residual solvents, differential scanning calorimetry (DSC) for determination of polymer glass transition temperature (T_g), contact angle goniometer for measurement of contact angle, and mechanical testing for evaluation of tensile properties; (3) fabrication and characterization of compression-molded films and three-dimensional scaffolds; (4) evaluation of *in vitro* degradation and erosion of TyrPCs; (5) evaluation of cytotoxicity and osteogenic properties using cells; and (6) evaluation of bone regeneration in a rabbit calvarial critical-sized defect. The results obtained from these studies demonstrate the potential utility of degradable 3D tyrosine-derived polycarbonate scaffolds in bone tissue engineering.

2.1.   Reagents

All chemicals used were reagent grade, HPLC grade and high purity. These chemicals were used as received except desaminotyrosyl-tyrosine ethyl ester (DTE, Integra Life Sciences, Plainsboro, NJ) which was purified further by washing with dichloromethane (DCM). Tyrosine *tert*-butyl ester (TtBu) was purchased from Bachem (Torrance, CA). Desaminotyrosine or 3-(4'-hydroxyphenyl) propionic acid (Dat) was purchased from Apin Chemicals (UK). Hydroxybenzotriazole (HOBt), *bis*(trichloromethyl)carbonate (triphosgene) and poly(ethylene glycol), M_w 1000 (PEG$_{1K}$) were obtained from Fluka (Switzerland). 1-Ethyl-3-(3-dimethylaminopropyl) carbodiimide hydrochloride (EDCI) was purchased from Kawaguchi Chemical Industry (Japan). Poly(ethylene glycol) M_w 2000 (PEG$_{2K}$) was purchased from Clariant Corporation (Charlotte, NC). Tetrahydrofuran (THF) and *N,N*-dimethylformamide (DMF) were obtained from EMD (Germany). Pyridine, dichloromethane (DCM), methanol (MeOH), 1,4-dioxane and isopropyl alcohol (IPA) were obtained from Fisher Scientific (Pittsburgh, PA). Dimethylsulfoxide-d$_6$ (DMSO-d$_6$), deuterated chloroform (CDCl$_3$), trifluoroacetic acid (TFA), HPLC water with 0.1% TFA, sodium chloride (NaCl) and Dulbecco's phosphate buffered saline, modified, without calcium chloride and magnesium chloride, (PBS), anhydrous calcium chloride (CaCl$_2$), and potassium phosphate dibasic trihydrate (K$_2$HPO$_4$ • 3H$_2$O) were obtained from Sigma-Aldrich Chemical Co. (St Louis, MO). Polystyrene standards used for GPC calibration, specifically, M_p 523,000, M_p 204,500, M_p 96,000, M_p 30,230,   and M_p 7,200 were obtained from Polymer Laboratories Inc., a subsidiary of Varian Inc. (Palo Alto, CA). Poly(lactide-*co*-glycolide) 85:15 (PLGA

85:15, Surmodics Pharmaceuticals formerly Lakeshore Biomaterials, Birmingham, AL), and Integra Mozaik Strip[TM] (Integra Life Sciences, Plainsboro, NJ) were used as controls for some *in vitro* or *in vivo* studies. Desaminotyrosyl-tyrosine (DT) was synthesized in-house by base hydrolysis of desaminotyrosyl-tyrosine ethyl ester (DTE).

2.2   Synthesis and characterization

2.2.1   Monomer synthesis

Desaminotyrosyl-tyrosine methyl ester (DTM) was prepared using a published synthesis procedure with minor changes[45] and as shown in the scheme below (Figure 2.1).
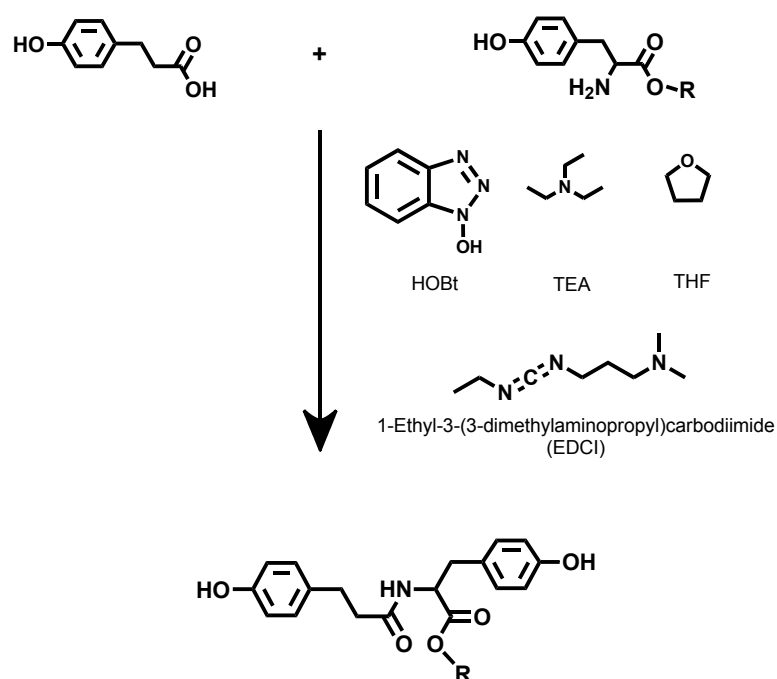
Figure 2.1 Synthetic scheme for the preparation of desaminotyrosyl-tyrosine alkyl esters (DTR).

A white powder was obtained after purification and vigorous stirring in hexane: yield 85%; m.p. 127 $^{\circ}$C; purity by melting point depression: 98.2%; ^{1}H-NMR (DMSO-d$_6$) δ: 2.31 (t, 2H), 2.62 (t, 2H), 2.75 (m, 1H), 2.88 (m, 1H), 3.58 (s, 3H), 4.38 (m, 1H), 6.65 (m, 4H), 6.95 (m, 4H), 8.23 (d, 4H), 9.12 (s, 1H), 9.23 (s, 1H).

2.2.2 Focused library of Tyrosine-derived polycarbonate terpolymers

Tyrosine-derived polycarbonate terpolymers were synthesized by condensation reaction of triphosgene and tyrosine-derived diphenol as shown in the scheme below (Figure 2.2).[34, 39, 44, 46]
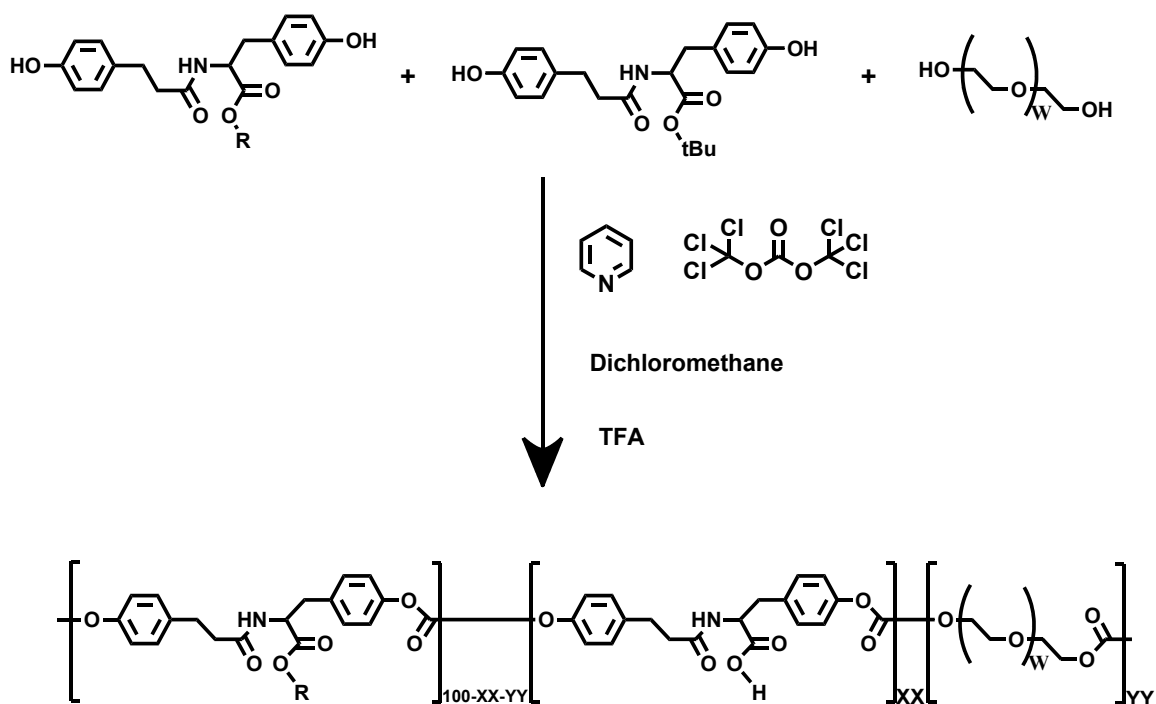
Figure 2.2 Synthetic scheme for the preparation of tyrosine-derived polycarbonate terpolymers.

The preparation of E2502(2K) described here serves as a typical example. A mixture of DTE (15 g, 0.04 mol), desaminotyrosyl-tyrosine tert-butyl ester (DTtBu) (5.5 g, 0.01 mol) and PEG2K (2.3 g, 10 mmol) was dissolved in 140 mL of DCM and 18 mL of pyridine in a round bottom flask that was continuously purged with N_2 gas. A solution of 6.3 g (60 mmol) of triphosgene in 20 mL of DCM was added to the reaction mixture with stirring over a two-hour period at room temperature. After the desired molecular weight was reached (around 200 kDa polystyrene equivalent MW by GPC using DMF as mobile phase), TFA (90 mL) was added to the reaction mixture. The polymer was precipitated using isopropyl alcohol (IPA, 400 mL) and then successively washed with IPA, IPA : H_2O (1:1) and H_2O. The precipitation and washings were carried out in a 4 L industrial blender. The polymer was allowed to dry by blowing N_2 gas overnight and then in a vacuum oven at 40 ^{o}C for 48 hours.

The polymer composition was determined by ^{1}H NMR in DMSO-d_6 or CDCl$_3$ at room temperature using 64 scans. Polymer sample of approximately 20 mg was dissolved in 0.75 ml of deuterated solvent and analyzed on a Varian VNMRS 400 or 500 MHz machine (Varian Inc., Palo Alto, CA). The molar ratio of DTR, DT and PEG was calculated by integrating ^{1}H NMR peaks.

Molecular weights (number average, M_n) and polydispersity indices (PDI) were determined using GPC relative to polystyrene standards. The GPC system consisted of a 515 HPLC pump, 717plus auto sampler, a 2414 RI detector and Empower Pro® Software (Waters Corporation, Milford, MA). Two PL gel columns (Polymer Laboratories, Amherst, MA), 1,000 and 100,000 Å, were used in series. DMF containing 0.1% TFA at a flow rate of 0.8 mL min^{-1} was used as the mobile phase. A sample of approximately 10

mg was dissolved in 1 mL of the mobile phase and filtered with a 0.45 µm Teflon® filter (13mm diameter, cat.# 6766-1304, Whatman Inc., Florham Park, NJ) into a GPC vial. The injection volume was 20 µl, run time was 24 minutes and analysis was carried out at room temperature.

Polymer decomposition temperature and residual solvent were measured using a Thermogravimetric Analyzer (TGA) Model TGA/SDTA851e with STARe software version 19.10 (Mettler-Toledo Inc., Columbus, OH). A sample of approximately 5 - 10 mg in an aluminum oxide crucible was heated from 25 to 400 °C at a rate of 10 °C per minute.

Polymer glass transition temperature (T_g) was measured using a Differential Scanning Calorimeter (DSC) Model DSC 823e (Mettler-Toledo Inc., Columbus, OH). A sample of approximately 5 - 10 mg in a sealed aluminum pan was heated from room temperature to 200 °C at a rate of 10 °C per minute, and then kept at 200 °C for 5 minutes to erase the thermal history of the polymer (first heat cycle). The sample was cooled and then heated again from -10 °C to 200 °C at a rate of 10 °C per minute (second heat cycle). The glass transition temperatures (T_g) of the polymers were determined in the second heat cycle as the midpoint of the transition.

The wet glass transition temperatures (wet T_g) of the polymers were also determined. Briefly, films were incubated in PBS for 24 hours at room temperature. The film was blotted dry to remove "free" water and then weighed (~ 7 mg). The film was then placed in an aluminum pan and sealed. The pan was cooled from room temperature to − 50 °C at a rate 0f -30 °C/minute, and then kept at -50 °C for 3 minutes. The sample was then heated to 90 °C at a rate of 10 °C/minute, and then kept at 90 °C for 3 minutes.

The sample was cooled and then heated again from -50 ^{o}C to 90 ^{o}C at a rate of 10 ^{o}C/minute (second heat cycle). The wet glass transition temperatures (wet T_g) of the polymers were determined in the second heat cycle as the midpoint of the transition.

Air-water static contact angles were measured at room temperature using NRL C.A. Goniometer Model #100-00115 (Rame-Hart, Inc (Mountain Lakes, NJ)). For each experiment, a drop (5-10 µL) of the DI water was placed on a polymer film and after 30 seconds, the left and right contact angles were measured for each drop. At least three drops were used for each polymer substrate that was analyzed.

To simplify the naming of the tyrosine-derived terpolymers, the notation RXXYY(M_w) is used to name poly(DTR-co-XX%-DT-co-YY%-PEGMW carbonate) where R is the alkyl pendent chain, XX is the mole percent of DT, YY is the mole percent of PEG and M_w is the weight average molecular weight of PEG. As an example, poly(DTE carbonate) will be designated as E0000 where E stands for ethyl while poly(DTE-co-25%-DT-co-02%-PEG$_{2K}$ carbonate) will have a notation of E2502(2K).

2.3   Preparation of compression-molded films

The dry polymer (400 – 500 mg) was molded at room temperature at 15000 psi for 5 seconds using a stainless steel pre-mold lined with Reynolds® parchment paper (Alcoa Consumer Products Inc., Richmond, VA). The pre-molded polymer film was then placed between stainless steel plates lined with Kapton® film (American Durafilm, Holliston, MA) and spaced apart by custom stainless steel shims that were 200 µm thick. The plates were placed between the platens of a Carver Press (model 4122, Carver Inc., Wabash, IN) that were preheated to the processing temperature ((T_g + 50) ^{o}C) (Table 2.1).

Table 2.1 Processing temperature for the preparation of compression-molded films.

Polymer	Processing temperature (^{o}C)	Polymer	Processing temperature (^{o}C)
E0000	144	M0000	161
E1002(1K)	140	M1002(1K)	152
E1502(1K)	145	M1502(1K)	158
E2002(1K)	148	M2002(1K)	157
E1001(1K)	148	PLGA 85:15	99
E2502(2K)	133		

The steps of the compression molding process were: (1) allow the polymer to soak in the heat at processing temperature with no pressure for 5 minutes, (2) ramp up the pressure slowly from 0 to 15,000 psi over 1.5 minutes, (3) hold the pressure at 15,000 psi for 1 minute and (4) release the pressure slowly from 15,000 psi to zero. Allow the plates to cool down to room temperature and remove the film. Samples were obtained by (1) punching 6 mm-diameter disks for *in vitro* degradation studies or (2) cutting 5 mm wide x 35 – 40 mm long strips for mechanical testing from the compression-molded films.

2.4 Scaffold fabrication

Scaffolds were fabricated using a combination of solvent casting/porogen leaching/phase separation techniques.[43, 44] Briefly, an amount of polymer was dissolved in a mixture of DI water and 1,4-dioxane. Sodium chloride (NaCl) which was sieved to 212–425 μm particle size was weighed into a Teflon dish. The polymer solution was slowly poured over NaCl and was allowed to diffuse undisturbed. The Teflon dish was covered to prevent evaporation of solvent. The mold was then frozen in liquid nitrogen for 15 minutes and then freeze-dried for 48 hours in either Labconco FreeZone 2.5L benchtop freeze dry system (Labconco, Kansas City, MI) or Millrock Laboratory Series Freeze Dryer LD85 (Millrock Technology, Kingston, NY). Dry scaffolds were cut to size using custom-made stainless steel punchers with inner diameter of 16.2 mm or 10.4 mm and incubated in DI water at room temperature to leach out NaCl. The presence of Cl^- ions was determined by addition of $AgNO_3$ (silver nitrate) solution to the wash. The formation of a white precipitate (AgCl) upon addition of the $AgNO_3$ solution indicated that NaCl was still leaching out from the scaffold. When no further precipitate could be detected, the leached scaffolds were removed from DI water, blotted dry and dried for 48 hours under vacuum at room temperature. The weight and dimensions (diameter and thickness) of the scaffolds were measured. Samples were set aside for GPC, ^{1}HNMR and SEM analyses.

Calcium ions were incorporated into the scaffolds by immersing preformed porous scaffolds in an aqueous solution of $CaCl_2$ with the aid of vacuum. The calcium-coated scaffolds were freeze-dried for 2-4 hours. Calcium ions in the scaffold were precipitated into calcium phosphate (CP) *in vitro* by addition of K_2HPO_4 trihydrate. The

CP-coated scaffolds were freeze-dried for 24 hours. The scaffolds were weighed again. The dimensions were not measured since the diameter and thickness were not affected by the coating process. CP-coated scaffolds (n=3) were set aside for GPC, ^{1}HNMR, and SEM analyses. The amounts (% weight element/weight of scaffold) of calcium, chloride, and phosphate (or phosphorus) ions were determined by elemental analysis using ICP-OES (Inductively coupled plasma-Optical emission spectroscopy, QTI Intertek, Whitehouse, NJ) (n=3 – 5).

Pore architecture of sputter coated scaffolds (SCD 004, 30 milliAmps for 120 seconds with gold/palladium (Au/Pd)) that were mounted on aluminum studs with adhesive was evaluated using a scanning electron microscope (SEM, Amray 1830I, acceleration potential of 20 kV). A 75x magnification was used to determine the gross structure and a 250x magnification was used to evaluate the microporous structure of the scaffolds.

2.5 Sterilization of test materials: Ethylene oxide (EtO) sterilization

Individual scaffold for *in vitro* cell studies and *in vivo* rabbit calvaria experiments was placed in a polystyrene petri dish (100 mm outer diameter x 15 mm height, Fisherbrand, Fisher Scientific, Pittsburgh, PA). Each dish was packaged in self-sealing pouches (Crosstex International, Hauppauge, NY) and was sterilized using a 12 hour cycle of ethylene oxide (EtO) sterilization at room temperature (AN74i, Andersen Products, Haw River, NC). Sterility was verified using a Steritest® (AN-80, Andersen Products, Haw River, NC). The samples were subsequently degassed in a vacuum oven (-

101.6 kPa) at room temperature for 14 days[47] and the absence of residual EtO was verified by ^{1}H NMR (absence of methylene proton peak at δ2.54 ppm).

2.6   *In vitro* degradation and erosion

The degradation and erosion profiles of tyrosine-derived polycarbonate scaffolds or films were measured by incubating scaffold or film disks (5 − 20 mg) in PBS (phosphate buffered saline, 10 mL) in scintillation vials with one scaffold or film per vial at 37 °C. To allow PBS to permeate into the scaffolds, the vial containing the scaffold and the PBS was subjected to several cycles of atmospheric and vacuum pressure before incubation.[48, 49] Scaffolds or films at t=0 were subjected to the same conditions for 24 hours except they were not incubated. Aliquots of the buffer and scaffolds or films were collected at predetermined time points. The retrieved scaffolds or films (n=3 for each composition) were rinsed three times with DI water, blotted dry, and freeze-dried. PBS was replaced with fresh solution at each time point.

GPC analysis of freeze-dried scaffold or film dissolved in 1 mL DMF with 0.1% TFA was used to determine the molecular weight loss. The percentage of molecular weight retained at each time point (%M_n) was calculated as M_n of the scaffold at each time point divided by the M_n of the scaffold at t = 0.

To measure mass loss, aliquots (0.5 mL) from the supernatant were treated with 0.5 mL 1 N NaOH to hydrolyze the terpolymer fragments to DT and PEG$_{MW}$. Acidification with 12 N HCl (100 μl) converted the carboxylate group of DT to carboxylic acid. The solution was filtered using a 0.45 μm filter into an HPLC vial and then followed by HPLC analysis to determine the amount of DT in the supernatant.

The HPLC system consisted of a Waters Alliance 2695 Module, Waters 2487 Dual l Absorbance Ultraviolet (UV) Detector and Empower Pro® Software (Waters Corporation, Milford, MA). The column was a Perkin-Elmer Pecosphere C18 (33 x 4.6 mm; 3 μm particle size; cat. # 0258-1064, Waltham, MA). The mobile phase was a mixture of water and methanol both containing 0.1% TFA with a gradient of 80:20 to 40:60 in 6 minutes. The column temperature was set at 25 ^{o}C. The injection volume was 5 or 10 μL. The concentration of DT in the hydrolyzed aliquot was determined from a DT standard calibration curve. The amount of DT that has leached into the buffer was a good approximation of the extent of erosion of the polymer. All analyses were done in triplicate. Samples were collected weekly except for E2502(2K) where samples were collected for days 1 and 2 and weekly thereafter.

The percentage of mass loss at each time point (% Mass loss) was calculated as the difference in the dry mass of the scaffold (film) at t = 0 and dry mass of the scaffold (film) at each time point divided by the dry mass of the scaffold (film) at t = 0.

2.7   Mechanical properties

2.7.1   Tensile properties

For mechanical testing, 200 μm-compression molded film that were pressed at 50 °C above T_g were cut into strips (approximately 5 mm wide x 35 – 40 mm long; n=3). A Sintech 5/D mechanical tester (MTS Systems Corp.) was used for all mechanical tests. Testing was performed at a rate of 10 mm/min, with a pre-load of 10 mm/min, using a 100 N load cell. The tensile modulus, yield, and failure point were reported for an average of at least 3 samples. Tensile properties of dry samples were measured at

ambient conditions while wet films which were incubated in PBS at 37 $^{\circ}$C for 24 hours were evaluated in wet state in PBS at 37 $^{\circ}$C.

2.7.2 Compressive properties

Compressive properties of porous scaffolds (n=3) at various time points were evaluated in wet state in PBS at 37 $^{\circ}$C using Sintech 5/D mechanical tester (MTS Systems Corp., Eden Prairie, MN). Scaffolds with diameter of about 10 mm and height of about 5 mm were tested. The rate of the measurement was set at 0.5 mm/min and using a load cell of 100 N. The compressive modulus (*E*) and yield stress were measured. Compressive properties of dry scaffolds were also evaluated at ambient conditions (n=3).

2.8   *In vitro* cell studies (performed by colleagues at Carnegie Mellon University)

In order to determine the osteogenic potential of TyrPC terpolymers, the following *in vitro* cell studies using MC3T3-E1 pre-osteoblasts were performed by our collaborators at Carnegie Mellon University: (1) cytotoxicity, (2) cell attachment, (3) proliferation, (4) alkaline phosphatase activity and total protein, (4) osteocalcin assay, and (5) mineralization assay.

In vitro cytotoxicity, proliferation and osteogenic differentiation of human-derived mesenchymal stem cells cultured on TyrPC scaffolds were also measured.

In vitro release kinetics and osteogenic activity of recombinant human bone morphogenetic protein – 2 (rhBMP-2) were also evaluated using MC3T3-E1 pre-osteoblasts.

The methods used in the in *vitro* cell studies are detailed in Appendix 2.

2.9   *In vivo* biocompatibility assessment in rabbit critical-sized calvarial defect

All surgical procedures involving animals were approved by the Institutional Animal Care and Use Committee (IACUC) at Rutgers University. The NIH Guide for Care and Use of Laboratory Animals was observed in the treatment of all experimental animals. Research was conducted in compliance with the Animal Welfare Act and other Federal statutes relating to animals and experiments involving animals. The research adheres to the principles set forth in the Guide for Care and Use of Laboratory Animals, National Research Council, 1996.

Skeletally mature New Zealand White male rabbits were used to assess *in vivo* biocompatibility. Following standard practices for aseptic surgery, a critical sized defect (CSD) in the calvaria was created in the parietal bone using a 15 mm surgical trephine as described previously[50] (Figure 2.3 a-k). A semilunar coronal incision was prepared through soft tissues with sharp dissection and the parietal bones were visualized. Using a surgical drill with a trephine supplemented with physiological saline for irrigation, a craniotomy (15 mm diameter) was prepared midway between the supraorbital ridge and across the mid-sagittal sinus. A tyrosine-derived polycarbonate scaffold was inserted into the single craniotomy and soft tissues were closed in layers with resorbable 4-0 Dexon sutures. The skin was closed with surgical staples.

After 12 weeks, rabbits were sacrificed humanely according to NIH and University guidelines with an intravenous (*i.v.*) overdose of barbiturate (200 mg kg^{-1} body weight). Selected tissues were placed immediately into formalin for histological processing and analysis.

Figure 2.3. Creating a critical-sized defect in the rabbit calvaria using a 15 mm surgical trephine (a-k).

In a second *in vivo* study that was carried out at Carnegie Mellon University and Allegheny General Hospital, the effect of rhBMP-2 dose on bone regeneration was determined. An FDA-cleared bone void filler, predicate device (PD), which is made from Type-1 collagen and 80% β-TCP (tricalcium phosphate), was used as a control. The rabbits were sacrificed at 6 weeks. The treatment table is described in Table 2.2.

Table 2.2. Treatment table for critical sized-defect rabbit calvaria using TyrPC scaffolds with or without rhBMP-2.

Groups	Rabbits (Survived/Total)		
	0 μg rhBMP-2	50 μg rhBMP-2	200 μg rhBMP-2
Predicate device	5/5	5/5	5/6
Tyr-PC	4/5	4/5	5/5
Tyr-PC+Ca	0/6	3/7	5/6
Total	13/21	17/23	20/22

Histology/Histomorphometry and micro-computed tomography (μ-CT or micro-CT) were performed by our colleagues from Carnegie Mellon University and Cleveland Clinic, respectively. Statistical analyses of data from in vitro cell studies and in vivo rabbit calvarial studies were performed at Carnegie Mellon University. These procedures are detailed in Appendix 3.

2.10   Statistical analysis

All data are represented as means ± standard deviations of n=3 samples, unless noted.

CHAPTER 3

Tyrosine-derived polycarbonate terpolymers as new biomaterials for bone tissue engineering: Synthesis and evaluation of a focused library

Preface

M. H. R. Magno, J. Kim, A. Srinivasan, S. McBride, D. Bolikal, A. Darr, J. O. Hollinger and J. Kohn, Synthesis, degradation and biocompatibility of tyrosine-derived polycarbonate scaffolds. *Journal of Materials Chemistry*, 2010, **20**, 8885-8893 – Reproduced by permission of the Royal Society of Chemistry

The use of degradable polymers as tissue engineering scaffolds is widely investigated. Within this area of research, a significant need exists for the development of tissue scaffolds for bone regeneration.[51, 52] However, the most commonly used degradable polymers, poly(α-hydroxyester)s, have drawbacks including the production of a local acidic environment upon degradation which has limited their potential utility in bone tissue engineering. [53, 54] The tyrosine-derived terpolymers introduced in this study are a potential alternative to poly(α-hydroxyester)s. The monomeric unit for all tyrosine-derived polycarbonates is desaminotyrosyl-tyrosine alkyl ester (DTR), a derivative of naturally occurring tyrosine dipeptide. This particular structure gives rise to a family of non-toxic diphenolic monomers. [34, 45, 46, 55]

A series of previous studies highlighted the potential of a specific tyrosine-derived polycarbonate, poly(DTE carbonate), for use in orthopedic applications due to its *in vivo* bone biocompatibility and physical properties.[36] The strength of poly(DTE carbonate) exceeds that of other degradable polymers including poly(ε-caprolactone) and poly(ortho ester)s [34]. Poly (DTE carbonate) exhibits a tensile modulus (2.5 GPa) comparable to that of high molecular weight poly(L-lactic acid) (2.4–10 GPa).[27, 56]

Poly(DTE carbonate) has been explored in several biomedical applications, including low or minimally load-bearing orthopedic implants. Poly(DTE carbonate) pins were found to degrade at about the same rate as high molecular weight PLLA pins [33] while erosion and complete resorption of poly(DTE carbonate) implants were too slow for most practical applications.[37] Previous efforts to accelerate the degradation rates of tyrosine-derived polycarbonates focused on the synthesis of copolymers of poly(ethylene glycol) (PEG) and DTE, such as poly(DTE-*co*-PEG carbonate)s.[39, 40] As an extension of

this approach, copolymers of DTR and desaminotyrosyl-tyrosine (DT), such as poly(DTR-*co*-DT carbonate) were also synthesized and tested. [38, 57]

Yu and Kohn [39] showed that poly(DTE-*co*-PEG carbonate)s undergo backbone degradation at a rate much faster than poly(DTE carbonate). However, the incorporation of PEG into the backbone of poly(DTE carbonate) also affected the mechanical and biological properties of the resulting polymers. The presence of PEG in the polymer backbone was associated with an increased tendency to absorb water and a significant reduction of mechanical strength.[39] The biological properties were also affected: the amount of adsorbed protein, *e.g.*, human fibronectin, on the polymers and its bioactivity decreased at PEG(M_w1000) molar fractions greater than 6%.[41] Additionally, cell motility of L929 mouse fibroblast cells had a biphasic response: cell motility increased with increasing molar fraction of PEG in the copolymer up to about 4 mol%, and then decreased at higher PEG molar fractions.[58] A study also evaluated the potential of PEG containing tyrosine-derived polycarbonates to influence the osteogenic differentiation of human mesenchymal stem cells.[59] Thus, incorporation of PEG into the polymer backbone allows for modification of bulk and surface properties.[39-41]

An alternative approach to using PEG in the polymer backbone to accelerate degradation, the study of poly(DTR-*co*-DT carbonate)s was carried out by Abramson. [60] Copolymers of DTR and DT degraded faster *in vitro* with increasing molar fraction of DT in the polymer backbone. Levene [48] showed a similar increase in the rate of polymer degradation *in vivo*, and demonstrated the potential of DT containing copolymers in bone tissue engineering. Based on these prior studies, DTR, DT, and PEG were combined to create a new terpolymer system, referred to as tyrosine-derived polycarbonate

terpolymers (TyrPC). These terpolymers may preserve the excellent bone biocompatibility of poly(DTE carbonate) while providing for precise control of (i) the rate of degradation and resorption, (ii) the bulk and surface properties, and (iii) the biological interactions of these polymers with cells and tissues. To further illustrate the versatility of the TyrPC terpolymers, the utility of these terpolymers with high DT or high PEG as carriers for cortical neural probes[61] and as carriers of a hydrophobic peptide molecule[62] has been investigated.

This chapter presents the synthesis and characterization of a focused library of TyrPC with potential utility as bone tissue engineering scaffolds.

3.1   Design of a focused library of tyrosine-derived polycarbonate terpolymers

The novel materials design strategy proposed for this thesis will incorporate free carboxylate side groups for tunable degradation and erosion, and PEG blocks for controlling the water uptake and thus, bulk and surface properties of the resulting polymer. The random linear terpolymer of tyrosine-derived polycarbonate will generally have the following composition, *poly(DTR-co-XX%-DT-co-YY%-PEG$_{MW}$ carbonate)*, where DTR is desaminotyrosyl-tyrosine alkyl ester, R is either ethyl or methyl, XX% is mole percentage of DT (desaminotyrosyl-tyrosine), YY% is mole percentage of PEG$_{MW}$ (poly(ethylene glycol)), and MW is the molecular weight of PEG. To simplify the naming of the tyrosine-derived terpolymers, the notation RXXYY(MW) is used to name poly(DTR-*co*-XX%-DT-*co*-YY%-PEG$_{MW}$ carbonate)s. See the Methods section for a detailed explanation of this polymer notation.

There are six polymer compositions in this focused library as shown in Table 3.1.

Table 3.1 List of terpolymers in the focused library of tyrosine-derived polycarbonates.

R	XX%	Polymer Notation
Methyl	10	M1002(1K)
	15	M1502(1K)
	20	M2002(1K)
Ethyl	10	E1002(1K)
	15	E1502(1K)
	20	E2002(1K)

The rationales for choosing the composition of tyrosine-derived polycarbonate terpolymers are:

(1) *Changing the alkyl ester pendent chain from ethyl to methyl*:

Ethyl as a pendent chain will be the standard to which other tyrosine-derived polycarbonates will be compared to. Ethyl as R group has been extensively studied in the Kohn lab but not yet for these specific compositions. Methyl, on the other hand, has not been considered because of the potential toxicity associated with its hydrolysis product, methanol. Since the methyl ester is hydrolyzed much faster than any other alkyl ester, the use of DTM as a monomer could result in promising new polymer compositions. Further, the tendency of a polymer to favor bone apposition rather than an undesirable encapsulation response is affected by alkyl chain length [37], with ethyl being far better than butyl or octyl. If this trend continues, then methyl as R group may have an even higher tendency for bone apposition than ethyl.

(2) *Mole percentage of desaminotyrosyl tyrosine (DT)*:

The mole percentage content of the focused library was determined from the results of preliminary studies. E0000 degraded to about 70% of molecular weight but no mass loss was observed *in vitro* during a 36-month period, while E2502(2K) and M2502(2K) degraded and eroded fast, within a week (Figure 3.1). Thus, 10, 15, and 20 mol% DT in the polymer backbone were chosen in order to optimize a chemical composition that will be used to fabricate bone regeneration scaffolds. In bone tissue engineering, an ideal scaffold should be intact for at least eight weeks and then degrade and erode thereafter.
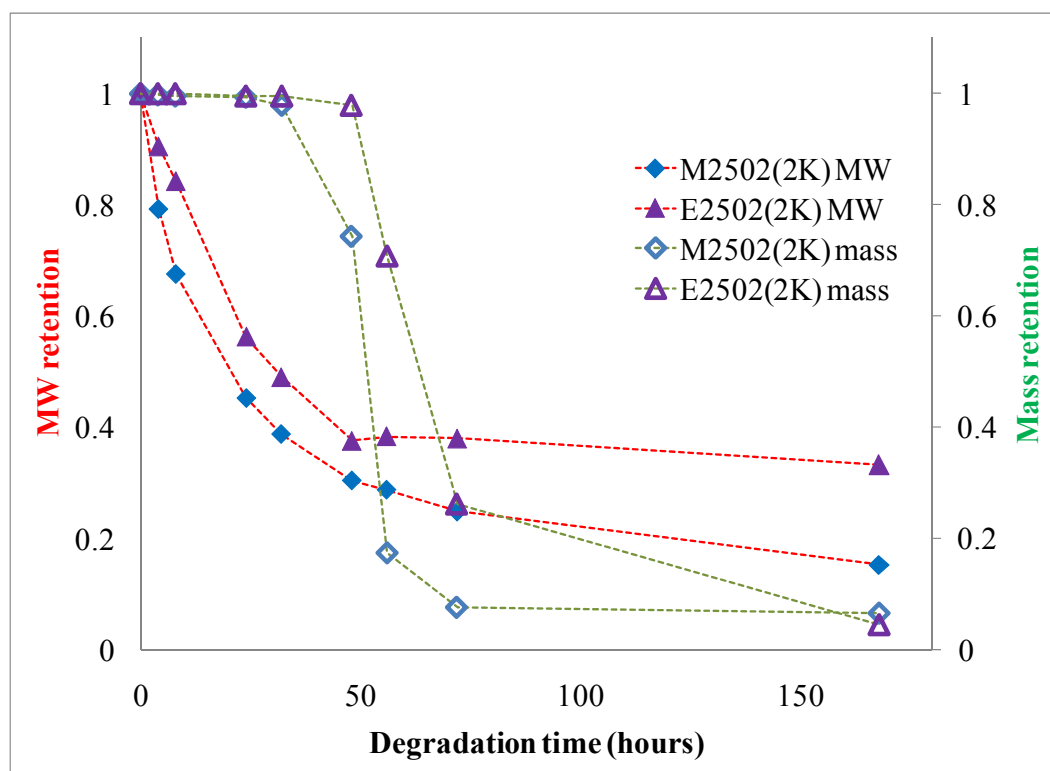
Figure 3.1. *In vitro* degradation and erosion of 15 mm diameter by 2 mm thick scaffolds in PBS at 37 °C.

(3) *Poly(ethylene glycol) block length and percentage mole composition:*

Poly(ethylene glycol) or PEG blocks will be fixed at 1,000 Da and at 2 mol%. In the preliminary degradation study, E2502(2K) dissolved within seven days (Figure 3.1). A polymer with the same DT content, E2500, but without PEG has not dissolved even after 4 weeks of incubation in PBS at 37 °C. This result clearly indicates that PEG plays a critical role in controlling the rate of degradation and erosion of tyrosine-derived polycarbonates by initiating the degradation of the polymer backbone through hydration of the PEG segments. [63] In order to modulate the overall effect of PEG on the rate of degradation, erosion, mechanical strength and osteoconductive properties, a shorter block length of PEG was used. In an *in vitro* study done by J. Khan[62], films made from random

linear terpolymers of DTE, DT and PEG_{1K}, whose compositions were different from the focused library being proposed, had significant MW loss in the initial stages of the study but there was minimal mass loss accompanying such degradation. After a few weeks (or months for some), still the loss in the MW started to stabilize with little to no signs of erosion. The hypothesis for such an occurrence is that water is associated with PEG blocks[63] and hydrolyzes adjacent carbonate bonds of the polymer backbone. This leads to significant MW loss. However, because the products of such hydrolysis are hydrophobic molecules which have low solubility in aqueous media, no mass loss is observed even with such dramatic decrease in the MW.

3.2   Synthesis and structure characterization

The tyrosine-derived polycarbonate terpolymers were synthesized using the methods described in Chapter 2. The chemical structures of these polymers were confirmed by ^{1}HNMR. A representative structure of TyrPC terpolymer and a typical ^{1}H NMR chemical shift assignment of the polymer are listed in Figure 3.2.
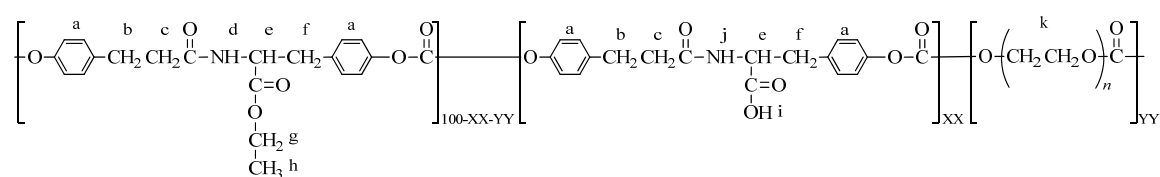
Hydrogen	Chemical shift (ppm)	Hydrogen	Chemical shift (ppm)
a	7.3	b	2.4
c	2.7	d	8.4
e	4.4	f	2.8, 3.0
g	4.0	h	1.1
i	12.8	j	8.3
k	3.5, 3.6, 4.1		

Figure 3.2. Chemical structure and ^{1}HNMR chemical shift assignment for poly(DTR-*co*-XX%DT-*co*-YY%PEG$_{MW}$ carbonate); here R = E or ethyl. XX and YY are mole percentages of DT and PEG, respectively. The mole percentage of DTR equals 100 – XX – YY, and *n* is the number of ethylene glycol repeat units in PEG.

In previous studies, Yu and Kohn[39] have shown that poly(DTR-*co*-PEG carbonate)s are random copolymers based on the integration of six carbonate peaks from

^{13}C NMR. These observations were confirmed by Pesnell[64] who showed that the iodinated versions of the polymers described here, poly(I$_2$DTR-*co*-I$_2$DT-*co*-PEG carbonate)s, also appear to be random copolymers. The terpolymers described in this study were synthesized using a similar polycondensation reaction, and are expected to possess random copolymer structure as well.

The optimized synthesis conditions yielded polymers with high molecular weight, around 200,000 Daltons, with small polydispersity indices (Table 3.2). The % mole composition of each monomer component was calculated using ^{1}HNMR, based on the integration of amide protons (d and j) at δ 8.3 and 8.4 ppm, aromatic protons (a) at 7.2 ppm and PEG methylene protons (k) at 4.1, 3.6 and 3.5 ppm. The polymer compositions were within ± 1 mole % of their theoretical value (Table 3.2).

Table 3.2. Characterization of TyrPC terpolymers and the homopolymers poly(DTE carbonate and poly(DTM carbonate)

TyrPC	Number average molecular weight (M_n, kDa)	Polydispersity index (M_w/M_n)	Composition from NMR		
			%DTR	%DT	%PEG$_{MW}$
E0000	194	1.6	100		
E1001(1K)	178	1.6	89.1	9.8	1.1
E1002(1K)	187	1.7	87.6	10.5	1.9
E1502(1K)	178	1.6	83.3	14.7	2.0
E2002(1K)	192	1.7	77.8	20.0	2.2
M0000	190	1.6	100		
M1002(1K)	168	1.6	88.1	9.7	2.2
M1502(1K)	183	1.6	83.3	14.6	2.1
M2002(1K)	200	1.5	78.8	19.0	2.2

3.3   Thermal properties

The effect of co-polymerization of poly(DTR carbonate)s on the glass transition temperature (T_g) was monitored using Differential Scanning Calorimetry (DSC). Yu and Kohn[39] observed that the dry T_g of poly(DTR-*co*-PEG carbonate)s decreased with increasing mole fraction of PEG and Abramson[60] observed that T_g increased with increasing mole fraction of DT in poly(DTR-*co*-DT carbonate)s. These results are confirmed in the present work.

For TyrPC terpolymers, T_g increased as DT was increased from 10 – 20 mol%, while keeping mol% PEG and PEG block length were kept constant at 1K. Furthermore, T_g decreased as the mole fraction of PEG$_{1K}$ was increased from 1 to 2 mol%, while keeping mol% DT constant as in the case of E1001(1K) and E1002(1K) (Table 3.3). Glass transition temperature is affected by stiffness of the polymer backbone, *i.e.*, the stiffer the backbone is the higher the T_g. Introducing DT, a rigid monomer, increases the T_g, while introduction of aliphatic chains, decreases the T_g by decreasing the stiffness of the polymer backbone. In the case of DTE- and DTM-based polycarbonates, higher T_g's are observed for the latter because of the shorter methyl pendent group in the polymer backbone that results in better packing of polymer chains.

After 24 hours of incubation in PBS, the wet T_g of the polymers was lesser than the corresponding dry T_g. The homopolymers had higher wet T_g than the terpolymers which indicate that either PEG(1K) and/or DT had an effect on the wet T_g of the polymers. However, for TyrPC terpolymers, the wet T_g did not increase as DT was increased from 10 – 20 mol%, while keeping mol% PEG at 1% and PEG block length

constant at 1K. This result indicates that the presence of PEG in the polymer backbone resulted to absorption of water which acted as a plasticizer that reduced the stiffness of the polymer backbone. The constant mol% and block length of PEG in the polymer backbone may also indicate that the amount of water that can be absorbed by TyrPC terpolymers is dependent on the amount of PEG present. This may be the reason why wet terpolymers films had very similar wet T_g.

Since the Td is considerably higher than T_g these terpolymers were expected to be stable at the processing temperature of $(T_g + 50)$ °C during compression molding.

Table 3.3. Thermal properties of TyrPC terpolymers.

Polymer Notation	T_g (^{o}C)	wet T_g (^{o}C)	Td (^{o}C)
E0000	95	68	276
E1001(1K)	98	61	275
E1002(1K)	90	52	265
E1502(1K)	95	53	279
E2002(1K)	98	56	277
M0000	111	68	289
M1002(1K)	102	55	278
M1502(1K)	108	60	271
M2002(1K)	107	51	269

3.4 Mechanical properties

The tensile properties of compression molded films made from TyrPC terpolymers were evaluated in the dry state in ambient conditions (Table 3.4) and after incubation in PBS at 37 $^{\circ}$C for 24 hours in the wet state in a PBS water bath maintained at 37 $^{\circ}$C (Table 3.5).

For both DTE- and DTM-based polycarbonates in the dry state, the tensile modulus (E) are similar, while the yield stress and tensile strength values indicate that terpolymer with higher mol% of DT and that are DTM-based are stronger polymers. However, the effect of the amount of PEG$_{1K}$ on the stiffness of E1001(1K) and E1002(1K) is not obvious. Both DTR and DT are stiff monomers and incorporating these monomers in the polymer backbone will result in stronger yet more brittle materials. Further, DTM-based polymers are generally stronger than DTE-based polymers because of the shorter alkyl pendent chain in former, which enables better packing of the polymer chain. In the dry state, PLGA 85:15 is a stiffer material than TyrPCs.

After 24 hours of incubation in PBS at 37 $^{\circ}$C, the films lost their stiffness and strength except for the homopolymers and E1001(1K). The decrease in the mechanical properties may be attributed to the amount of PEG in the polymer backbone. PEG is a hydrophilic polymer that will attract water to the polymer backbone. The water that gets adsorbed on the polymer acts as a plasticizer which results in the decrease in the tensile properties of the terpolymers. For the DTE-based terpolymer films in the wet state, the higher the DT, the stronger the wet films were. The reverse was true for DTM-based terpolymers, which could indicate that as early as 24 hours incubation in PBS, degradation of M2002(1K) and M1502(1K) may have commenced, resulting in brittle

films. This is reflected in the significant decrease in the tensile strength of the films. After

incubation in PBS, the mechanical property of PLGA 85:15 were significantly reduced.

Table 3.4. Mechanical properties of compression-molded polymers in the dry state. Data reported are mean values with standard deviation in parentheses.

Polymer	Modulus (E), GPa	Yield stress (σ_y), MPa	Strain at yield, %	Tensile strength, MPa	Strain at break, %*
E0000	2.5 (0.2)	40.8 (3.1)	2.5 (0.2)	34.3 (3.3)	15.1 (6.3)
E1001(1K)	2.6 (0.1)	17.8 (1.6)	1.1 (0.2)	6.4 (3.6)	12.3 (1.0)
E1002(1K)	2.6 (0.3)	20.7 (3.0)	1.2 (0.5)	13.1 (3.4)	12.4 (3.3)
E1502(1K)	2.4 (0.1)	24.6 (1.3)	1.7 (0.1)	18.7 (2.0)	10.2 (1.5)
E2002(1K)	2.1 (0.1)	26.9 (0.5)	1.9 (0.2)	18.8 (4.1)	11.5 (2.0)
M0000	2.7 (0.1)	27 (1.6)	1.6 (0.2)	15.3 (2.7)	9.3 (0.8)
M1002(1K)	2.5 (0.2)	21.8 (4.7)	1.4 (0.3)	12.6 (1.5)	10.8 (3.9)
M1502(1K)	2.6 (0.2)	31.3 (7.5)	2.2 (0.6)	21.7 (3.6)	12.0 (4.3)
M2002(1K)	2.6 (0.2)	35.3 (4.9)	1.9 (0.6)	24.0 (7.8)	8.8 (3.9)
PLGA 85:15	3.4 (0.2)	13.6 (3.2)	0.5 (0.1)	9.0 (1.8)	10.8 (2.0)

Table 3.5. Mechanical properties of compression-molded polymers in the wet state after incubation in PBS at 37 $^{\circ}$C for 24 hours. Data reported are mean values with standard deviation in parentheses.

Polymer	Modulus (*E*), GPa	Yield stress (σ_y), MPa	Strain at yield, %	Tensile strength, MPa	Strain at break, % *
E0000	2.6 (0.1)	34.5 (0.5)	2.2 (0.6)	24.4 (2.3)	47.1 (25.0)
E1001(1K)	2.4 (0.1)	30 (2.6)	1.6 (0.1)	18.2 (1.8)	92.4 (53.4)
E1002(1K)	1.6 (0.2)	17.9 (2.9)	2.0 (0.1)	9.5 (2.4)	59.7 (28.4)
E1502(1K)	1.7 (0.2)	22.4 (0.4)	1.9 (0.4)	15.4 (2.4)	164.7 (55.8)
E2002(1K)	1.6 (0.4)	21.4 (2.8)	1.9 (0.2)	13.3 (8.0)	154.1 (97.2)
M0000	2.9 (0.3)	32.2 (3.1)	1.3 (0.1)	24.9 (4.1)	174.4 (38.0)
M1002(1K)	2.4 (0.3)	26.7 (2.2)	1.6 (0.3)	17.2 (2.2)	129.7 (8.5)
M1502(1K)	2.1 (0.2)	21.0 (2.4)	1.3 (0.1)	16.2 (2.9)	3.7 (1.7)
M2002(1K)	1.9 (0.1)	20.0 (1.4)	1.5 (0.1)	18.6 (1.0)	2.2 (0.1)
PLGA 85:15	0.6 (0.03)	4.0 (0.6)	1.8 (0.6)	2.2 (0.2)	77.0 (13.9)

large standard deviations are due to sample slippage from the grips

3.5   Contact angle measurements

The wettability of the compression-molded polymer surface was analyzed by measuring the contact angle of water on the surface of a film (Figure 3.3). The homopolymers, E0000 (literature value 73° [34]) and M0000, and PLGA 85:15 (literature value 84° [65]) had the highest contact angles among the test specimens. The higher the contact angle of the surface is with water, the more hydrophobic is the surface. Between, E1001(1K) and E1002(1K), the latter's surface had a lower contact angle with DI water which indicates that the higher concentration of PEG_{1K} in the polymer backbone decreases the hydrophobicity of the polymer. An increase in mol% DT, results in a decrease in the contact angle which indicates that higher mole percentage of DT in the polymer backbone also results in a less hydrophobic polymer. This trend was most obvious for the DTM-based polycarbonates. Between DTE- and DTM-based polycarbonates, the contact angles of the DTM-based polycarbonates were generally lower than the former and this is an indication that the DTM-based surfaces are less hydrophobic than the DTE-based surfaces. The lower contact angle of DTM-based polycarbonates could also indicate better water uptake which will result in faster degradation of the polymer.
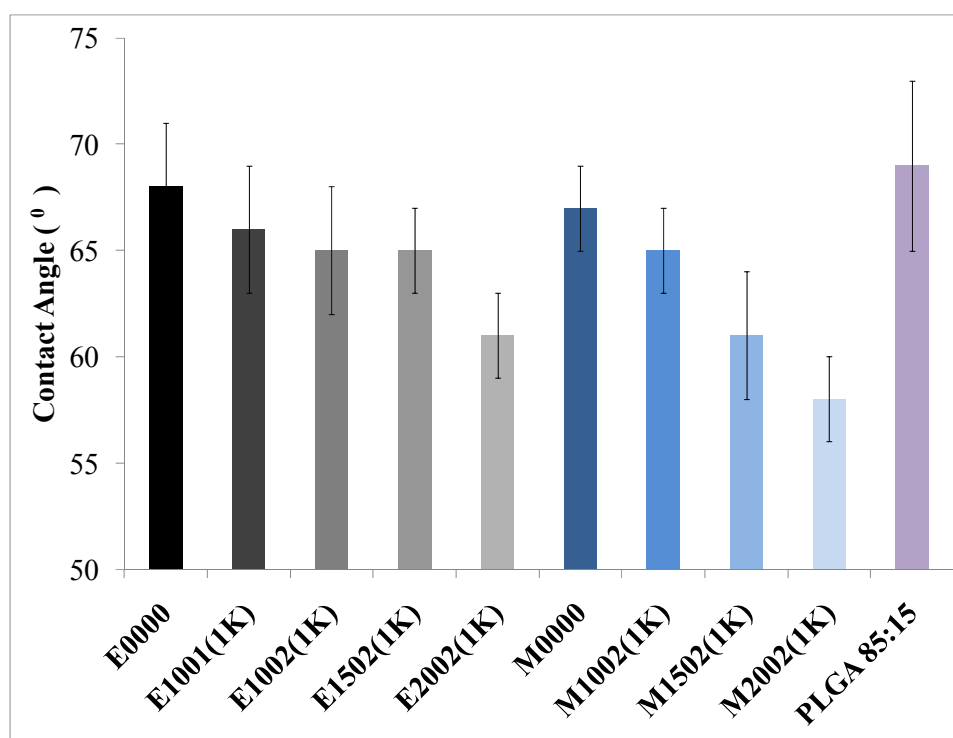
Figure 3.3. Air-water contact angle using DI water as liquid probe on compression-molded films measured at room temperature. Data is reported as mean ± standard deviation for 3 drops where both left and right contact angles were measured.

3.6   Conclusion

A comprehensive evaluation of tyrosine-derived polycarbonate terpolymers as a new class of degradable biomaterials was presented. The evaluation included synthesis and chemical structure proof, thermal properties, mechanical properties, and contact angle. These results indicate that variations in the molar fractions of either DT or PEG within the polymer backbone can be used to tune the properties of these polymers.

The effect of varying the chemical composition of TyrPC terpolymers on degradation and erosion will be discussed in the next chapter (Chapter 4).

CHAPTER 4

Hydrolytic degradation of tyrosine-derived polycarbonate terpolymers

In bone-related injuries or defects, the implant is only needed for a short period of time, only until the defect has healed, which can take as little as about eight to ten weeks [4]. Thus, there is a need for biomaterials that degrade and resorb in a timeframe parallel to fracture healing. Some terms, related to degradation and erosion, are defined for clarification [24, 66, 67]. Degradation involves enzymatic or hydrolytic cleavage of labile bonds in the polymer that results in the breakdown of the polymer to low molecular weight fragments or to the corresponding monomers. Resorption involves the complete elimination of the degradation products in the body either by metabolism or excretion. Erosion is a process that is accompanied by mass loss and physical changes in size and shape of the implant.

Implanted materials degrade in biological environment in two ways: (1) through chemical events such as hydrolysis or oxidation, and (2) through enzyme-mediated degradation. Although degradation experiments that take into account *in vivo* conditions may increase the significance of the results, the complex biological milieu cannot be replicated *in vitro*. Enzyme-mediated degradation of TyrPC may also be unlikely due to the inherent stiffness of the polymer. Often, *in vitro* studies, which are carried out in phosphate buffered saline (PBS) and at 37 $^\circ$C approximate physiological conditions and results obtained can give us an understanding on how materials degrade in aqueous conditions.

The ability of tyrosine-derived polycarbonates (TyrPC) to degrade on a time scale relevant to bone healing was an important objective for this project. During the *in vitro* degradation studies, incubated films, around 200 μm thick, and scaffolds, around 10 mm in diameter x 2.5 mm thick, and aliquots of the supernatant were collected at predetermined time points to determine occurrence of hydrolytic degradation and erosion. In an attempt to elucidate the mechanism and kinetics of the hydrolysis of TyrPC terpolymers, changes in physical appearance, molecular weight retention, mass retention, and compositional changes were monitored during the study. Water uptake for incubated films was also monitored.

4.1   Physical appearance of TyrPC terpolymer films during incubation

During the 16-week incubation period, the homopolymers, specifically, E0000 and M0000, and E1001(K) remained transparent. In contrast, the transparent films became opaque faster with increasing amounts of DT during incubation and this transition coincided with an observable increase in water uptake.

In the case of M2002(1K), which degraded and eroded completely within 4 weeks of incubation, the physical appearance changed from clear to opaque to swollen, and finally the films became brittle. Similar changes were observed for the other TyrPC terpolymers but the changes occurred over a longer period of time than M2002(1K) films. For comparison, compression-molded films made of PLGA 85:15 which were transparent became white in less than a week in PBS at 37 $^{\circ}$C.

4.2   Molecular weight retention

The degradation and erosion behavior of TyrPC terpolymers were evaluated in PBS at 37 ^{o}C and compared with the degradation of E0000, M0000 and PLGA 85:15. The values of weight- average molecular weights of the compression-molded films were close in values except for E0000 and M0000 (Table 4.1), thus making the comparison of the degradation of these polymers valid.

Table 4.1. Weight-average molecular weights (M_w) and PDI of compression-molded films made of tyrosine-derived polycarbonates and poly(lactide-*co*-glycolide) 85:15 used in this study. Data is reported as mean with standard deviation in parentheses of n=3.

Compression molded Films	M_w, kDa	PDI (M_w / M_n)
E0000	247 (9)	1.7 (0)
E1001(1K)	184 (29)	1.7 (0)
E1002(1K)	216 (13)	1.7 (0)
E1502(1K)	202 (31)	1.7 (0)
E2002(1K)	211 (10)	1.9 (0)
M0000	262 (20)	1.6 (0)
M1002(1K)	176 (26)	1.6 (0)
M1502(1K)	191 (32)	1.8 (0.3)
M2002(1K)	174 (9)	1.6 (0)
PLGA 85:15	173 (2)	1.5 (0)

All polymers lost molecular weight to varying degrees as a function of incubation time (Figure 4.1). As expected, increasing the DT content significantly increased the polymers' susceptibility to hydrolytic degradation. Specifically, the degradation of polymers increased when the DT content was changed from 10 to 20 mol%, while keeping the PEG content constant. In addition, changing the PEG mol% from 1 to 2, while keeping the DT constant, also increased the degradation rate, as in the case of E1001(1K) and E1002(1K). Thus, it is believed that DT and PEG synergistically accelerate the hydrolytic degradation of TyrPC terpolymers. DT accelerates degradation by increasing the acidity and hydrophilicity of the polymer matrix, while PEG increases the hydrophilicity of the polymer backbone which results in a concomitant increase in water uptake.
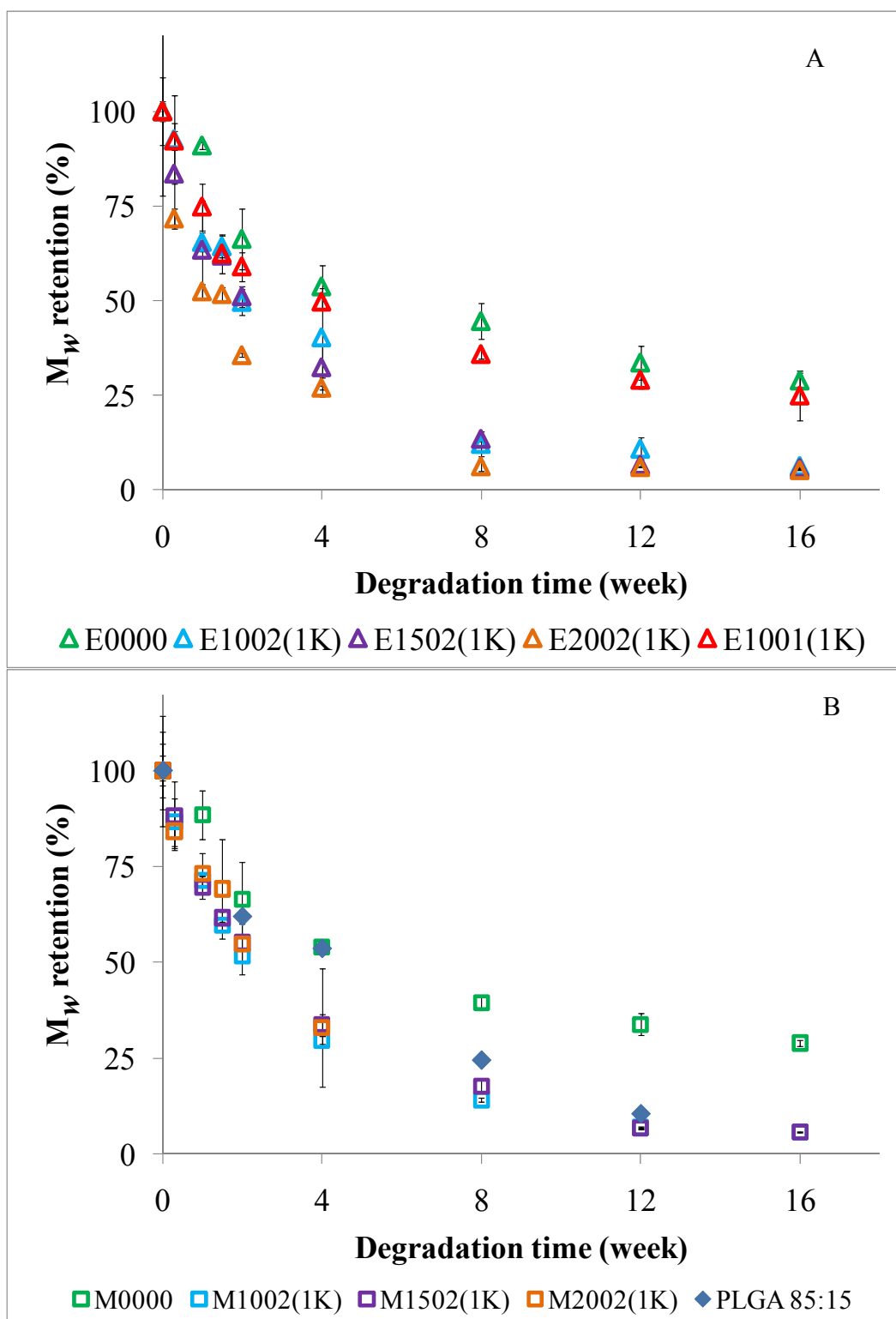
Figure 4.1. Molecular weight retention of compression-molded films (A) DTE-based, (B) DTM-based polycarbonates and compared with PLGA 85:15 as a function of degradation time in PBS at 37 ^{o}C. Data is reported as mean ± standard deviation of n=3.

Replacing DTE with DTM in the polymer backbone did not result in faster degradation. It is expected that decreasing the length of the pendent chain will increase the hydrophilicity (see contact angle measurements in Chapter 3, contact angle with water: DTE > DTM) of the polymer backbone that will result in faster degradation. However, the shorter methyl groups on DTM terpolymers allow for better packing of the polymer strands decreasing water permeability of the polymer matrix. A measurable physical quantity that approximates the flexibility of polymer strands is the glass transition temperature (Tg). Between DTE and DTM, the latter has a higher Tg. Although DTM terpolymers are more hydrophilic than DTE terpolymers, the permeability of water into the polymer network is the rate determining step in the degradation of these terpolymer systems.

However, increasing the amount of DT in DTM-based terpolymers did not have an effect on the rate of degradation because these terpolymers lost molecular weight at almost the same rate. In this case, increasing the DT content increases the stiffness of the polymer, *i.e.*, higher Tg, but also increases the hydrophilicity of the polymer, *i.e.*, lower contact angle with water. In the case of the DTM-based terpolymers, the effect of stiffness is counterbalanced by hydrophilicity. Thus, similar degradation was observed.

The overall goal of this dissertation was to fabricate scaffolds for bone regeneration. A scaffold that can maintain its shape, pore architecture and strength, while degrading in a time frame that is parallel to new bone formation is an ideal bone regeneration scaffold. Scaffolds were fabricated using the polymers in the focused

library and their degradation and erosion were compared with PLGA 85:15 and E0000 (Figure 4.2).

The degradation of both DTE-based and DTM-based polycarbonate scaffolds is a function of the mole percentage of DT, i.e., the higher the mole percentage of DT, the faster the degradation. For instance, E1502(1K) lost around 80% of its initial molecular weight while E1002(1K) lost around 25% after 1 week of incubation.

PEG also affected the degradation of the scaffolds as seen between E1001(1K) and E1002(1K).

DTM-based scaffolds degraded faster than DTE-based scaffolds, specifically, E1002(1K) and M1002(1K).

What is interesting is that for the E1001(1K) composition, the device configuration has actual effect on the rate of degradation. Where E1001(1K) compression-molded films degraded at the same rate as E0000 film, there was a vast difference in the degradation rates of these compositions in scaffold form. These results indicate that porosity increases the rate of degradation because a porous material has a greater surface area exposed to the aqueous solution than a solid disc of film.
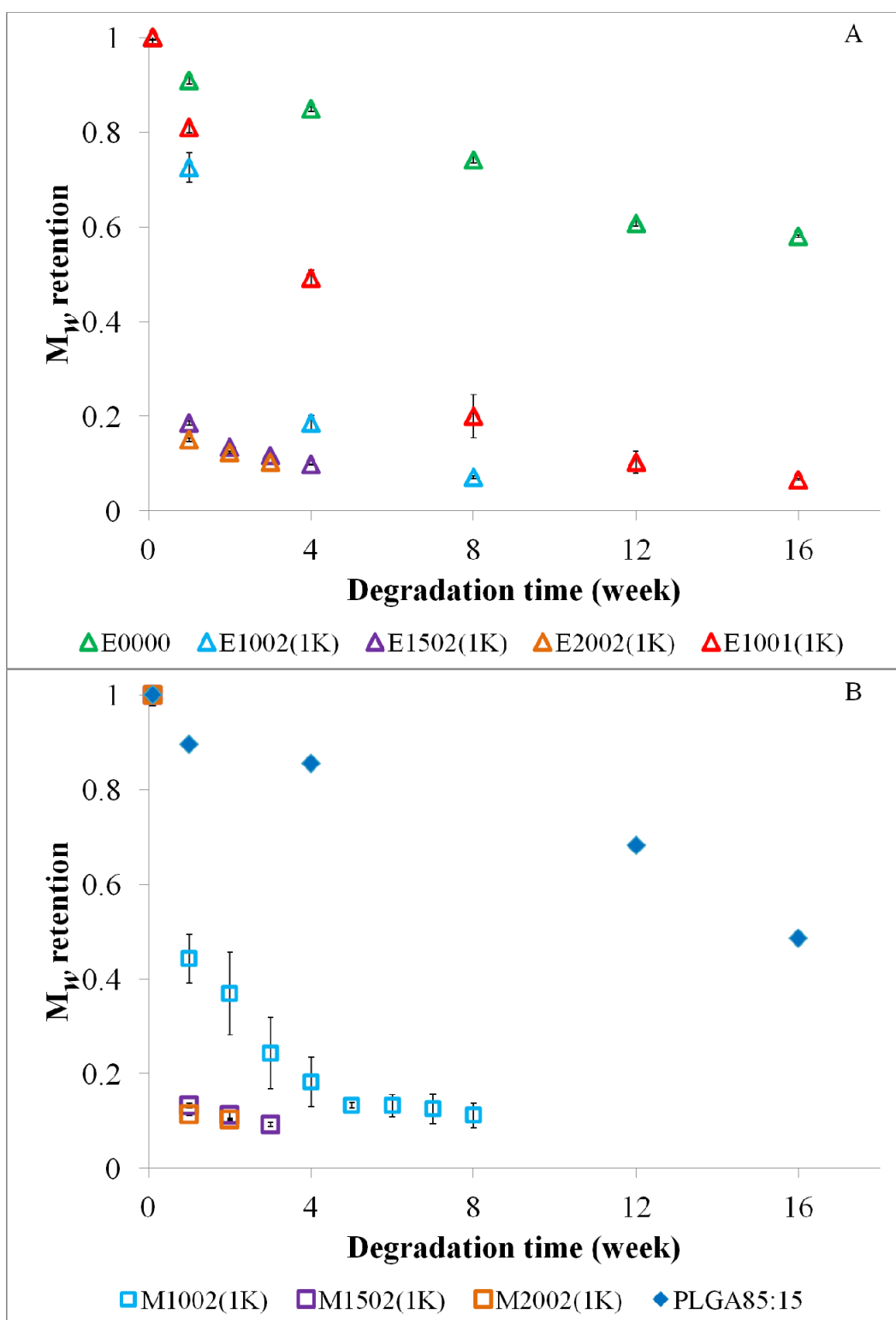
Figure 4.2. Molecular weight retention of scaffolds (A) DTE-based, (B) DTM-based polycarbonates and compared with PLGA 85:15 as a function of degradation time in PBS at 37 $^{\circ}$C. Data is reported as mean ± standard deviation of n=3.

Before incubation of M2002(1K) scaffolds (Figure 4.3), uniform pore morphology was observed in all scaffolds where the characteristic bimodal pore distribution, high degree of interconnectivity and oriented micropores were seen. After 1 week of incubation, morphological changes started to occur with the micropores decreasing in size. As the scaffolds degraded further, the pore architecture starts to collapse. For this scaffold composition, the scaffolds became brittle after week 3 and no sample can be analyzed by SEM for morphological changes.

Diminished pore size was observed with PDLLA, PLGA 75:25 and PLGA85:15 also and that these morphological changes are a function of the degradation rate of the scaffold. [68]
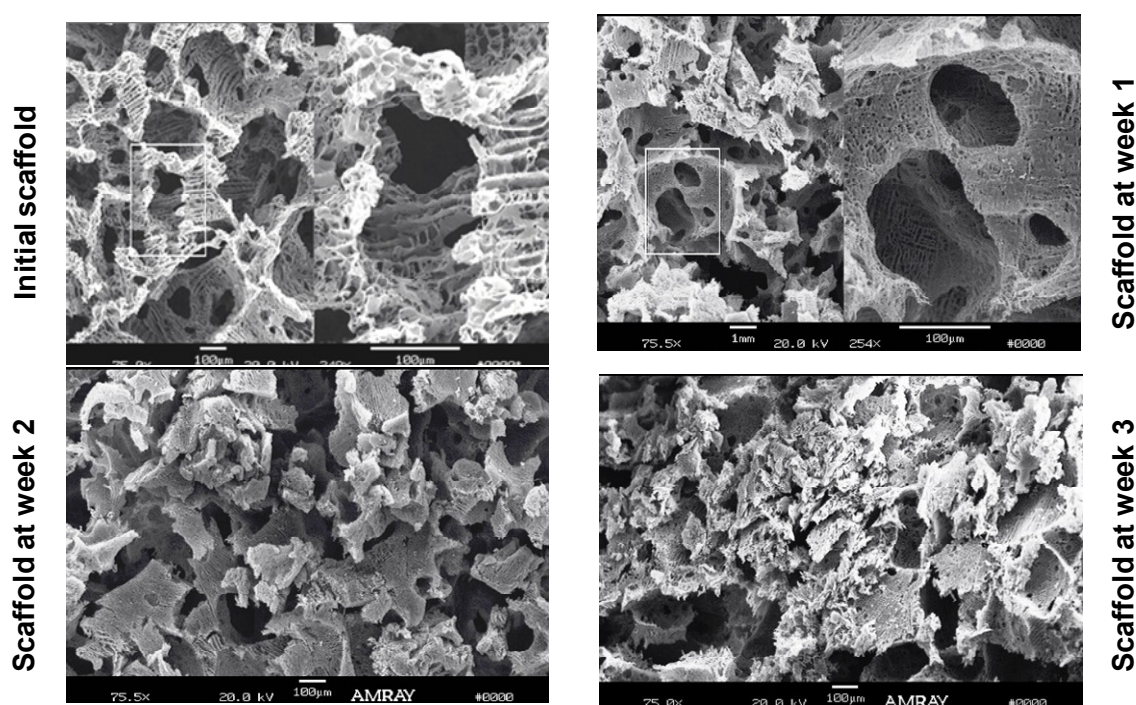
Figure 4.3. SEM images of M1002(1K) scaffold as it degrades in PBS at 37 $^{\circ}$C.

4.3   Mass retention

For E0000, M0000, E1001(1K) and E1002(1K), no mass loss was detected during the course of the 20-week degradation study (Figure 4.4 A and B). The results for the other terpolymers clearly showed that erosion is a function of the amount of DT, with the terpolymer containing the highest DT, at 20 mol%, eroding fastest. The higher DT provides a more hydrophilic and acidic environment around the hydrolysable bonds which results in faster hydrolysis of the carbonate bonds in the polymer backbone and faster hydrolysis of the ester pendent chain. These two events lead to formation of soluble degradation products that leach out of the polymer matrix resulting in mass loss.

Moreover, between DTE-based and DTM-based terpolymers, the latter eroded faster in PBS at 37 ^{o}C. The solubility of DTE in PBS at 37 ^{o}C was around 1.2 mg/mL (in water at 37 ^{o}C, 1.2 mg/mL) while the solubility of DTM in PBS (37 ^{o}C) was 1.6 mg/mL (in water at 37 ^{o}C, 1.6 mg/mL). The higher solubility of DTM than DTE resulted in a less hydrophobic polymer backbone that caused the accelerated degradation of the DTM-based polycarbonates and subsequent erosion *in vitro*.

However, very minimal erosion was observed for TyrPC scaffolds. These scaffolds, specifically, the scaffolds with the highest mole% DT only lost around 15% of their initial mass during the 16-week study. This is quite unexpected because the greater surface area of the scaffold resulted in faster degradation (see Figures 4.1 and 4.2). When the scaffolds degrade the soluble degradation products easily leach out through the pores so there's a measurable amount of mass lost, although very minimal. As the scaffolds degrade there are two possible events that are taking place, (1) the pore architecture collapses and traps the soluble oligomers in the scaffold framework and (2) the

composition of the remaining scaffold is essentially that of a homopolymer or a co-polymer which are more hydrophobic than the starting terpolymers compositions.
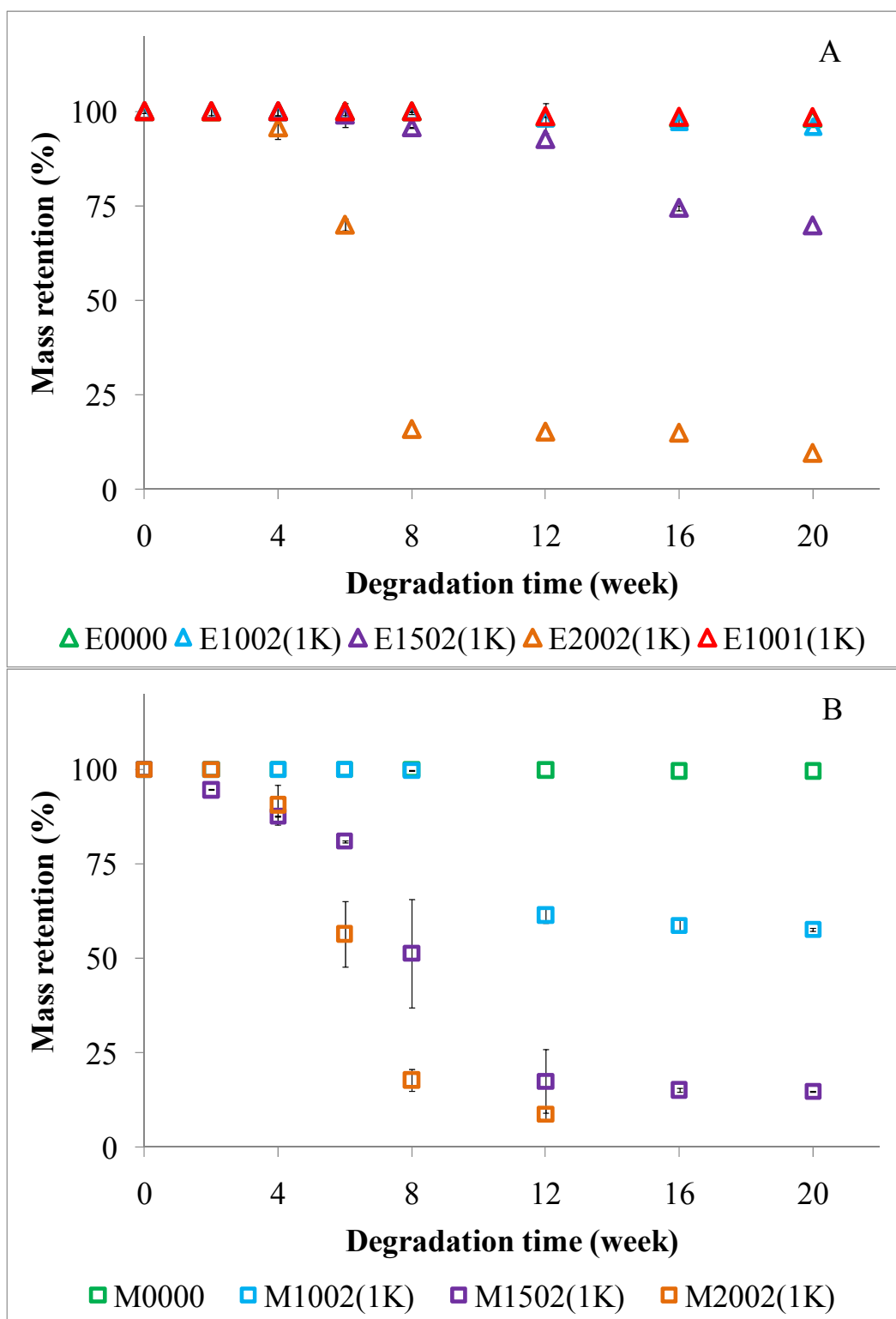
Figure 4.4. Mass retention of compression-molded films (A) DTE-based, (B) DTM-based polycarbonates as a function of degradation time in PBS at 37 $^{\circ}$C. Data is reported as mean ± standard deviation of n=3.

4.4   Water uptake

The effect of the polymer backbone composition was also evaluated in terms of water uptake (Figures 4.5 A and B, films). At each time point during *in vitro* degradation of the films in PBS at 37 $^{\circ}$C, the amount of water uptake was calculated as the amount of water absorbed by the film with respect to the dry weight of the film.

The water uptake for E0000 was between 2 to 3 % while that for M0000 films was around 5%. These values remained unchanged during the 10-week study.

Among the DTE-based polycarbonates (Figure 4.5 A), the trend in water uptake was unexpected, *i.e.*, E2002(1K) < E1502(1K) < E1002(1K). This observation may be due to the greater stiffness of higher DT containing terpolymers which results to lower water permeability and lower water uptake. However, no increase in water uptake was observed for E1502(1K) and E2002(1K) in the preceding time points because these films started eroding and any increase in the water uptake may be counterbalanced by mass loss. Between E1002(1K) and E1001(1K), there was a significant difference in water uptake as early as 2 weeks indicating that PEG facilitates water uptake. Although E1001(1K) has both DT and PEG in the backbone, its water uptake is similar to E0000.

DTM-based terpolymers (Figure 4.5 B) absorbed about 5% water during the course of the 10 week study. The wet weight of DTM-based films, specifically, M1502(1K) and M2002(1K), could only be measured accurately during the early time points due to film embrittlement. Further during the degradation, these films started losing mass too (Figure 4.4B). The amount of water uptake among the tyrosine-derived polycarbonates was very small when compared with the water uptake, ~80%, by PLGA 85:15 during the same 10-week period. The difference in the water uptake between

PLGA 85:15 and TyrPC is due to the hydrophilic polymer backbone composition of PLGA, namely, lactic acid and glycolic acid, which result in higher hydration of the PLGA 85:15 than the TyrPC terpolymers.
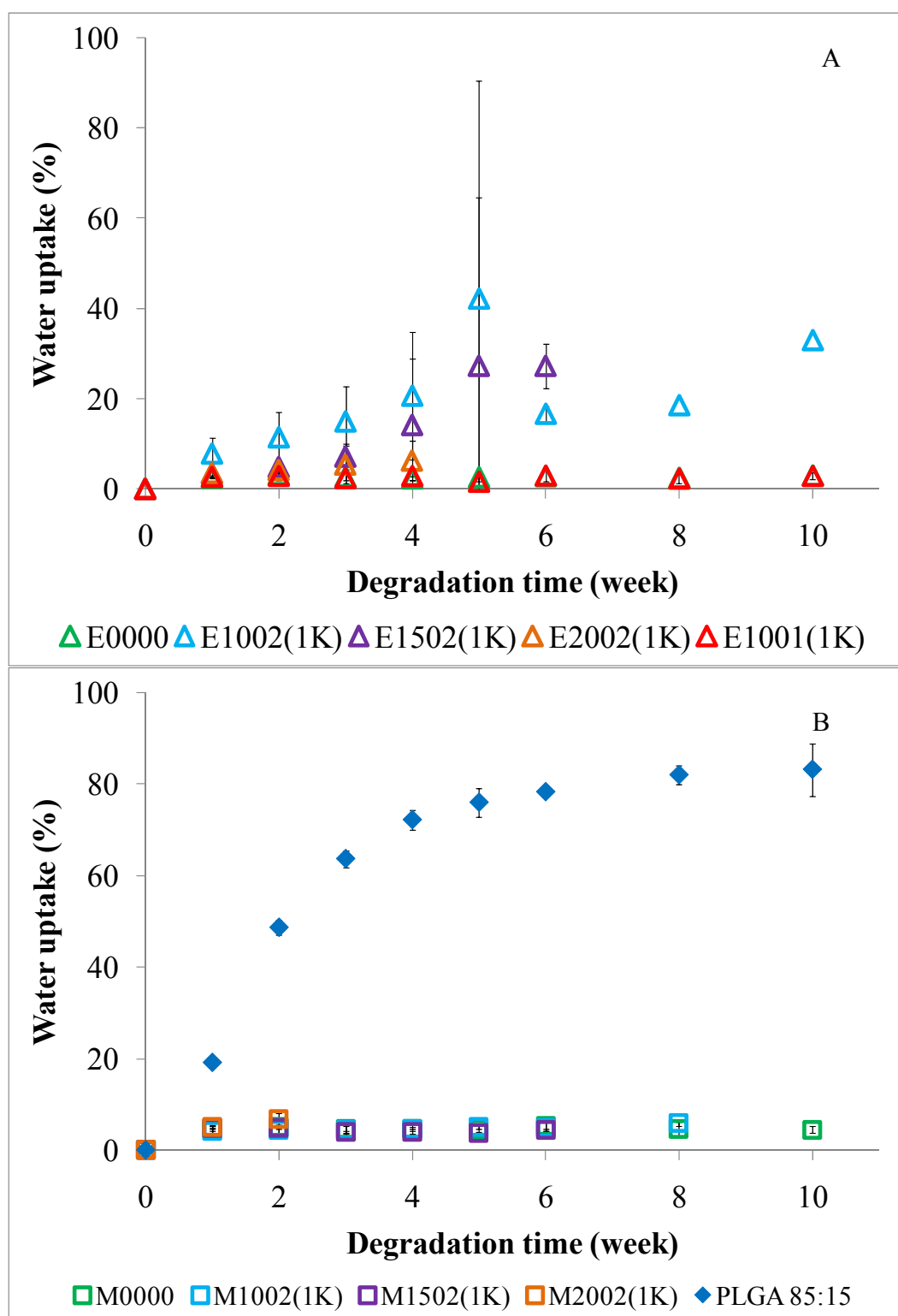
Figure 4.5. % Water uptake of compression-molded films (A) DTE-based, (B) DTM-based polycarbonates and compared with PLGA 85:15 during *in vitro* degradation in PBS at 37 $^{\circ}$C. Data is reported as mean ± standard deviation of n=3.

4.5   **Degradation kinetics and mechanism**

The rate of degradation of TyrPC terpolymers can be evaluated using a kinetic equation suggested by Zhu et al. that is based on the mechanism of carbonate bond hydrolysis. [69] The carbonic acid formed during the hydrolysis of the carbonate bonds is less acidic and unstable further decomposing into carbon dioxide and alcohol. Because of this, autocatalysis by carbonic bonds is not expected and therefore, the hydrolysis of the polycarbonates can be considered to follow a first order kinetics:

$$\ln\left(\frac{DP - 1}{DP}\right) = \ln\left(\frac{DP^\circ - 1}{DP}\circ\right) - k't$$

where DP° and DP represent the degree of polymerization before and after incubation, k' is the rate of degradation and t is time.

The kinetic equation provided good fits, with R^2 (Pearson's coefficient) close to 1, to the data points for all the polymers (Figure 4.6).
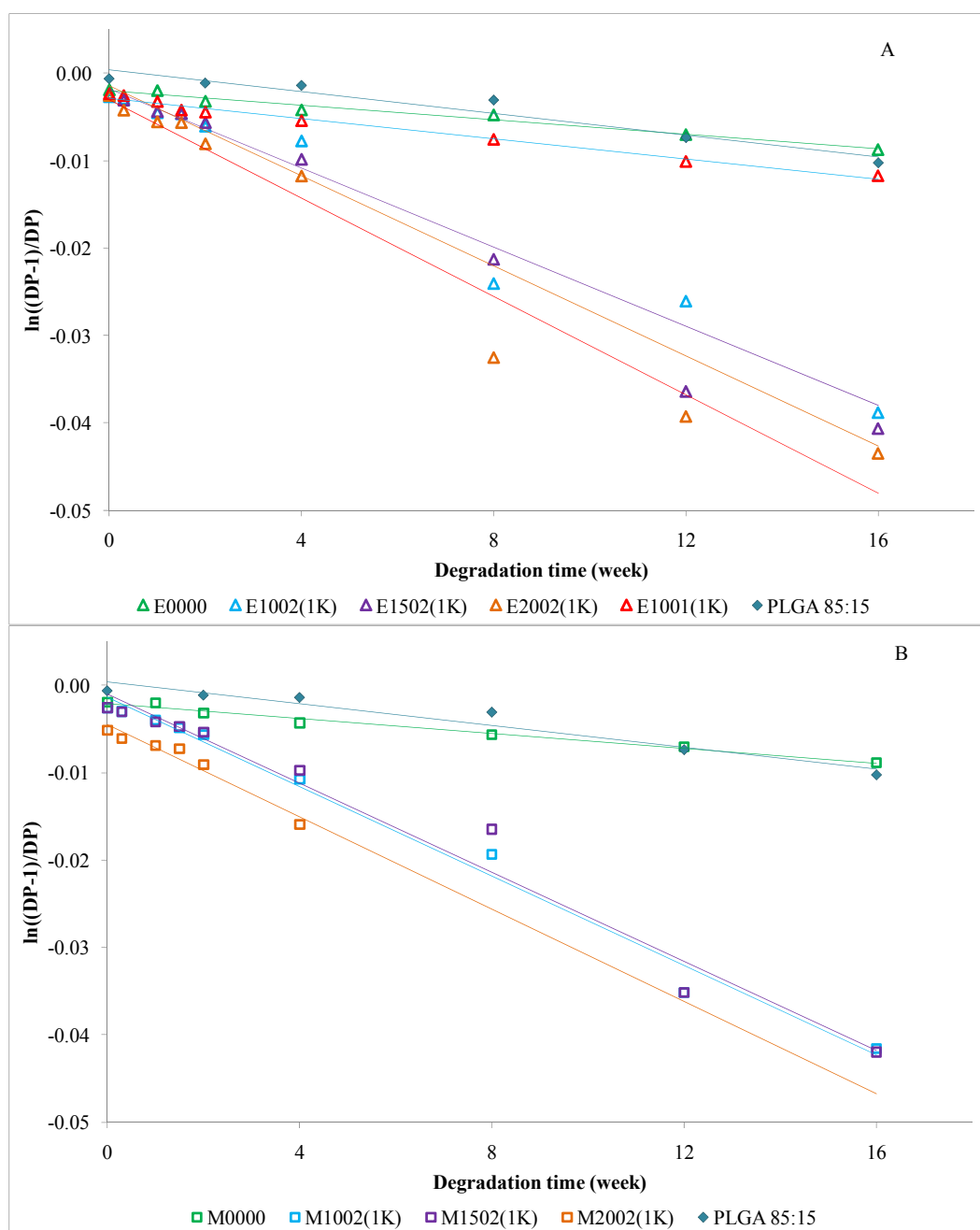
Figure 4.6. Plot of ln((DP-1)/DP) as a function of time of compression-molded films of (A) DTE- based and (B) DTM-based polycarbonates as compared to PLGA 85:15.

The initial rate constants of degradation which were calculated from residual molecular weight of the compression-molded films are summarized in Table 4.2.

Table 4.2. Initial rate constants of TyrPC degradation.

Polymer Notation	Rate constant (week^{-1}) at 37 ^{o}C in PBS
E0000	.0004
E1001(1K)	.0006
E1002(1K)	.0023
E1502(1K)	.0026
E2002(1K)	.0028
M0000	.0004
M1002(1K)	.0026
M1502(1K)	.0025
M2002(1K)	.0026
PLGA 85:15	.0006

For DTE-based polycarbonates, the rate of carbonate bond hydrolysis increased as the mole percentage of DT increased while the PEG concentration was kept constant. The observed trend for this family of TyrPCs is probably due to the increased hydrophilicity of the polymer matrix caused by the increased amount of DT. However, this trend was

not observed for the DTM-based terpolymers, *i.e.*, the rate of degradation was the same for all DTM-based terpolymers.

The significant effect of PEG concentration on the degradation rate was seen between E1001(1K) and E1002(1K) and the rate of degradation of E1001(1K) was similar to the TyrPC homopolymers and PLGA 85:15.

Based on the initial rate constants calculated from these experiments, the time required for TyrPC homopolymers, PLGA 85:15 and E1001(1K) to degrade to dimers in PBS at 37 $^{\circ}$C could be as long as 35 years and in the case of the TyrPC terpolymers, approximately 5 years. However, the degradation rates predicted using the initial rate constants do not agree with results from *in vitro* degradation and *in vivo* studies, where complete erosion of some of the terpolymers was seen as early as 8 weeks, and complete resorption of fast resorbing terpolymers was evident at 12 weeks post-implantation.

Tangpasuthadol, et al, [70, 71] also observed that the predicted rates using the initial rate constants deviated from what was observed experimentally due to the hydrolysis of the ester bond that results in accelerated hydrolysis of the carbonate bond.

Tyrosine-derived polycarbonates have three bonds that are susceptible to hydrolysis, namely, carbonate, ester and amide[70] (Figure 4.7). Generally, this is how poly(DTR carbonate)s degrade: The hydrolysis of the carbonate bond occurs first. While cleavage of the carbonate bonds leads to loss of molecular weight due to formation of low molecular weight oligomers (degradation), no significant mass loss is observed (erosion). For complete erosion to take place, ester hydrolysis must occur that yields DT which is more soluble than DTR (solubility of DT in water is 9.1 mg/mL vs. 1.4 mg/mL for DTE [70]).
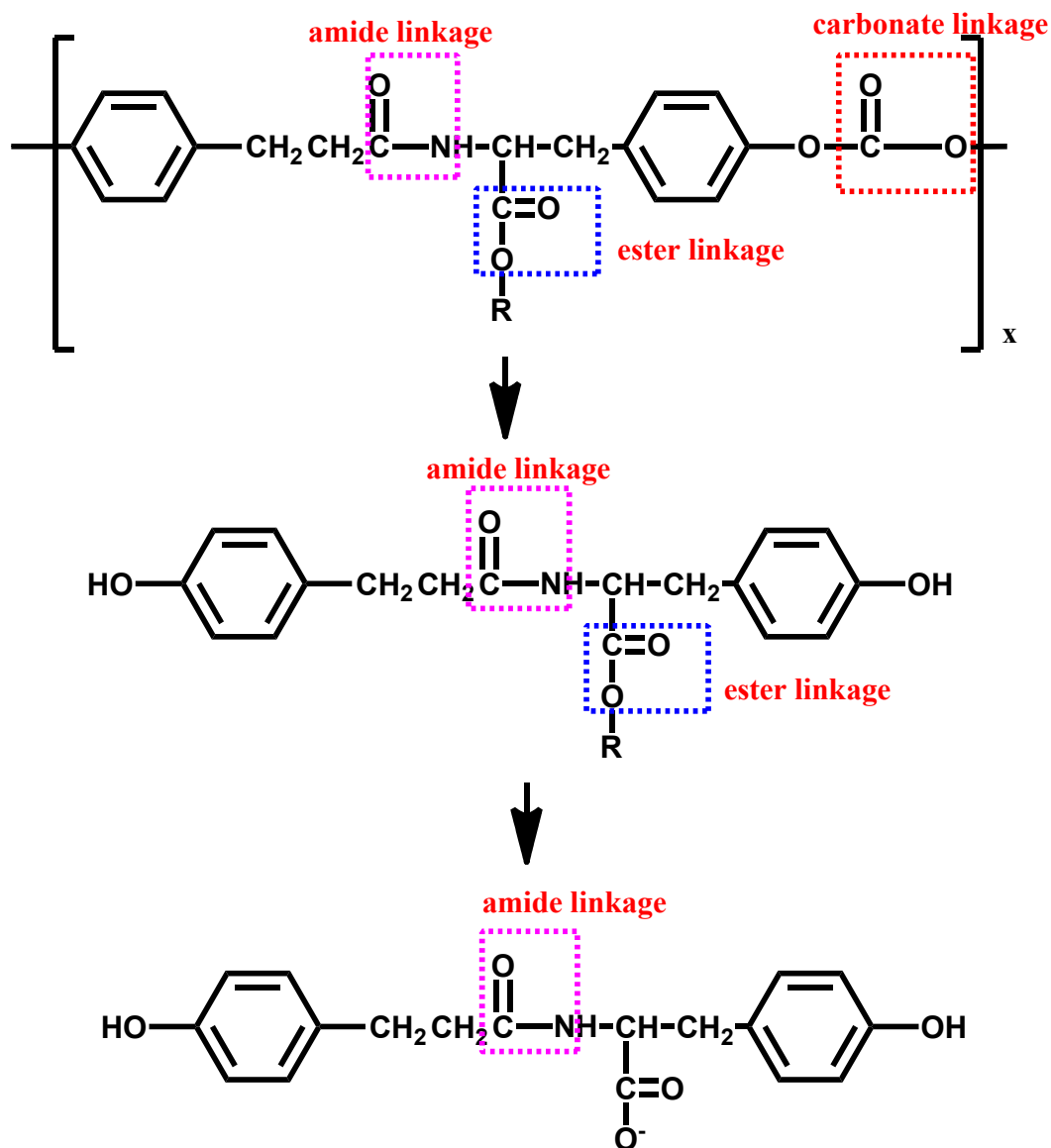
Figure 4.7. Degradation pathway of poly(DTR carbonate)s.

In the case of TyrPC terpolymers, there are also three hydrolysable bonds present in the polymer backbone and pendent chain similar to the homopolymers. However, what's different is the kind of carbonate bonds present in the polymer backbone (Figure 4.8).
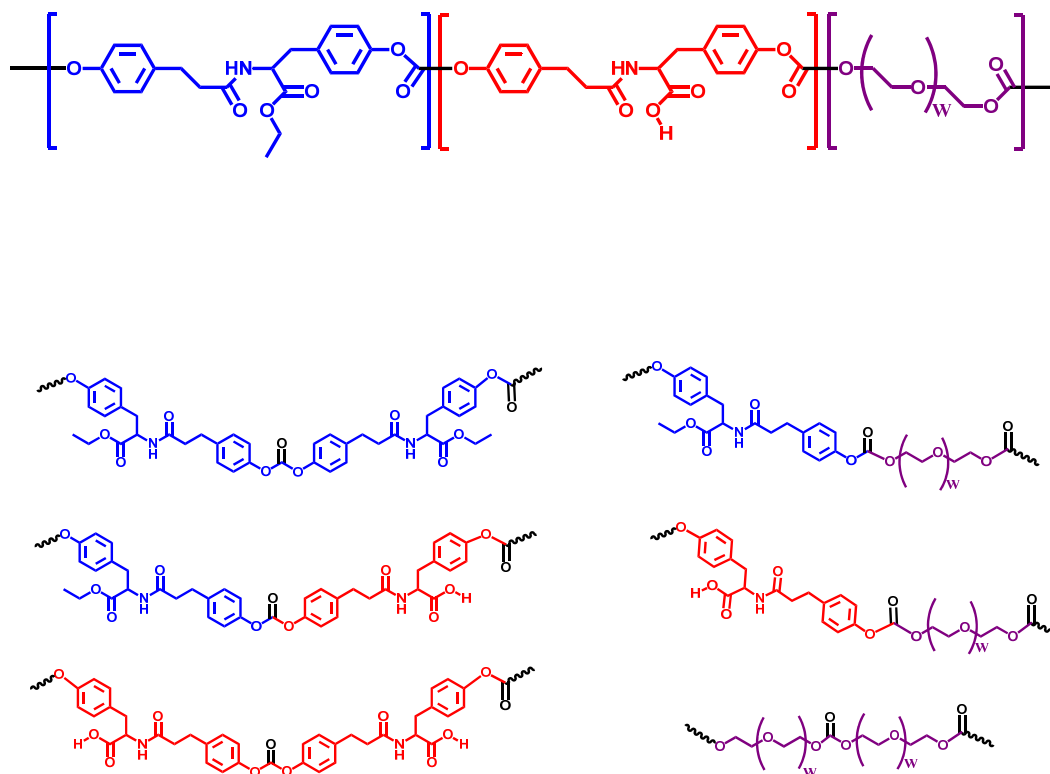
Figure 4.8. There are different types of carbonate bonds present in poly(DTR-*co*-DT-*co*-PEG carbonate), namely, DTR-DTR, DTR-DT, DT-DT, DTR-PEG, DT-PEG and PEG-PEG.

The following carbonate linkages are present in TyrPC terpolymers: DTR-DTR, DTR-DT, DT-DT, DTR-PEG, DT-PEG and PEG-PEG (Figure 4.8). In carbonate linkages associated with DTR and DT, the carbonate bonds can be further classified into head-head (HH), head-tail (HT) or tail-tail (TT) attachments (Figure 4.9). HH attachment of the carbonate bonds will be the least sterically hindered with respect to the proximity of the alky pendent chain in DTR or free carboxylate group in DT to the carbonate bond, followed by HT and then by TT.
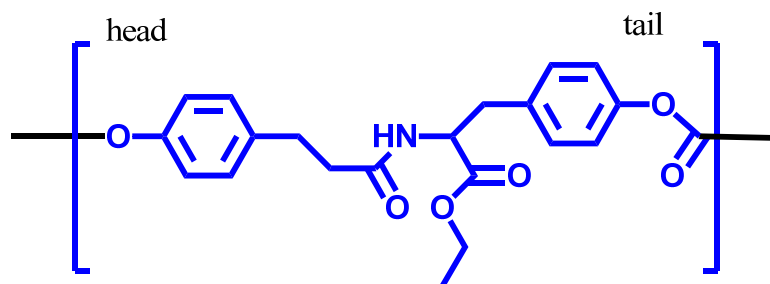
Figure 4.9. In poly(DTE carbonate), the phenolic hydroxyl groups can be classified in terms of its position, *i.e.*, head or tail, as illustrated above.

Considering these variables, there will be 12 types of carbonate linkages present in the TyrPC terpolymer backbone. These different bonds will affect the rate of hydrolysis of the carbonate bonds present in the terpolymer backbone because of differences in the rate of chain scission of the carbonate bond types and by the access of water into the polymer matrix.

In the study performed by Tangpasuthadol, et al., on small model compounds that mimic the repeat unit of poly(DTR carbonate)s, they assumed that the group (ethyl) on the para position of the aromatic ring with respect to the hydroxyl group neither affects the reactivity of the phenolic hydroxyl group nor affects the hydrolysis of the carbonate bond formed.[70] Thus, the carbonate linkage in DTR-DTR will be the same in terms of rate of hydrolysis irrespective of attachment.

Since the first step in the degradation of polymers is water uptake, carbonate bonds attached to either DT or PEG will considerably be more susceptible to hydrolysis because of the hydrophilic nature of these monomers.

In order to study the mechanism by which TyrPC terpolymers degrade and erode, low molecular weight polymers were synthesized and then incubated in PBS at 37 $^{\circ}$C. It

is assumed that the polymer backbone hydrolysis will be faster in low molecular weight polymers than higher molecular weight polymers in order to yield monomers or soluble oligomers that will be detectable by ^{1}HNMR. At each time point, the supernatant from three samples of each polymer composition was combined, then freeze-dried. Dry residue was analyzed by ^{1}HNMR in order to determine the composition of the soluble degradation product. The remaining polymer powder was freeze-dried and then subjected to GPC analysis to evaluate molecular weight loss.

The low molecular weight polymers were synthesized using the established protocol for the synthesis of TyrPCs. However, no excess of triphosgene was used in the synthesis. The structures and compositions of these polymers were confirmed by ^{1}HNMR.

The following polymers were synthesized, specifically, (1) E0000 (M_n 36 kDa) where only one kind of carbonate bond is present (DTR-DTR), (2) E0002(2K) (M_n 28 kDa) where three kinds of carbonate bonds are present (DTR-DTR, DTR-PEG, PEG-PEG), (3) E2500 (M_n 32 kDa ,DTR-DTR, DT-DT, DTR-DT), (4) poly(DT-co-2%PEG$_{2K}$ carbonate) (M_n 36 kDa, DT-DT, DT-PEG, PEG-PEG), (5) poly(DT carbonate) (M_n 22 kDa, DT-DT), (6) poly(PEG$_{2K}$ carbonate) (M_n 17 kDa, PEG-PEG) and (7) E2502(2K) (M_n 27 kDa, all the different types of carbonate bonds are present).

In the cases, of E0000, E0002(2K), and E2500 no detectable peaks were seen on the ^{1}HNMR spectrum that will indicate preferential cleavage of DTE-PEG or DTE-DT carbonate bonds over DTE-DTE. These observations are confirmed by minimal molecular weight loss at the end of 4 weeks for these polymer compositions.

In the case of poly(DT carbonate), a polymer that is composed of 100% DT, molecular weight loss was evident as early as week 1 (36%) with further decrease in the molecular weight at week 4 (77%). Analysis of the supernatant by ^{1}HNMR revealed the presence of peaks corresponding to DT.

In the case of R9802(2K), a polymer that is composed of 98 mol% DT and 2 mol% PEG(2K), loss in the molecular weight was also observed at week 1 (67%) and week 4 (75%). Analysis of the supernatant by ^{1}HNMR revealed the presence of peaks corresponding to oligomers of DT and PEG$_{2K}$ starting at week 1 until week 4.

In the case of poly(PEG$_{2K}$ carbonate) a 50% drop in the molecular weight was observed in week 1. Analysis of the supernatant by ^{1}HNMR revealed the presence of peaks corresponding to PEG$_{2K}$.

In the case of E2502(2K), a polymer that is composed of 73 mol% DTE, 25 mol% DT and 2 mol% PEG$_{2K}$, molecular weight loss was observed on day 1 (33%) and on day 4 (44%). Analysis of the supernatant by ^{1}HNMR on day 1 revealed the presence of peaks corresponding to DTE-DT-PEG$_{2K}$ oligomers while analysis of the remaining polymer indicated the presence of DTE and PEG$_{2K}$. Water uptake experiments showed that E2502(2K) absorbed 81% of water on day 1 and 181% of water on day 2. The presence of a significant amount of water in the polymer may have resulted in the hydrolysis of the DTE in the backbone to DT which in turn resulted in the complete erosion of the polymer by day 7.

These results clearly indicate that co-polymers of DTR with 1 to 2 mol% of PEG, or DTR with 5 to 25 mol% DT degrade and erode the same way as TyrPC homopolymers during the study period. The greater amount of the hydrophobic DTR in the polymer

backbone makes the polymer matrix hydrophobic and less permeable to water. Although the carbonate bonds in the polymer backbone are cleaved, no concomitant mass loss is observed because the degradation products are insoluble in phosphate buffered saline.

In the cases of pure DT or pure PEG in the polymer backbone, molecular weight loss was observed in as early as the first week. This result indicates that in PBS, these carbonate bonds, specifically, DT-DT and PEG-PEG, are highly susceptible to hydrolysis. However, the presence of both DT and PEG as in the case of R9802(2K), accelerated both degradation and erosion of the polymer in PBS at 37 $^{\circ}$C, faster than poly(DT carbonate) or poly(PEG carbonate) which may indicate that DT and PEG have synergistic effect on degradation and erosion.

4.6 Conclusion

The degradation of TyrPC terpolymers is a function of water uptake, hydrophilicity of the polymer, and T*g*. These studies indicate that the simultaneous presence of PEG and DT within the terpolymer structure has a synergistic effect on accelerating both the rate of degradation and the rate of erosion. Replacing DTE with DTM also resulted in the faster degradation and erosion of TyrPC films. The higher solubility of DTM than DTE resulted in a less hydrophobic polymer backbone that caused the accelerated degradation of the DTM-based polycarbonates and subsequent erosion *in vitro*.

The terpolymers degrade by cleavage of carbonate bonds and erode due to the release of soluble degradation products. The carbonate bonds that are cleaved faster are those that are adjacent to hydrophilic groups such as DT and PEG. However, due to the

high degree of hydrophilicity of PEG, the erosion that occurs is through dissolution of PEG or PEG-containing oligomers.

Based on these results, two polymer compositions have potential utility as scaffold materials for bone regeneration, specifically, M1002(1K) and E1001(1K).

CHAPTER 5

**Fabrication of bone tissue engineering scaffolds using tyrosine-derived
polycarbonate terpolymers**

The purpose of this chapter was to optimize an established scaffold fabrication method in order to create tyrosine-derived polycarbonate (TyrPC) scaffolds for bone regeneration. The first study describes how the mechanical properties, degradation behavior and pore architecture of scaffolds are affected by changing two parameters in the fabrication process, namely, the concentration of the polymer concentration and the amount of porogen used. The second study describes how pre-treatment of the scaffold surface with a surfactant, such as poly(vinyl alcohol) (PVA), helped in the efficient incorporation of aqueous solution into TyrPC scaffolds. The third study describes a method for coating the TyrPC scaffold surface with calcium phosphate. The fourth study describes a method for sterilizing TyrPC scaffolds.

5.1   Optimization of a bone regeneration scaffold composition

The scaffolds were designed to mimic the structure of trabecular bone, which has a similar size range of pores and also has high levels of pore interconnectivity. The scaffolds that were fabricated using a combination of solvent casting, particulate leaching and phase separation techniques showed (1) a bimodal pore distribution of macropores in the 200-400 μm and micropores in the < 20 μm size range; (2) high degree of interconnectivity through the macropores and micropores; and (3) oriented alignment of micropores around the macropores. The macropores are created from porogen leaching while the aligned and organized microstructure was formed from the phase separation and crystallization of 1,4:dioxane and water during freezing.[55]

The pore architecture of these scaffolds was assessed using Scanning Electron Microscopy (SEM). In order to determine the reproducibility of the scaffold fabrication process, E0000 was used to fabricate scaffolds that were made at different times. Different E0000 batches show the expected pore architecture as described above (Figure 5.1 a) and the decrease in the molecular weight after fabrication is 20% or less (Figure 5.2). Other polymers were used to fabricate scaffolds using the same fabrication process, these scaffolds exhibit very open, porous architecture with bimodal pore distribution (Figure 5.1). These results indicate this fabrication method may be used to fabricate scaffolds with pore architectures that are open and highly interconnected regardless of polymer composition.
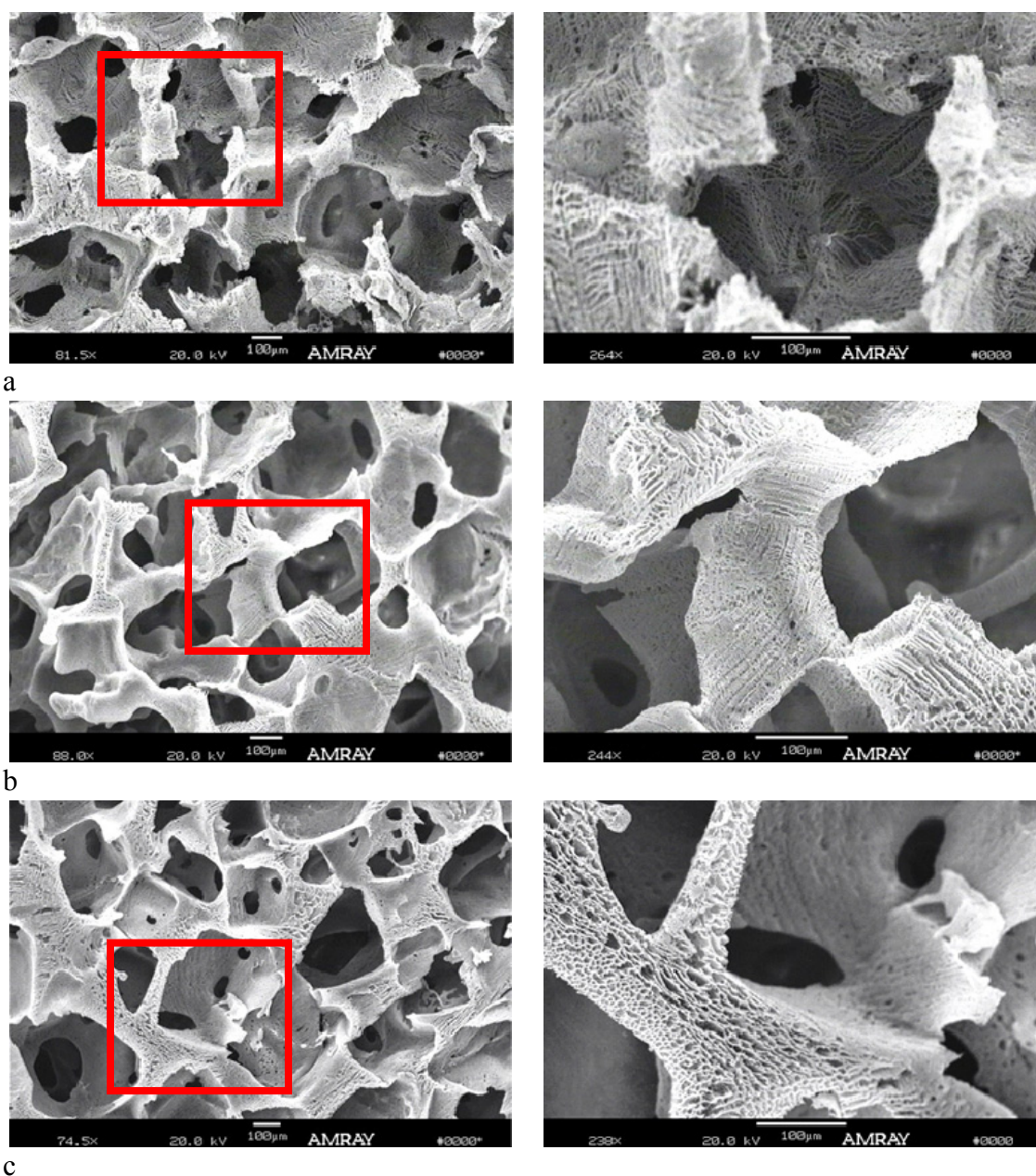
Figure 5.1. SEM images of scaffolds fabricated from a) E0000, b) E2502(2K) and c) M2502(2K) using the combined solvent casting/porogen leaching/phase separation techniques. The first column shows images using ~75x magnification while the second column shows a close-up at 250x magnification. These images of the scaffolds show macropores and micropores, interconnectivity of pores and aligned/oriented structure of the micropores.
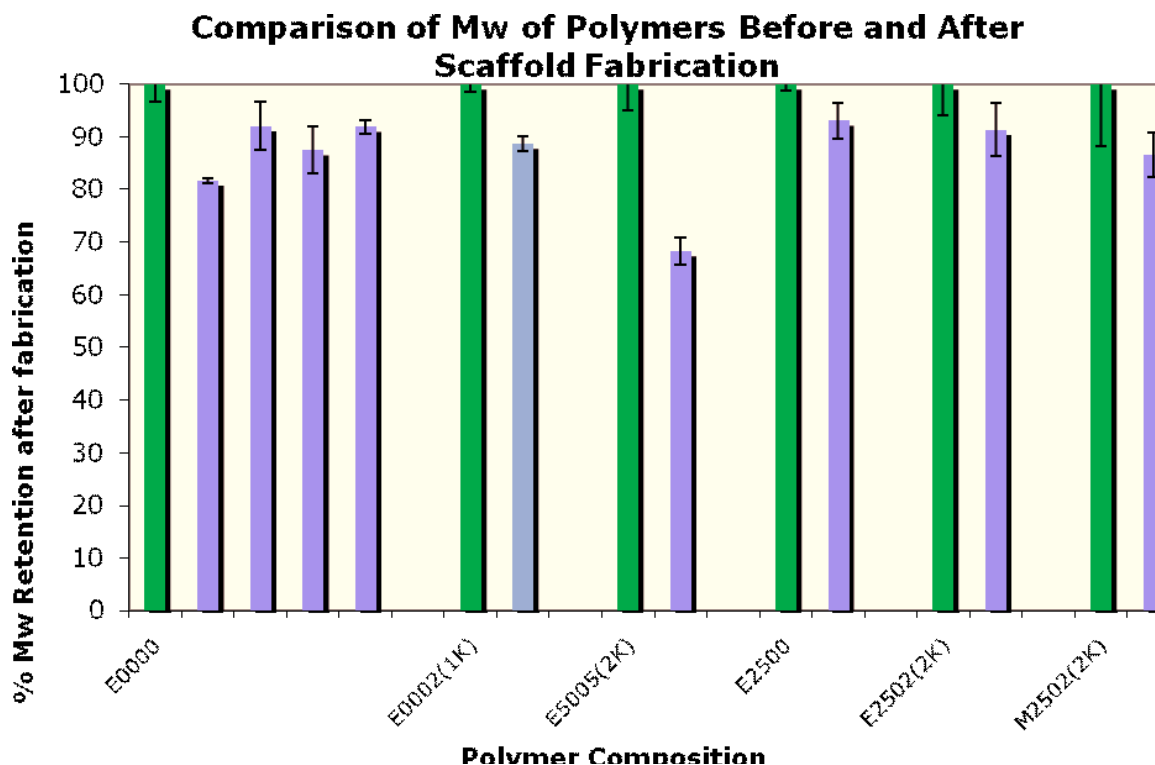
Figure 5.2. Molecular weight of the polymers before (green) and after scaffold fabrication (blue) using GPC (in DMF). Data is reported as mean and error bars represent the standard deviation for n=3 samples. In the case of E0000, several batches of scaffolds were fabricated to verify reproducibility of the fabrication technique across batches.

This graph (Figure 5.2) indicates that fabrication of polymer into a scaffold by using the aforementioned technique has a minimal effect on the molecular weight of the polymer used except for the scaffold fabricated out of E5005(2K) where there was about 30% loss in the molecular weight. This result is expected because of the high DT content of the polymer that resulted in the degradation of the polymer matrix during the leaching process.

Due to the rapid *in vitro* degradation of scaffolds that contained 25mol% DT and 2mol% PEG$_{2K}$, scaffolds were prepared from TyrPC terpolymers that varied in the amount of DT, from 10 to 20 mol%, and PEG$_{1K}$, from 1 to 2 mol%. The scaffolds degraded *in vitro* from several days to several weeks depending on the mole percentages of DT and PEG. Generally, the higher the DT and PEG content, the faster is the degradation of the scaffolds. Based on the results of the *in vitro* degradation (Chapter 4), *in vitro* cell studies at CMU (Chapter 6) and a preliminary *in vivo* study using a critical sized rabbit calvarial model (Chapter 7), E1001(1K) or (poly(DTE-*co*-10%DT-*co*-1%PEG$_{1K}$)), was chosen as the optimal composition of the TyrPC scaffold.

In order to determine the effect of the concentration of the polymer solution and amount of NaCl used in the fabrication of three-dimensional scaffolds, two scaffold formulations were used for this study, specifically, (1) 8% (*w/v*) E1001(1K) solution in 1,4-dioxane:water and 98% (*w/w*) NaCl, and (2) 20% (*w/v*) E1001(1K) solution in 1,4-dioxane:water and 90% (*w/w*) NaCl. The first formulation was chosen because it was the lowest polymer concentration that resulted in scaffolds that retained their shape during salt leaching. The second formulation was chosen as the highest polymer concentration with a consistency that can be efficiently poured onto the salt particles.

The effect of the formulations on the pore architecture as assessed by SEM, on the changes in molecular weight during degradation in PBS at 37 ^{o}C as calculated from gel permeation chromatography (GPC) in relation to polystyrene standards, and on the compressive properties as evaluated using a mechanical tester in compression mode.

The scaffolds that were fabricated using formulation #1 (8% E1001(1K) solution, 98% NaCl) showed a pore architecture that is very open and highly interconnected as

seen from SEM images (Figure 5.3). However, these scaffolds degraded rapidly and lost

mechanical properties in as early as 4 weeks of incubation in PBS at 37 $^{\circ}$C (Figure 5.4).
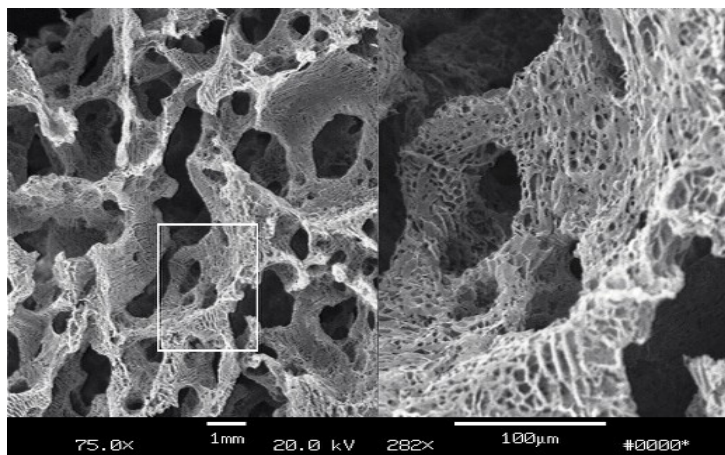
Figure 5.3. A representative SEM image of scaffolds fabricated using formulation #1. Left panel shows bimodal pore distribution and highly interconnected pore architecture. Right panel shows oriented and aligned micropores (< 20 μm) surrounding the macropores (212 – 425 μm).
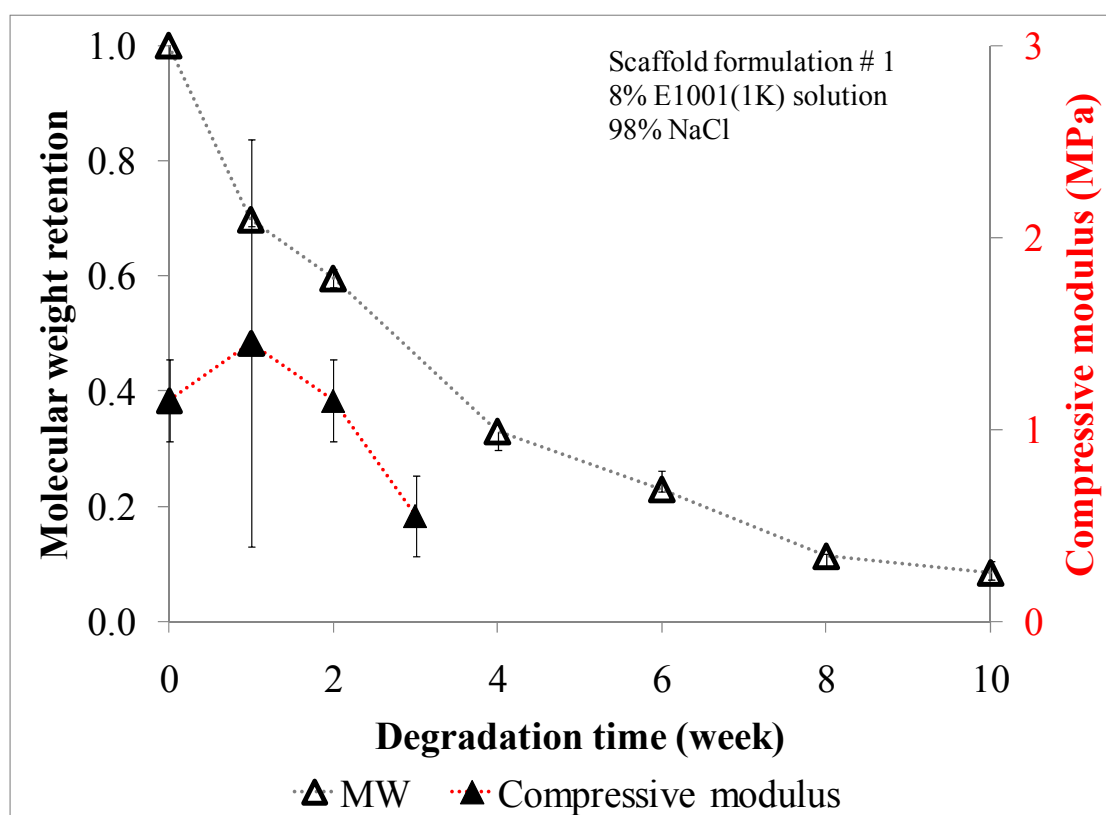
Figure 5.4. Changes in molecular weight and compressive modulus of scaffolds fabricated using 8% E1001(1K) solution and 98% NaCl as a function of degradation time (in PBS at 37 $^{\circ}$C). The compressive properties were evaluated using the wet scaffold and compression testing was performed in PBS at 37 $^{\circ}$C. Data is reported as mean and error bars represent the standard deviation for n=3 samples.

Scaffolds that were fabricated using formulation #2 (20% E1001(1K) solution, 90% NaCl) showed bimodal pore distribution, interconnected pores and a greater wall thickness than scaffolds fabricated using formulation #1 as seen from SEM images (Figure 5.5).
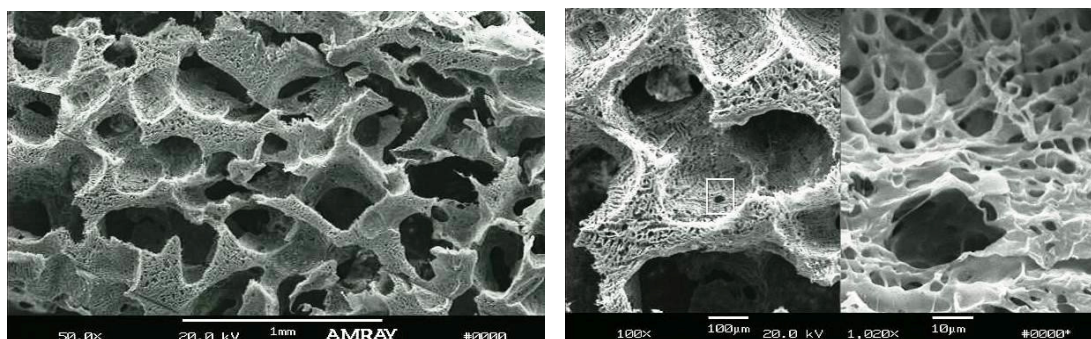
Figure 5.5. Representative SEM images of scaffolds fabricated using formulation #2. Images on left and right (left panel) show the pore distribution and the pore architecture. Right image (right panel) shows oriented micropores (< 20 μm).

The *in vitro* degradation, erosion and mechanical properties of these scaffolds (10 mm in diameter x 5 mm in thickness) were evaluated in PBS at 37°C at various time points (Figure 5.6). Formulation #2 scaffolds displayed a higher dry compressive modulus than formulation #1 (2.7 ± 0.3 MPa vs. 2.3 ± 0.9 MPa).   Qualitatively, formulation #2 felt stronger and tougher when held. Thus, it was easier to handle scaffolds that were fabricated using formulation #2 than scaffolds fabricated using formulation #1.

Even at 8 weeks, the wet compressive modulus of formulation #2 scaffolds was greater than 0.4 MPa, the target mechanical property of calvarial implants[72]. At 8 weeks,

the molecular weight was down to 20%. Although the scaffolds looked intact and did not

show signs of swelling at 8 weeks, they were very fragile and crumbled easily when held.
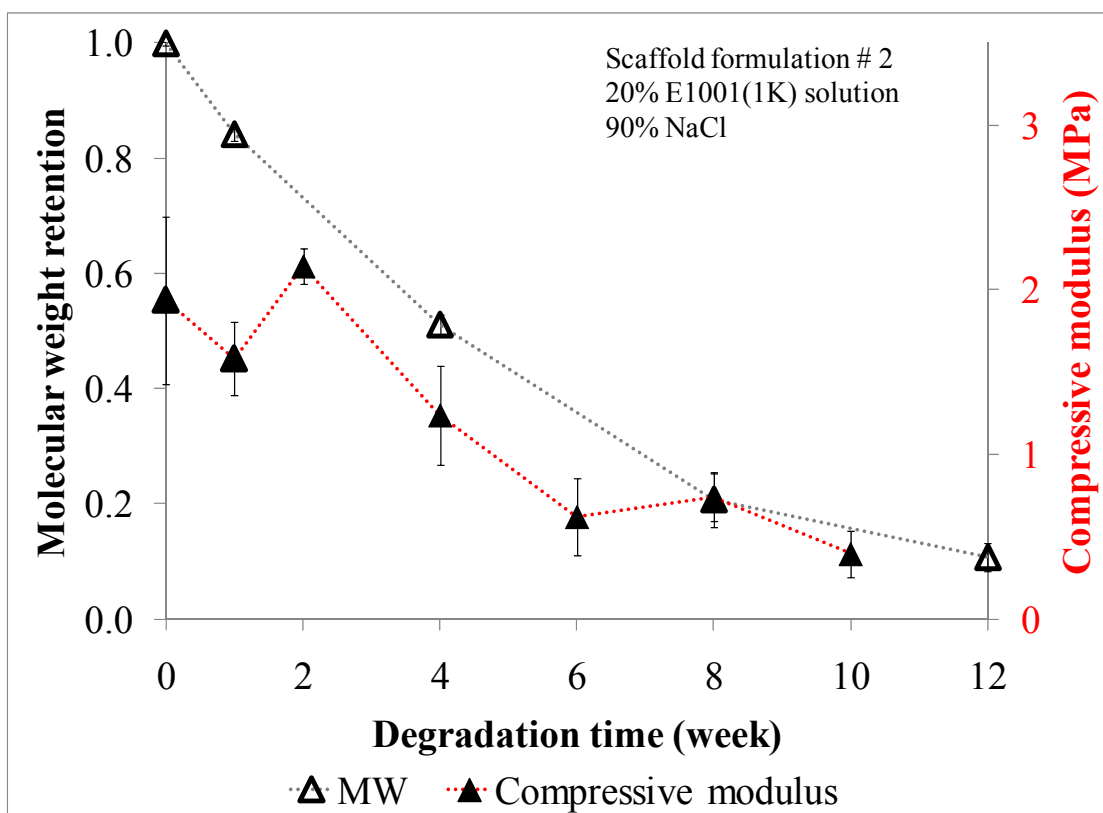
Figure 5.6. Changes in molecular weight and compressive modulus of scaffolds fabricated using 20% E1001(1K) solution and 90% NaCl as a function of degradation time (in PBS at 37 ^{o}C). The compressive properties were evaluated using the wet scaffold and compression testing was performed in PBS at 37 ^{o}C. Data is reported as mean and error bars represent the standard deviation for n=3 samples.

A comparison of the *in vitro* degradation of scaffolds fabricated using two different formulations (Figure 5.7) revealed that the scaffolds fabricated using formulation # 1 degraded faster than formulation #2.
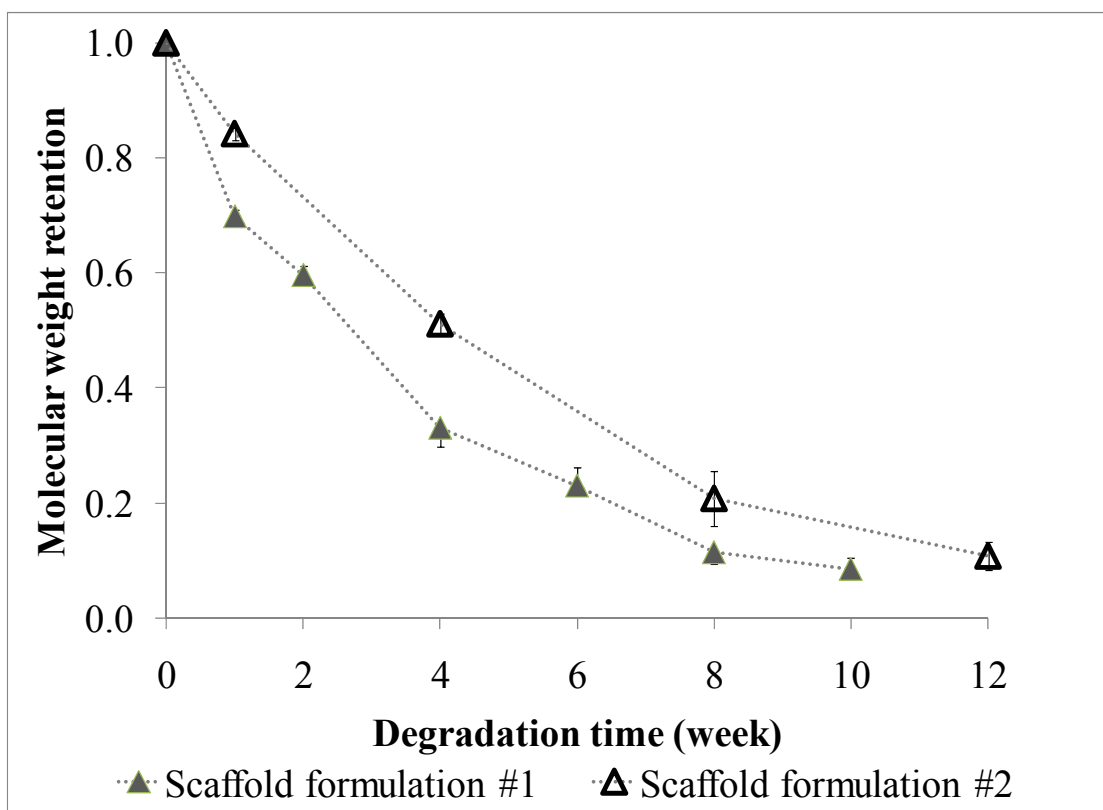
Figure 5.7. A comparison of the *in vitro* degradation of two different scaffold formulations in PBS at 37 ^{o}C.

During the 12-week study period, both scaffold formulations did not show signs of mass loss.

By changing the concentration of the polymer solution and the amount of salt used during fabrication, two scaffolds with different pore architecture, compressive properties and degradation profiles were obtained. Studies have shown the inverse

relationship between porosity and mechanical properties of 3D scaffolds, *i.e.*, the greater the degree of porosity is, the weaker the scaffold and vice versa.[73, 74] However in bone tissue engineering, both porosity and mechanical properties need to be optimized. Porosity plays a role in osteoconduction[42], transport of nutrients, and excretion of waste, while maintaining adequate mechanical strength during the formation of new bone tissue is also important.

5.2   Improved scaffold penetration of growth factor solutions

One approach of bone tissue engineering involves the incorporation of growth factors, which are dissolved in aqueous solutions, into 3D scaffolds. The TyrPC scaffolds produced are intended for combination with buffered saline solutions containing the growth factor of choice at the time of implantation. In order to improve infiltration of these growth factor solutions, TyrPC scaffolds were pre-treated with a surfactant such as poly(vinyl alcohol) (PVA). A solution containing PVA (1% mass by volume) in phosphate buffered saline (PBS) was added onto the surface of an otherwise hydrophobic TyrPC scaffold matrix (Figure 5.8). When the scaffold was pretreated with PVA, a drop of PBS solution was absorbed by the pre-treated scaffold in less than 5 minutes. However, a drop of PBS on an untreated TyrPC, beaded up on the scaffold surface and was not absorbed.   It was determined that the addition PVA resulted to more efficient incorporation of aqueous solution such as PBS and would imply more efficient incorporation of aqueous solutions of growth factors in TyrPC scaffolds.
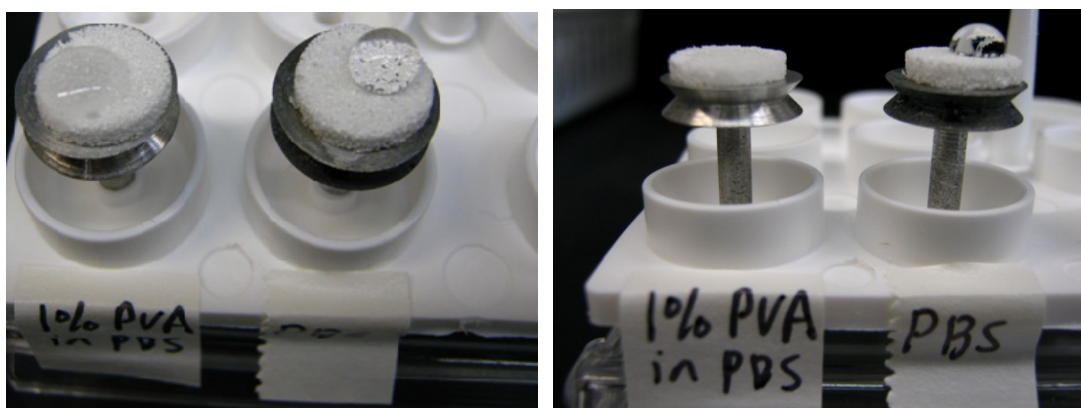
Figure 5.8. TyrPC scaffold pretreated with PVA in PBS (left scaffold) and untreated Tyr-PC scaffold (right scaffold) immediately after addition of PBS (left image) and 5 minutes after (right image).

5.3   Development of bioactive TyrPC scaffolds

In an attempt to make Tyr-PC scaffolds more bioactive, soluble Ca^{+2} ions in the form of $CaCl_2$ were incorporated into Tyr-PC scaffolds (Figure 5.9). It was hypothesized that adding calcium would enable better host-scaffold integration, and that the presence of calcium in the defect site would promote the deposition of hydroxyapatite or calcium phosphate *in vivo* that might in turn enhance bone formation.[7, 8, 28, 75-77]
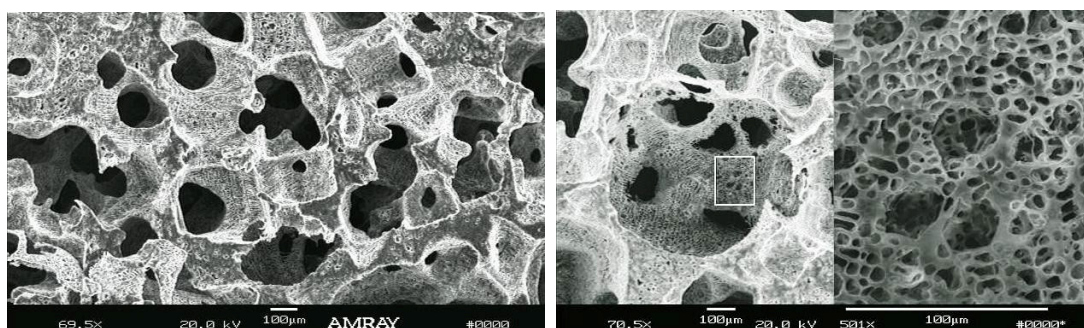
Figure 5.9. Representative SEM images of TyrPC + Ca^{+2} scaffolds. Images on left and right (left panel) show the pore distribution and the pore architecture. Right image (right panel) shows micropores.

However, some difficulties were encountered with TyrPC + Ca^{+2} which resulted to a number of rabbit deaths during the first *in vivo* study using a critical-sized defect (15 mm diameter defect) in the rabbit calvaria that was carried out at CMU (Carnegie Mellon University). The deaths may have been caused by a significant increase in the temperature and decrease in the pH as calcium chloride dissolved in the the implant site.

A study was carried out to check for changes in temperature and in the pH of 1 mL of PBS after immersion of TyrPC + Ca^{+2}. It was found that the dissolution of calcium salt resulted to a gradual increase in the temperature of PBS over time and a decrease in the pH. The amount of calcium chloride in the scaffold proportionally affected temperature and pH, *i.e.*, the higher is the amount of calcium chloride, the

greater is the change in temperature and pH. It was concluded that due to the minimal extracellular fluid available in the CMF environment, and the proximity to the brain, even small amounts of soluble calcium chloride were unfavorable.

To eliminate the temperature and pH changes, other sources of calcium were also considered, specifically, (1) calcium chloride dihydrate, (2) calcium chloride hexahydrate, (3) calcium gluconate monohydrate (used for the treatment of hypocalcemia), (4) calcium citrate tetrahydrate (commonly used food additive), and (5) amorphous calcium phosphate. Dissolution of choice (1) in water is less exothermic than anhydrous $CaCl_2$ while choice (2) dissolves in water endothermically. These two salts were considered in order to decrease the change in temperature during dissolution. However, freeze-drying of scaffolds coated with these salts resulted in the dehydration of the calcium salt. This would mean that the calcium salt in the scaffold would then dissolve exothermically in an aqueous environment, similar to anhydrous calcium chloride. Choices (3) and (4) have low solubility in water and low calcium content per mole of the salt would require the use of more of these salts to achieve 10% Ca by weight per scaffold. In the case of choice (5), which has been used as a component of composite devices used in tissue engineering, it was water insoluble and obtaining a scaffold that has a uniform coating of this salt would be a problem.

Another alternative to minimize the extent of change in temperature and pH is the precipitation of calcium into calcium phosphate. After calcium ions were incorporated into the scaffolds and following scaffold drying, a solution of dibasic potassium phosphate (K_2HPO_4 x 2 H_2O) was added to each scaffold to completely convert the calcium in the scaffold to calcium phosphate (TyrPC + CP scaffolds, Figure 5.8 and 5.9).

By doing this, minimal changes in temperature (< 1 ^{o}C) and pH (< 1) of PBS were observed *in vitro*.

SEM images of TyrPC scaffolds coated with CP are shown below (Figures 5.10 and 5.11).
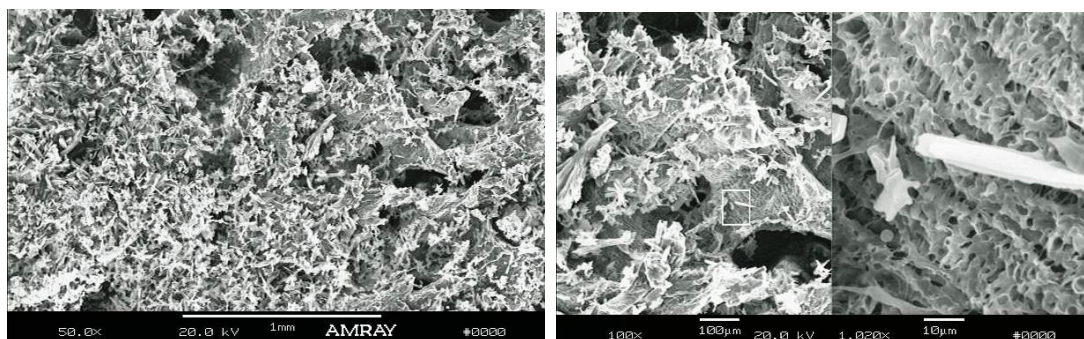
Figure 5.10. Representative SEM images of TyrPC + CP scaffolds. The macropores in TyrPC scaffolds were swamped by calcium phosphate (left and right (left panel)). CP crystals were much bigger than the micropores (right (right panel)).
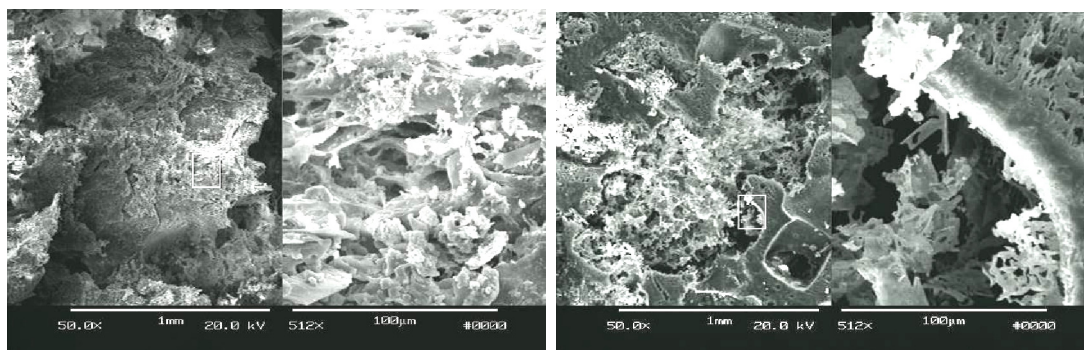
Figure 5.11. SEM micropgraphs of TyrPC + CP scaffolds showing distribution of coating on the periphery (left panel, left (50x) and right (500x) images) and cross section (right panel, left (50x) and right (500x) images). The periphery of the scaffold (left panel) showed a dense layer of CP coating. Scaffold cross section of the central portion (right panel) revealed incorporation of the CP coating well into the center of the scaffold. The coating inside the scaffold was more dispersed.

A comparison of the *in vitro* degradation (Figure 5.12 A) and changes in compressive modulus (Figure 5.12B) of TyrPC and TyrPC+CP scaffolds showed that coating the TyrPC with calcium phosphate did not affect the degradation while there was a minimal increase in the compressive modulus of TyrPC+CP as compared to TyrPC.
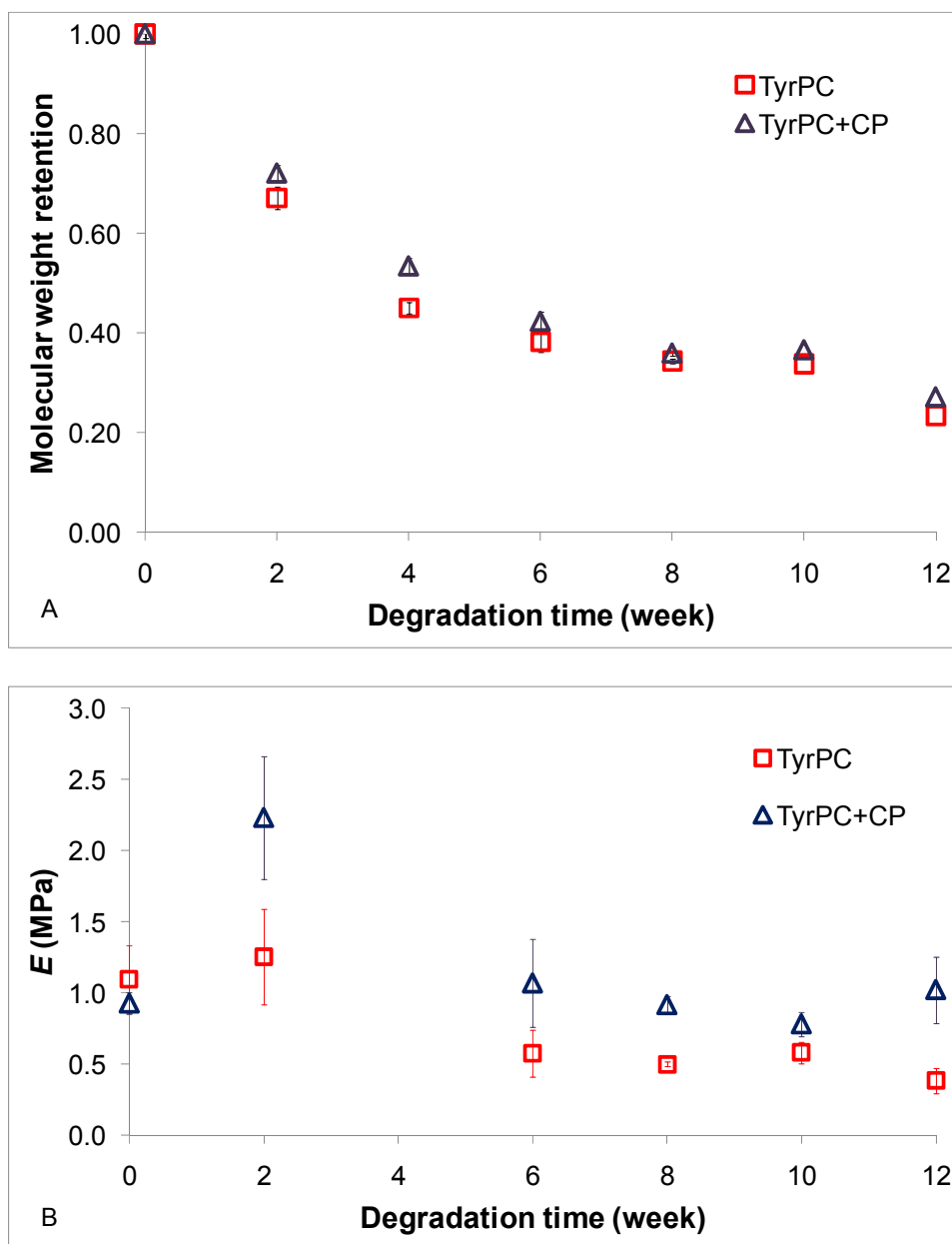
Figure5.12. (A) Molecular weight retention and (B) changes in the compressive modulus of TyrPC and TyrPC+CP (15 mm in diameter x 2.5 mm in thickness) scaffolds as a function of degradation time in PBS at 37 $^{\circ}$C.

The molecular weights (M_n) calculated by GPC relative to polystyrene standards (in DMF with 0.1% TFA), polydispersity index (PDI), composition by ^{1}H NMR and calcium content (% by weight of scaffold) of TyrPC scaffolds are given in Table 5.1.

Table 5.1. Tyr-PC scaffold characterization.

Scaffold composition	M_n, kDa / PDI	Tg (^{0}C)	Composition from NMR			Calcium content (% by weight of scaffold)
			mol% DTR	*mol% DT*	*mol% PEG$_{1K}$*	
Formulation #1	**187** / 1.3	95	89	10	1	n/a
Formulation #2	**175** / 1.4	95	89	10	1	n/a
TyrPC+Ca^{+2}	**165** / 1.5	99	90	9	1	8.6
TyrPC+CP	**163** / 1.4	96	93	6	1	7 – 12 %

5.4   Sterilization

Samples that will interact with cells or biological tissues need to be sterilized first. In the case of TyrPCs, Hooper, et al., has demonstrated that ethylene oxide is a suitable method for the sterilization of TyrPC homopolymers including poly(DTE carbonate), poly(DTB carbonate), poly(DTH carbonate) and poly(DTO carbonate). These polymers retained 99% of their initial molecular weight following EtO sterilization[47]. In addition, Yu and Kohn reported that copolymers of DTE and PEG could be sterilized using EO with at least 88% of their initial molecular weight being retained post-sterilization[39]. Thus, EtO sterilization was used with TyrPC terpolymers.

Following ethylene oxide (EtO) exposure of the TyrPC terpolymer scaffolds, no change in color and physical appearance (thickness and diameter) were observed. There were also no significant changes in the molecular weights and polydispersity of the scaffolds as measured by GPC. TyrPC and TyrPC+CP scaffolds retained approximately 85% of their initial molecular weight (from MW of polymer) after EtO sterilization. Absence of methylene proton peak at $\delta 2.54$ ppm from ^{1}H NMR indicated that residual EtO was completely removed by degassing in vacuum at room temperature for 14 days.

5.5 **Conclusion**

The chemical composition and formulation of a TyrPC terpolymer scaffold for bone regeneration has been optimized. *In vitro* characterization showed that at 8 weeks of incubation in PBS at 37° C, the compression modulus of scaffolds that were fabricated using formulation # 2 was greater than 0.4 MPa, the minimum mechanical property target for calvarial implants. In order to make the scaffolds less hydrophobic prior to implantation they were pretreated with 1% PVA solution, and this addition resulted in a more efficient incorporation of aqueous solutions. TyrPC scaffolds coated with calcium phosphate (TyrPC + CP) have been prepared and may show improved *in vivo* biological performance in the rabbit calvarial critical-sized defect model (Chapter 7). Finally, ethylene oxide is a suitable method for the sterilization of TyrPC terpolymer scaffolds, with or without calcium phosphate coating.

CHAPTER 6

Osteogenic differentiation of pre-osteoblasts on biomimetic tyrosine-derived polycarbonate scaffolds

Preface

"Reprinted with permission from J. Kim, M. H. R. Magno, P. Alvarez, A. Darr, J. Kohn and J. O. Hollinger. Osteogenic differentiation of pre-osteoblasts on biomimetic tyrosine-derived polycarbonate scaffolds. *Biomacromolecules*, 2011, **12** (10), 3520 – 3527. Copyright 2011 American Chemical Society"

This chapter summarizes the results of the *in vitro* cell studies that were done at Carnegie Mellon University to evaluate the *in vitro* cytotoxicity and osteogenic potential of the tyrosine-derived polycarbonate (TyrPC) terpolymer scaffolds using MC3T3-E1.4 pre-osteoblasts and hMSCs. In the first set of experiments, *in vitro* biocompatibility of fast resorbing TyrPC was evaluated. The second set of experiments was designed to determine if TyrPC scaffolds supported osteogenesis of MC3T3-E1.4 cells cultured on the scaffolds. The third set was to determine the bioactivity of rhBMP-2 released from TyrPC scaffolds compared to the exogenous rhBMP-2. DTE-based scaffold, specifically, E1001(1K), was down-selected based on the data from the 2nd and 3rd sets of experiments. The fourth set was to determine if osteogenesis of MC3T3-E1 cells were further enhanced when the cells were cultured on DTE-based scaffolds containing

rhBMP-2. The last study determined the *in vitro* biocompatibility of DTE-based TyrPC scaffolds including cytotoxicity, proliferation and osteogenic differentiation of hMSCs.

Please refer to Appendix 2 for the complete manuscript that has been published in Biomacromolecules.

Investigation of the potential of materials to support the osteogenic process *in vitro* provides a valuable guide for the fine tuning of scaffold matrices for tissue engineering. Two kinds of cells were used for this study, MC3T3-E1.4 pre-osteoblasts, a cell line that is used in bone cell biology, and human mesenchymal stem cells, a clinically relevant cell line.[78] MC3T3-E1.4 cells were derived from murine calvaria and have a predisposition to become osteoblasts. Human mesenchymal stems cells (hMSCs), on the other hand, were obtained from human bone marrow and have the ability to differentiate into chondrogenic, adipogenic, myogenic and osteogenic lineages.

Prior to *in vivo* applications, *in vitro* data provide a valuable guide for the fine-tuning of potential tissue mimetics for use in tissue engineering. Valuable data was obtained in this study with the goal of progressing to *in vivo* work.

For the initial *in vitro* cell culture study, the test polymers were intentionally designed to be fast degrading to ensure that cells are exposed to high concentrations of degradation products, increasing the sensitivity of the cytotoxicity assays. Exposure of the cells to only the degradation products such as monomers or oligomers was achieved by using transwell inserts (membrane pore size: 3.0 μm) to evaluate the *in vitro* cytotoxicity of the scaffolds as a function of incubation time while polymers stay in the transwell without directly having contact with cells.[79, 80] Despite their exposure to high concentration of polymer degradation products, MC3T3-E1.4 pre-osteoblasts remained

viable when compared to polymer-free tissue culture medium over 14 days (Figures 6.1

6.2 and 6.3).
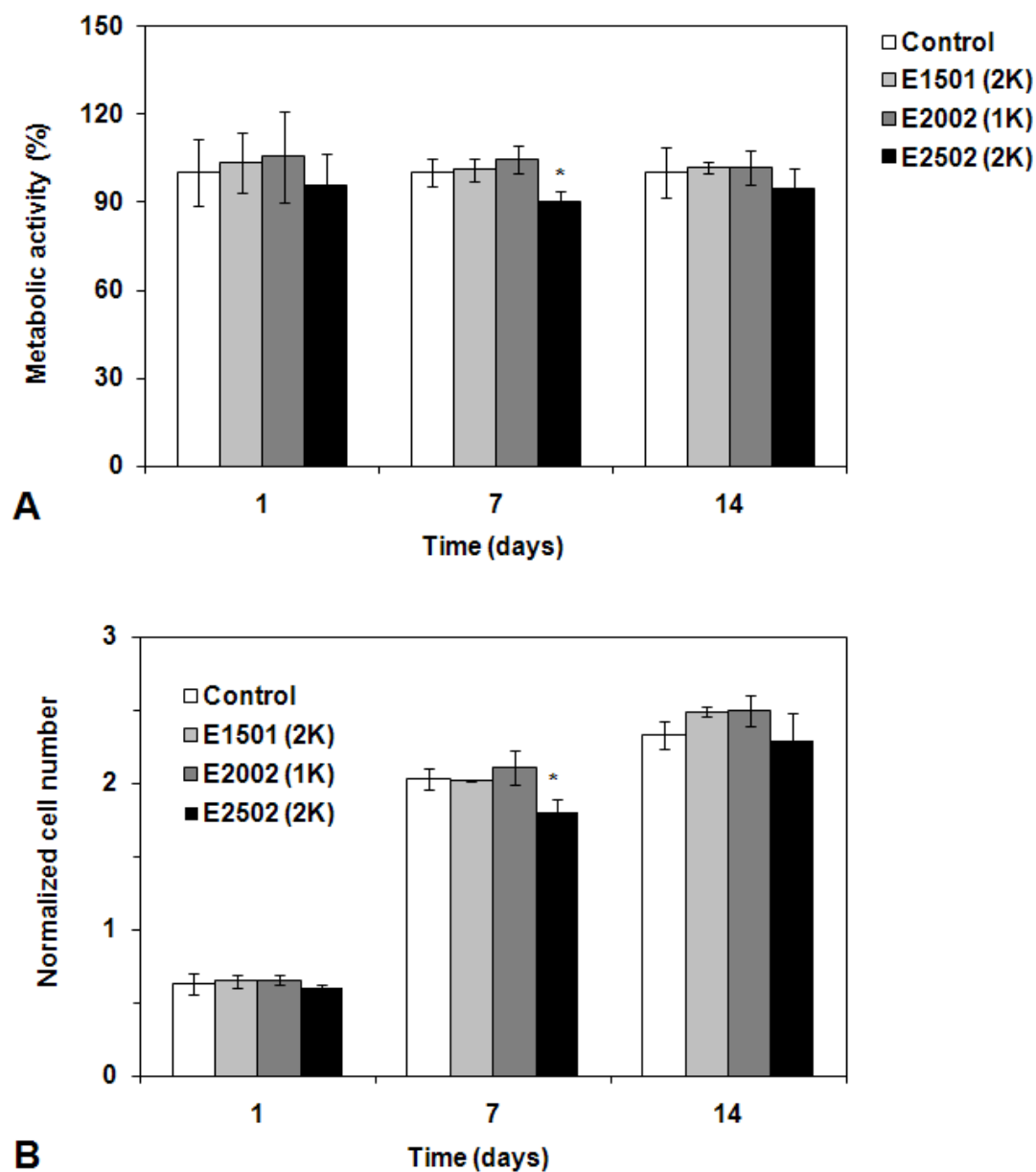
Figure 6.1. (A) The percent metabolic activity and (B) the normalized cell number of MC3T3-E1.4 cells cultured in the presence of various TyrPC scaffolds up to 14 days of incubation at 37 °C. Error bars represent means ± standard deviation for n=3 samples. * indicates significant ($p < 0.05$) difference from the control which is MC3T3-E1.4 cells cultured on TCPS without the scaffolds.
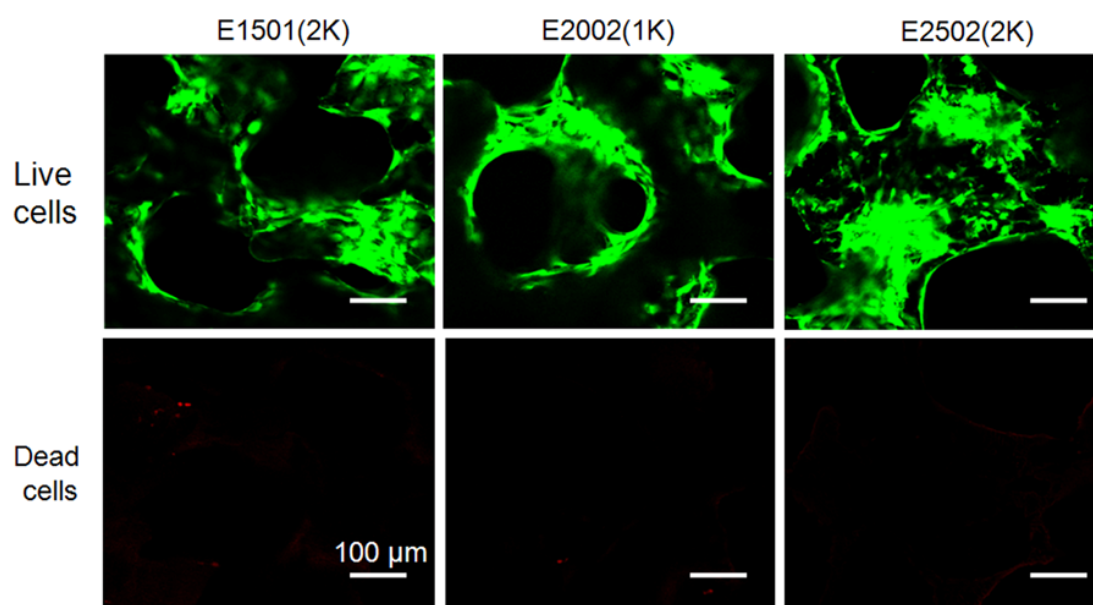
Figure 6.2 Confocal microscopic images of MC3T3-E1.4 cells on different TyrPC scaffolds after 1 day of culture. Live cells fluoresce green and dead cells red.
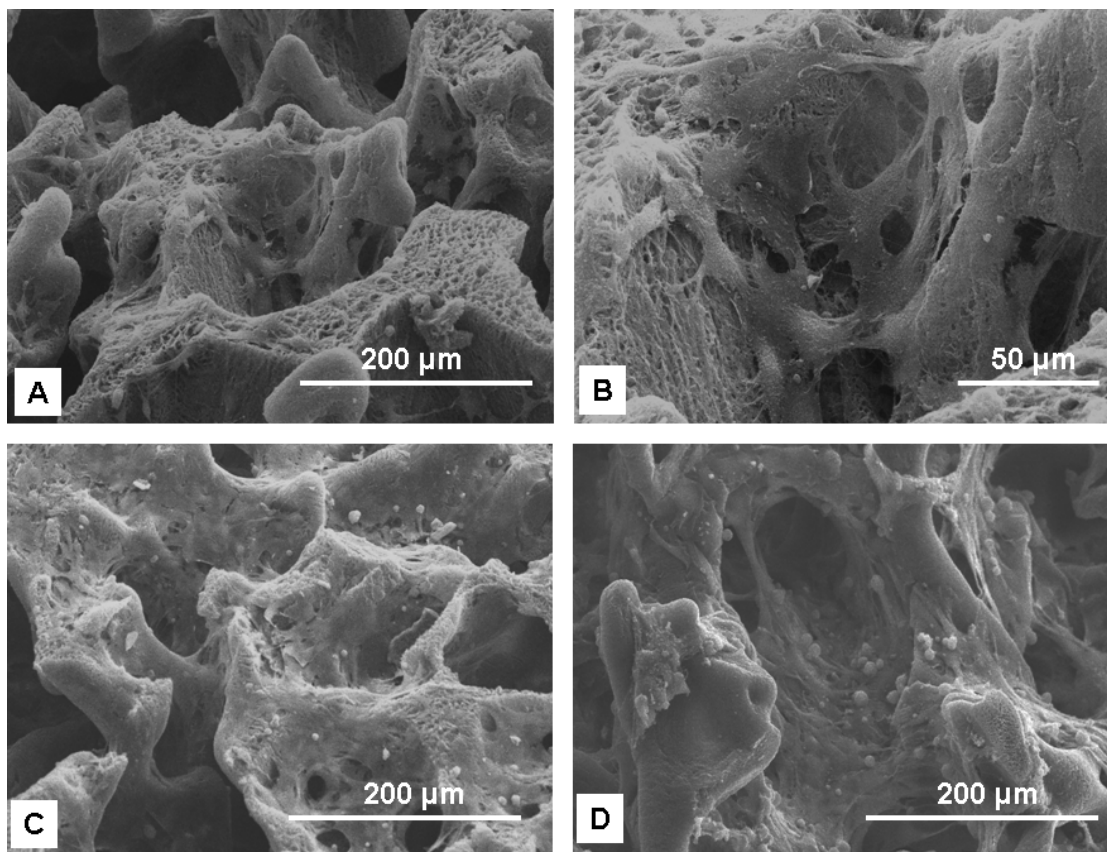
Figure 6.3. SEM images of MC3T3-E1.4 cells after 24 hours of culture on different TyrPC scaffolds. (A) E1501(2K) with low and (B) high magnification, respectively, (C) E2002(1K), and (D) E2502(2K) scaffolds.

In addition, there was no significant pH change in the media throughout the test period between the test groups and the polymer-free medium. Robust cell attachment was also observed on all TyrPC scaffolds as early as 24 hours following cell seeding. Cell attachment behavior was not studied beyond 24 hours on E2502(2K) due to significant disintegration of the scaffold.

The purpose of the second *in vitro* study was to determine the osteogenic properties of DTE and DTM-based TyrPC scaffolds as a substratum for MC3T3-E1 cells, as well as a carrier for rhBMP-2 and the promotion of osteogenic differentiation. TyrPC scaffolds containing an ethyl pendent chain promoted greater expression of ALP and OCN as well as mineralization when compared to the scaffolds with a methyl ester pendent chain. Initially, we hypothesized that the DTM-based TyrPCs will be more conducive to osteogenesis than DTE-based scaffolds due to the faster hydrolysis of DTM to DT. A previous study by James et al.,[37] showed that better bone apposition was observed for TyrPC implants that had shorter alkyl pendent chains than the ones with longer pendent chain. They suggested that this may be due to the faster hydrolysis of the shorter alkyl pendent chain into DT which has a free carboxylate group and which may provide calcium chelation sites on the polymer surface that resulted in better bone bonding *in vivo*. However, the *in vitro* cell studies data suggested otherwise. The observations may be due to the difference in the hydrophobicity and/or surface properties of the polymers[34], formation of reactive oxygen species by PEG[81], or the possible effect of ethanol or methanol, which are products from the hydrolysis of the alky pendent chain of DTR, and not simply on whether DTE or DTM was used.

One possible explanation for such an observation is that the more hydrophobic (*i.e.*, DTE) terpolymer backbone may provide a more permissive substrate for cell adhesion proteins such as fibronectin and vitronectin, as compared to the more hydrophilic DTM. This response is encouraging in light of the fact that fibronectin is reported to induce cell attachment.[82] Extracellular matrix (ECM) proteins, especially fibronectin and vitronectin, mediate osteoblastic-ECM interactions via integrin receptors

$\alpha_5\beta_1$ or $\alpha_v\beta_3$.[83, 84] Hence, it is reasonable to deduce that the outcome we measured may be a consequence of the hydrophobic segments of the polymer backbone initially recruiting cell adhesion proteins from the serum. The proteins may preferentially attach to the more hydrophobic TyrPC scaffolds (*i.e.*, DTE vs. DTM) and induce cell attachment to the scaffolds. Purportedly, the cells attached on the scaffolds may secrete significantly more ECM proteins, including osteogenic proteins, which initiate a differentiation cascade for the pre-osteoblasts.[85]

Although 3D scaffolds are more relevant for the simulation of *in vivo* environments, previous studies reported cellular responses have not been favorable on 3D porous substrates such as poly(lactide-*co*-glycolide) (PLGA), which is probably due to the burst release of acidic degradation products.[86] Absence of or limited pore interconnectivity in 3D scaffolds may significantly hinder or delay osteogenic differentiation and mineralization, likely due to the mass transit limitation of nutrients and oxygen throughout the scaffolds. In this study, however, MC3T3-E1.4 cells cultured on 3D TyrPC scaffolds supported cell ingrowth and subsequent osteogenic differentiation surpassing the 2D counterpart (compression-molded film) and tissue culture polystyrene (TCPS). We deduce this outcome is likely a result of the pore architecture of TyrPC scaffolds that is similar to bone. The TyrPC scaffolds displayed a bimodal pore distribution of macropores (200 – 400 μm) and micropores (< 20 μm) that were highly interconnected and open.[44] Consequently, this 'bone-mimetic' pore architecture may provide topographical and physical cues as well as proper mass transfer of nutrients and oxygen, which are crucial for osteoblast lineage progression. The 3D topographical and

physical cues cannot be replicated on 2D surfaces and thus, this distinction may offer a compelling feature for the superiority of outcome with the 3D TyrPC scaffolds.

In addition, when TyrPC scaffolds were supplemented with rhBMP-2, ALP activity and calcium deposition increased as compared to TyrPC alone without rhBMP-2. This is not an unexpected outcome. However, it is highly noteworthy to underscore that controlled release of a biological molecule from a delivery scaffold does not ensure biological activity, *i.e.*, change in the conformation of the biological molecule may diminish receptor-ligand binding, subsequent internalization, and upregulation of cellular activity. In fact, rhBMP-2 released from TyrPC scaffold was equivalent in biological activity to the rhBMP-2 administered exogenously.

The *in vitro* cytotoxicity of TyrPC scaffolds was similar to PLGA scaffolds when hMSCs were cultured on these scaffolds. PLGA is a polymer used in FDA-approved devices for certain applications and is considered a 'safe' biomaterial. Although both scaffolds were non-cytotoxic, TyrPC scaffolds promoted osteogenic differentiation of hMSCs by producing significantly greater ALP activity on days 7 and 14 than PLGA and TCPS.

The results of these studies showed that TyrPC scaffolds supported osteogenic differentiation of two cell types, MC3T3-E1.4 and hMSCs. Moreover, based on the favorable *in vitro* outcome, it is anticipated that there will be a positive outcome for the utility of TyrPC scaffolds for bone regeneration *in vivo*.

CHAPTER 7

Bone regeneration in a rabbit critical-sized calvarial model using tyrosine-derived polycarbonate scaffolds

Preface

The second *in vivo* study described below and the histology/histomorphometric evaluation of the explants were done at CMU. The micro-CT evaluation of the explants was performed at the Cleveland Clinic by Dr. Amit Vasanji.

Portions of this chapter have been reproduced from:

(1) **M. H. R. Magno**, J. Kim, A. Srinivasan, S. McBride, D. Bolikal, A. Darr, J. O. Hollinger and J. Kohn, Synthesis, degradation and biocompatibility of tyrosine-derived polycarbonate scaffolds. *Journal of Materials Chemistry*, 2010, **20**, 8885-8893 – Reproduced by permission of the Royal Society of Chemistry

(2) J. Kim[1], **M. H. R. Magno**[2], H. Waters[3], B. A. Doll[2], S. McBride[1], S. McBride[1], P. Alvarez[1], A. Darr[2], A. Vasanji[4], J. Kohn[2] and J. O. Hollinger[1], Bone regeneration in a rabbit critical-size calvarial model using tyrosine-derived polycarbonate scaffolds. *Tissue Engineering*, accepted for publication – Reproduced by permission of Mary Ann Liebert, Inc. Publishers

More than 500,000 bone graft procedures are performed annually in the United States [87] and approximately 30,000 surgical procedures involve the craniofacial complex [88]. Escalating global demands for bone grafting procedures and recognized challenges with autografts and allografts used in craniofacial procedures have stimulated a need for bone graft substitutes.

Bone graft substitutes must fulfill specific biological and biomechanical criteria that include functioning as a template for cell attachment, amplification and differentiation with subsequent expression of extracellular matrix (ECM) proteins that will mineralize [42] and eventually regenerate bone. Moreover, the bone substitute must include performance properties of biocompatibility, biodegradability, osteoconductivity (ease of infiltration of cell and nutrient on the scaffold [89]), osteoinductivity (stimulation of the recruitment of and differentiation of mesenchymal stem cells into bone forming cells [89, 90]), as well as biomechanical functionality [91].

A porous micro- and macro-architecture must be exploited to enable angiogenesis, cell migration and viability and osteoconduction [42, 92]. Incorporation of recombinant human bone morphogenetic factor-2 (rhBMP-2) will initiate osteoinduction [93]. In addition, the bone substitute must have adequate mechanical strength during bone healing, including non-load bearing zones of the cranium where cyclic stresses occur due to dural pulsation [94].

Despite vigorous efforts to mimic physical and biological properties of bone in the design of biomaterials for bone tissue engineering, contemporary scaffolds fail to match stringent clinical performance criteria for bone regeneration[95, 96]. Some materials

have produced compelling outcome in rodent models; however, there is little fidelity between rodent and human bone physiology [3].

Biomaterials based on tyrosine-derived polycarbonates (TyrPC) have been developed in the Kohn Lab. Specifically for orthopedic applications, poly(DTE carbonate) demonstrated osteoconductive potential in the distal femur and proximal tibia of rabbits [37, 97], a canine bone chamber model [36], a delayed healing rabbit calvarial defect [48] and rabbit mandibular defects [98, 99]. It is noteworthy that in contrast to poly(α-esters), the TyrPCs have consistently produced superior biocompatibility [36, 71].

In spite of the reported osteoconductive outcomes from those studies, bone regeneration was limited. These observations may have been caused by a mismatch between the poly(DTE carbonate) degradation rate to the rate of new bone formation. To mitigate against this mismatch, a new class of TyrPC terpolymers has been developed that is composed of desaminotyrosyl-tyrosine alkyl ester (DTR), desaminotyrosyl-tyrosine (DT) and poly(ethylene glycol) (PEG). By combining these three building blocks, the terpolymers will provide precise control of physical, chemical, biomechanical and biological properties requisite for bone regeneration. Moreover, the addition of carboxylate groups into the polymer backbone in the form of DT can result in possible formation of nucleation sites for hydroxyapatite layer by chelation of calcium ions from blood, thus promoting bone formation. [37, 100]

In an attempt to make Tyr-PC scaffolds more bioactive, the scaffold surface was coated with calcium phosphate. It was hypothesized that adding calcium phosphate (CP) would enable better host-scaffold integration, and that CP's presence in the defect site would promote the deposition of hydroxyapatite *in vivo* that might in turn enhance bone

formation [7, 8, 28, 75-77]. Polymers in combination with calcium phosphates have been used as grafts for bone repair to improve bone-scaffold integration, to enhance bone regeneration by promoting the deposition of hyrdoxyapatite *in vivo*, and to enhance adhesion and differentiation of osteoprogenitor cells.[7, 8, 28, 75]. Calcium phosphates have been coated on the polymer surface or have been prepared as polymer-calcium phosphate composites. Polymer surfaces can be coated by immersion in solutions resembling body fluids, such as simulated body fluid,[101, 102] or solutions of calcium and phosphate.[103]

This chapter describes the work done to evaluate the *in vivo* performance of the tyrosine-derived polycarbonate terpolymer as bone tissue engineering scaffolds in a critical-sized defect (CSD) in the rabbit calvaria. The first animal study evaluated the biocompatibility of resorbing scaffolds at 12 weeks in a CSD rabbit calvaria model. In the second animal study, the effects of CP coating and incorporation of recombinant human bone morphogenetic protein-2 (rhBMP-2) on the osteogenic performance of TyrPC scaffolds in the same rabbit model were evaluated six weeks post-implantation using micro-computed tomography (micro-CT or μCT) and histomorphometry.

7.1   *In vivo* biocompatibility of resorbing TyrPC scaffolds

To assess *in vivo* performance of the polymers, we chose the rabbit cranial critical sized defect model, which has been well established and widely used as an *in vivo* model to evaluate bone formation as well as *in vivo* characteristics of tissue engineering scaffolds.[104, 105]

The CSD showed some soft tissue healing in the specimens at 12 weeks post-implantation (Figure 7.1.A). The host implant bones were bridged by extensive fibrous connective tissue (Figure 7.1.A and D) and the degradation of the polymer was quite marked, >90% of the implant had resorbed by 12 weeks (Figure 7.1.D and E). Neither osteolysis or bone resorption nor any severe inflammatory response was observed within the specimens as a consequence of the implanted material.

New cancellous bone formation was very limited to small areas along the implant/host calvaria tissue interface and only to the degree that is anticipated in the normal sequence of wound healing (Figure 7.1.B). There was no evidence of either pericranial or dural bone growth. Likewise, there was no evidence of bulk new bone formation within the implant probably as a result of the rapid degradation profile of the polymer. Within the medullary cavity of the calvaria, there was evidence of osteoblast activity, regions of newly formed osteoid and the presence of erythrocytes, all of which suggest a normal wound healing response (Figure 7.1.C and F). Overall, the implant materials did not elicit severe inflammatroy response, although histological assessment of their biological performance was not possible due to their rapid degradation profile.
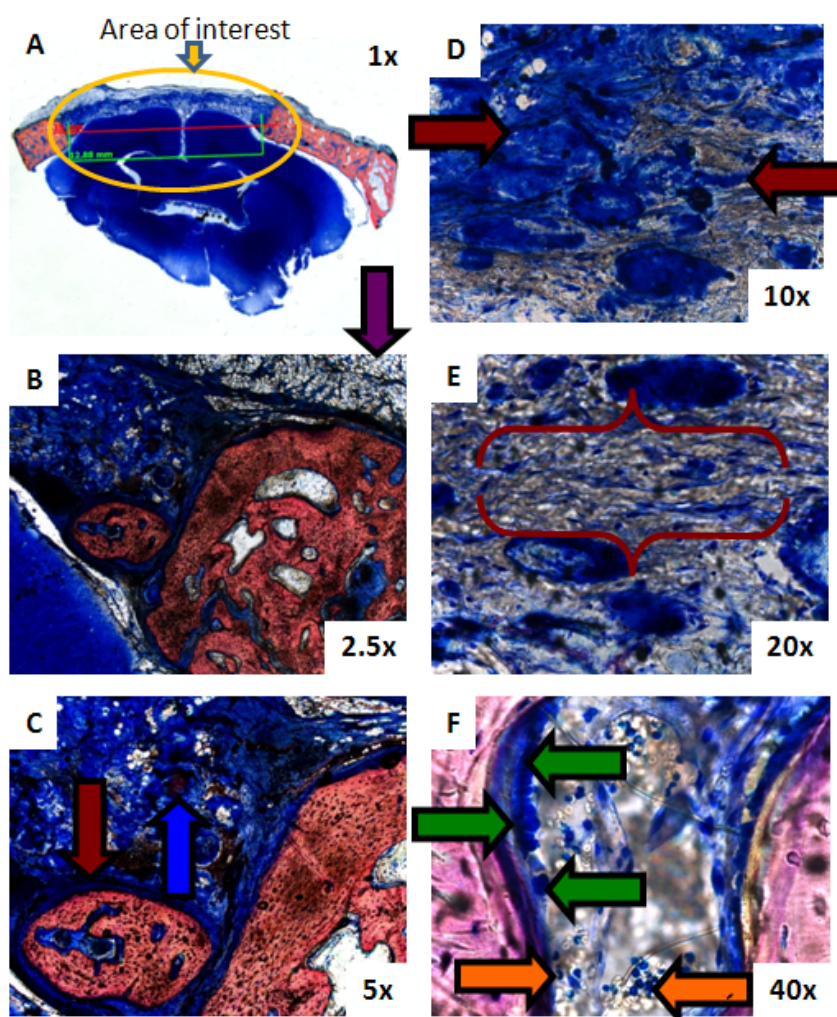
Figure 7.1. A typical section of the implanted tyrosine-derived polycarbonate (E1501(2K)) after 12 weeks of implantation. The specimens were cut and ground to 30 μm thick sections and stained with Sanderson's Rapid Bone Stain and counterstained with van Gieson's picrofuchsin. Soft tissue was stained blue and bone was pink/red. (A) Implant area is devoid of significant new bone growth (orange circle). (B) Fat cells were filling the pericranial region of the defect (purple arrow) and (C) a few islands of new cancellous bone formation were seen (blue arrows) surrounded by fibrous tissue (dark red arrow). (D) Defect area pervaded by fibrous connective tissue (dark red arrows). (E) Fibrous connective tissue filling the void left by the polymer degradation (dark red brackets). (F) Plump osteoblast cells lining the osteoid (green arrows) and erythrocytes (red blood cells, orange arrows) were seen in a medullary cavity of the calvaria (orange arrows).

7.2   Bone regeneration in CSD rabbit calvaria

In the second *in vivo* study, scaffolds made from E1001(1K), with optimized mechanical properties, and degradation and resorption rate (see Chapter 4) were fabricated using TyrPC terpolymers. During bone healing, including non-load bearing zones of the cranium, cyclic stresses occur due to dural pulsation [94] and a mechanically stable scaffold will be needed in the defect site.

TyrPC scaffolds were compared to a predicate device, a Food and Drug Administration (FDA)- approved device with clinical indications for use as bone void filler in the extremities, spine, and pelvis. This predicate device is a porous and resorbable scaffold strip that is made of 80% tricalcium phosphate (TCP) and 20% type-1 bovine collagen. Representative SEM images of these test materials are shown in Figure 7.2.
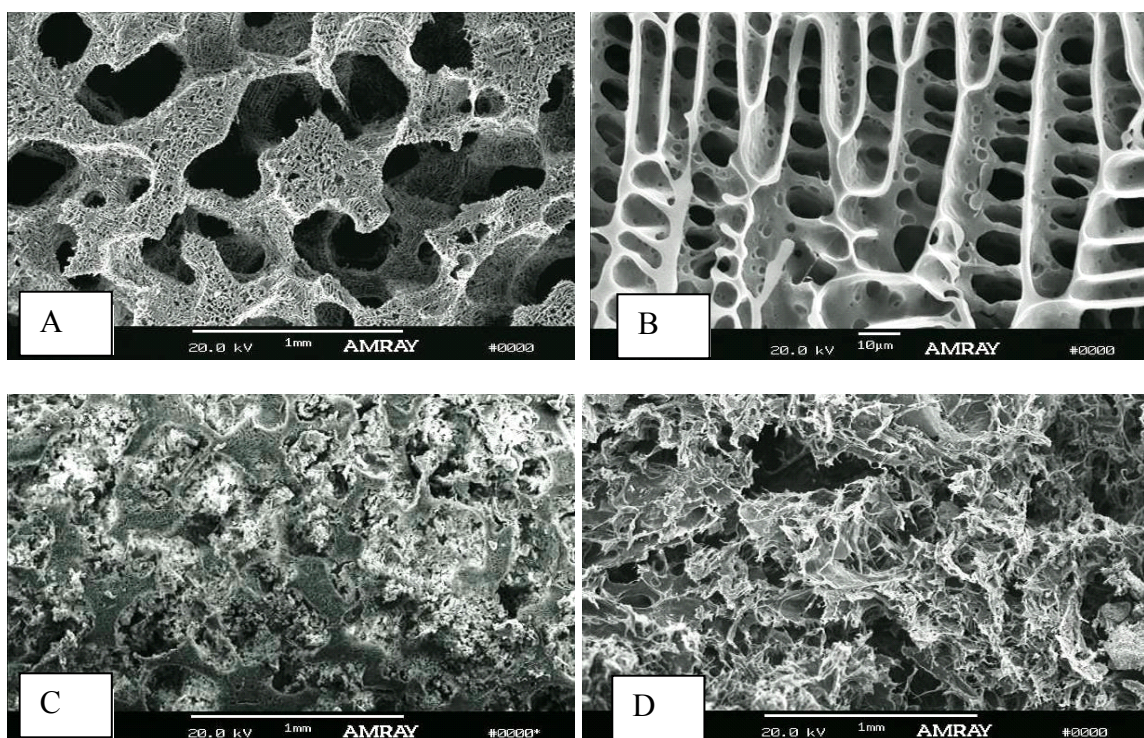
Figure 7.2. (A and B) Representative SEM images of TyrPC scaffold at 50x and 1000x, respectively, (C) TyrPC+CP scaffold at 50x and (D) predicate device scaffold at 50x.

It has also been shown that the pore architecture of scaffold matrices is important for osteoconduction[42, 92]. The highly open and interconnected pore architecture of TyrPC scaffolds resembles trabecular bone. Moreover, micropores (< 20 µm) aligned around the macropores benefit angiogenesis and osteoconduction by increasing surface area, thus enhancing endogenous protein adsorption, exogenous protein retention, as well as ion exchange for apatitic formation [42]. During surgery, the pores imbibed blood which helped in localizing pro-angiogenic and pro-osteogenic factors needed for the bone healing cascade[106].

The surgical properties of TyrPC and TyrPC+ CP (TyrPC+CP) scaffolds were better than the predicate device (PD). PD was friable and difficult to handle during insertion into the defects. In contrast, TyrPC and TyrPC+CP were sturdy, if deformed,

they 'rebounded' and upon surgical implantation, they imbibed blood. This property is significant in that the clotted blood contains stimulatory, influential osteogenic and angiogenic cues [106]. Moreover, at necropsy (6 weeks post-implantation), all recipient sites implanted with tested materials displayed normal-appearing tissues with neither swelling nor tissue necrosis (Figure 7.3).
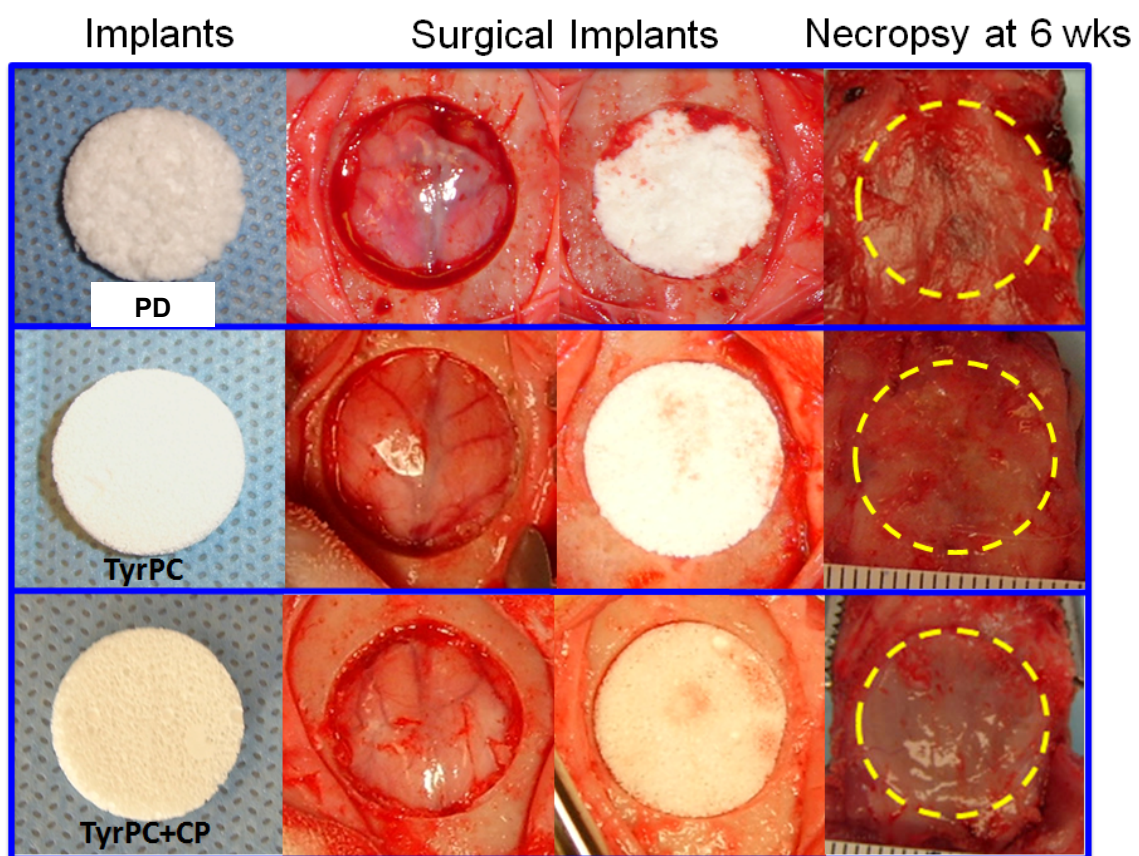
Figure 7.3. Implant images before and after surgery using the CSD (15 mm-diameter) rabbit calvarial defect. All test implants fit snugly into the craniotomy sites. There were no adverse tissue observations at necropsy (yellow dotted circle showed the implant site).

Two-dimensional sections (coronal and transverse planes) of micro-computed tomographic (micro-CT or μCT) images of the calvarial specimens revealed that without rhBMP-2, PD-treated and TyrPC-treated CSDs had marginal new bone formation. In distinction, rhBMP-2-supplemented scaffolds (50 μg rhBMP-2/scaffold) had significant bone regeneration at 6 weeks (Figure 7.4**)**. Micro-CT images of PD without rhBMP-2 suggested bone regeneration in isolated zones at the periphery of the scaffolds. In addition, micro-CT revealed PD fragments were still present in the recipient CSD.
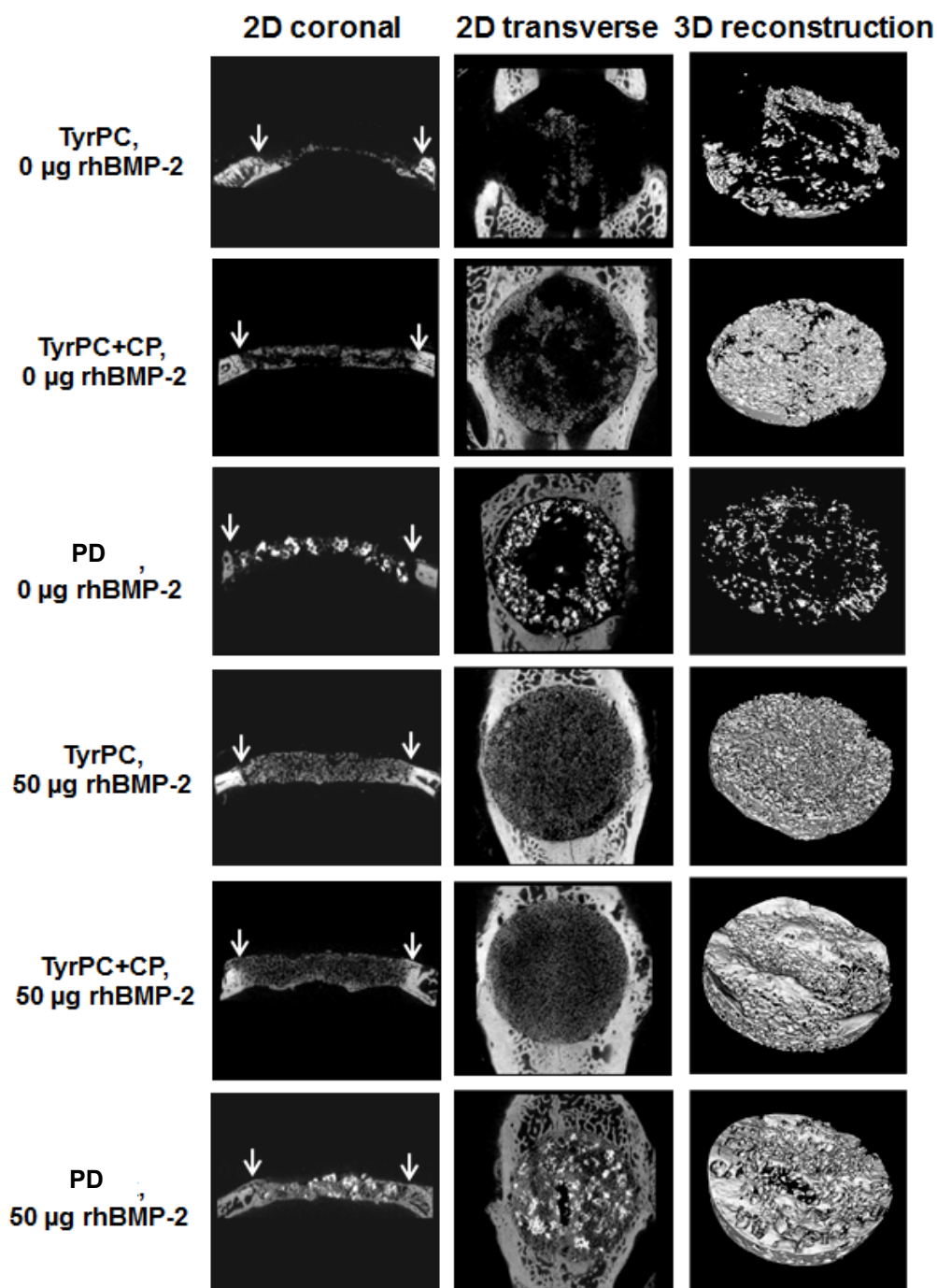
Figure 7.4. Micro-CT images of bone regeneration in the rabbit calvarial CSD model at 6 weeks post-implantation. White arrows in the first column identify the defect site. Remaining β-TCP fragments are identified as bright specks in the 2D transverse images of PD scaffolds.

Trabecular bone volume was calculated using the image analysis (MicroView, GE Healthcare) of µCT data (Figure 7.5A). Data suggested that rhBMP-2-treated scaffolds had significantly greater trabecular bone volume than scaffolds without rhBMP-2, regardless of scaffold type. There were no significant differences in trabecular bone volume between PD and TyrPC scaffolds without rhBMP-2, while TyrPC+CP scaffolds had more trabecular bone volume than both TyrPC and PD.

Among the rhBMP-2-treated scaffolds, there was a significant difference in trabecular bone volume between TyrPC+CP and PD treatment groups (Figure 7.5A), that is, TyrPC+CP regenerated significantly more new trabecular bone at the defect site than PD.

New bone bridging was also obtained by measuring a projected image from the 3D data sets resulting in bone coverage data (Figure 7.5B)[96]. A similar trend was found in bone coverage data compared to trabecular bone volume data, except on the effects of rhBMP-2 with TyrPC+CP and PD, where no significant differences were measured between the groups with and without rhBMP-2.
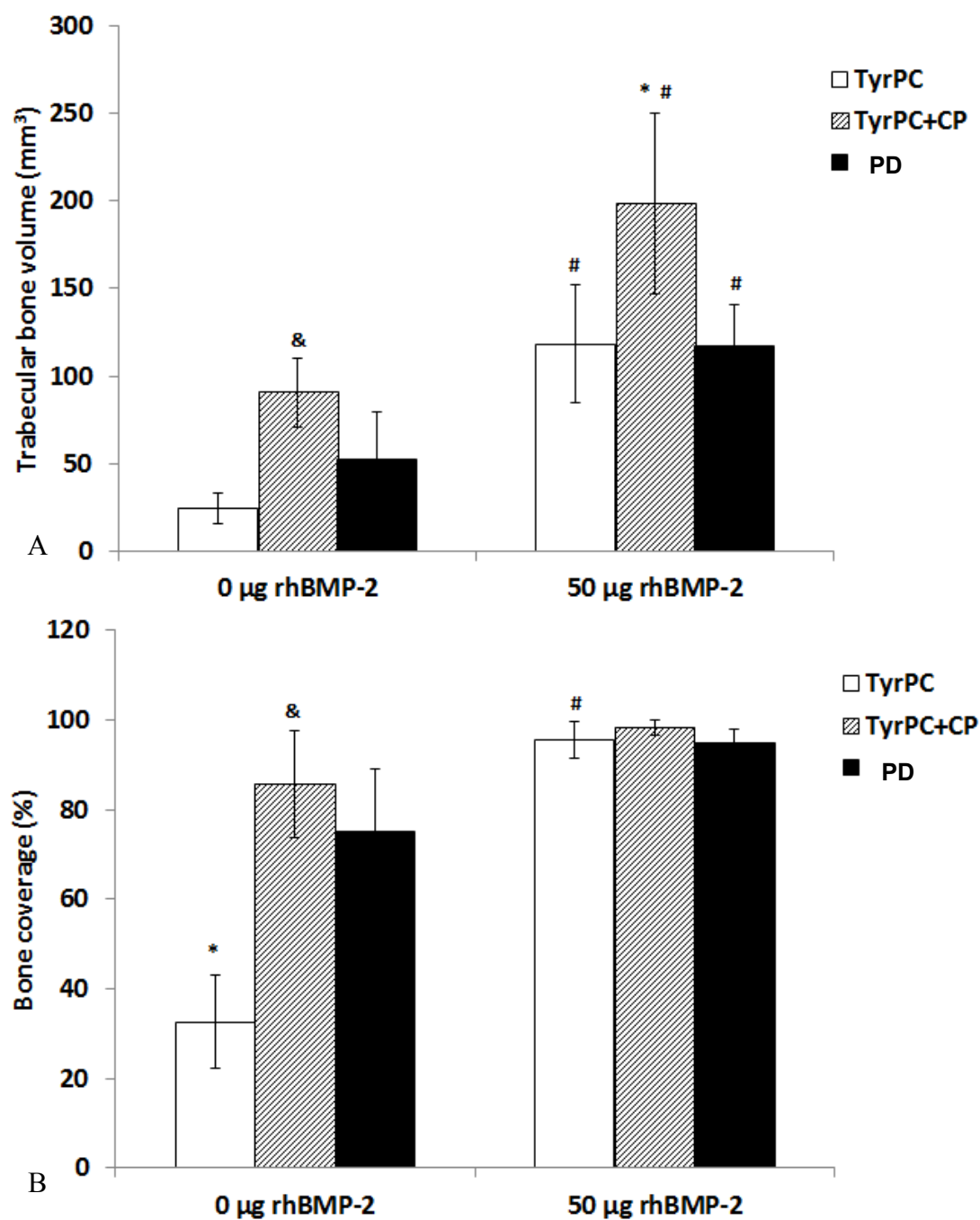
Figure 7.5. (A) Trabecular bone volume (mm^3 of new bone in the defect) and (B) bone coverage (%) of the defect as determined from image analysis of micro-CT data. Data are reported as a mean ± standard deviation for n ≥ 4. * and & represent significant difference vs. PD and TyrPC, respectively. #: significant differences between each group without and with rhBMP-2 (p<0.05).

The coronal plane of the histological sections were stained with Sanderson's Rapid Bone Stain and counterstained with van Gieson's picrofuchsin (Figure 7.6, panels on the left at 1.5x magnification; insert: yellow dotted lines at 5x magnification on the right) where bone stained red while soft tissue stained blue. The images suggested bone formation along the dural surface and modest osteoconduction in the TyrPC scaffolds as indicated by the red stained tissues lining the dural surface (Figure 7.6A). In contrast to TyrPC, there was substantial bone formation throughout TyrPC+CP scaffolds (Figure 7.6B). CP's presence in the defect site would promote the deposition of hydroxyapatite *in vivo* which resulted in enhanced bone formation.[7, 8, 28, 75-77] The predicate device (PD), on the other hand, did not regenerate as much trabecular bone in the defect site as TyrPC+CP. The defect site treated with PD was pervaded by soft tissue (Figure 7.6C). It is a bone void scaffold filler composed of β-TCP and type-1 bovine collagen. Collagen is a natural biomaterial that may elicit an immunological response[107] from the host which may have affected new bone formation.

A possible explanation for the performance superiority of TyrPC-based scaffolds may be attributable to chemical and physical properties that promoted cell attachment, amplification and differentiation to an osteogenic phenotype (see Chapter 6 and Appendix 2 for details) and degradation in register with bone regeneration.

Further histological examination suggested the rhBMP-2-treated scaffolds had robust bone formation as indicated by the almost complete red staining of the defect site which is outlined by two black arrows (Figures 7.6 D, E and F).

Incorporation of recombinant human bone morphogenetic factor-2 (rhBMP-2) resulted in regeneration of bone in the defect site, regardless of scaffold composition,

most likely a result of osteoinduction [93]. Studies using the rabbit CSD calvarial model have reported rhBMP-2 dosing up to 290 µg/defect site delivered with a collagen sponge [108] and coral [109]. In this study, at 6 weeks, we achieved remarkable bone regeneration in a stringent rabbit CSD model with all the rhBMP-2 supplemented implants at a much lower dosage of 50 µg/defect site. The minimal dose of rhBMP-2 supplementation of TyrPC scaffolds significantly enhanced bone formation. There is a profound clinical impact and patient benefit when a delivery system (*i.e.*, bone substitute) provides a physiological, calibrated dose of rhBMP-2. A localized and physiological dose for therapeutic effect is safer and more economical than a supra-physiological dose of rhBMP-2. In addition, a localized effective dose of rhBMP-2 may mitigate against ectopic bone formation [110].

In vivo resorption of all of the implants appeared to be almost complete by 6 weeks and likely a consequence of enzymatic and/or cellular interactions [111]. Furthermore, biodegradability of TyrPC scaffolds appeared to match the bone formation rate (~2 µm/day)[72]. The clinical predicate had the most bulk remaining after 6 weeks as indicated by the black stained fragments on the histological images and highlighted by orange arrows. TyrPC+CP had lesser bulk remaining in the defect site than PD. This observation may be due to a slower resorption rate of the calcium phosphate in contrast to the TyrPC alone (Figures 7.6 A, B and C).

Although bone healing speed between rabbit and human is quite different, rabbit sigma correlates with the temporal groups we selected. In addition, a rabbit model provides a sequential, systematic approach to assess the biomaterial in a clinically relevant pre-clinical model.[3] A precise match between the biodegradation of the biomaterial eventually will have to be made in the appropriately designed clinical study.

Nevertheless, the literature teaches and biology underscores the fact that biodegradation in the rabbit pre-clinical model is a compelling antecedent to the clinical model and further, can be exploited to predict accurately the likely outcome in the clinical condition.

The *in vivo* outcome data revealed that TyrPC alone had marginal bone formation and may lack innate osteogenic capacity to regenerate bone in a rabbit calvarial CSD model. However, when TyrPC was supplemented with either rhBMP-2 or CP, new bone formation in the defects significantly increased (Figure 7.6 C).
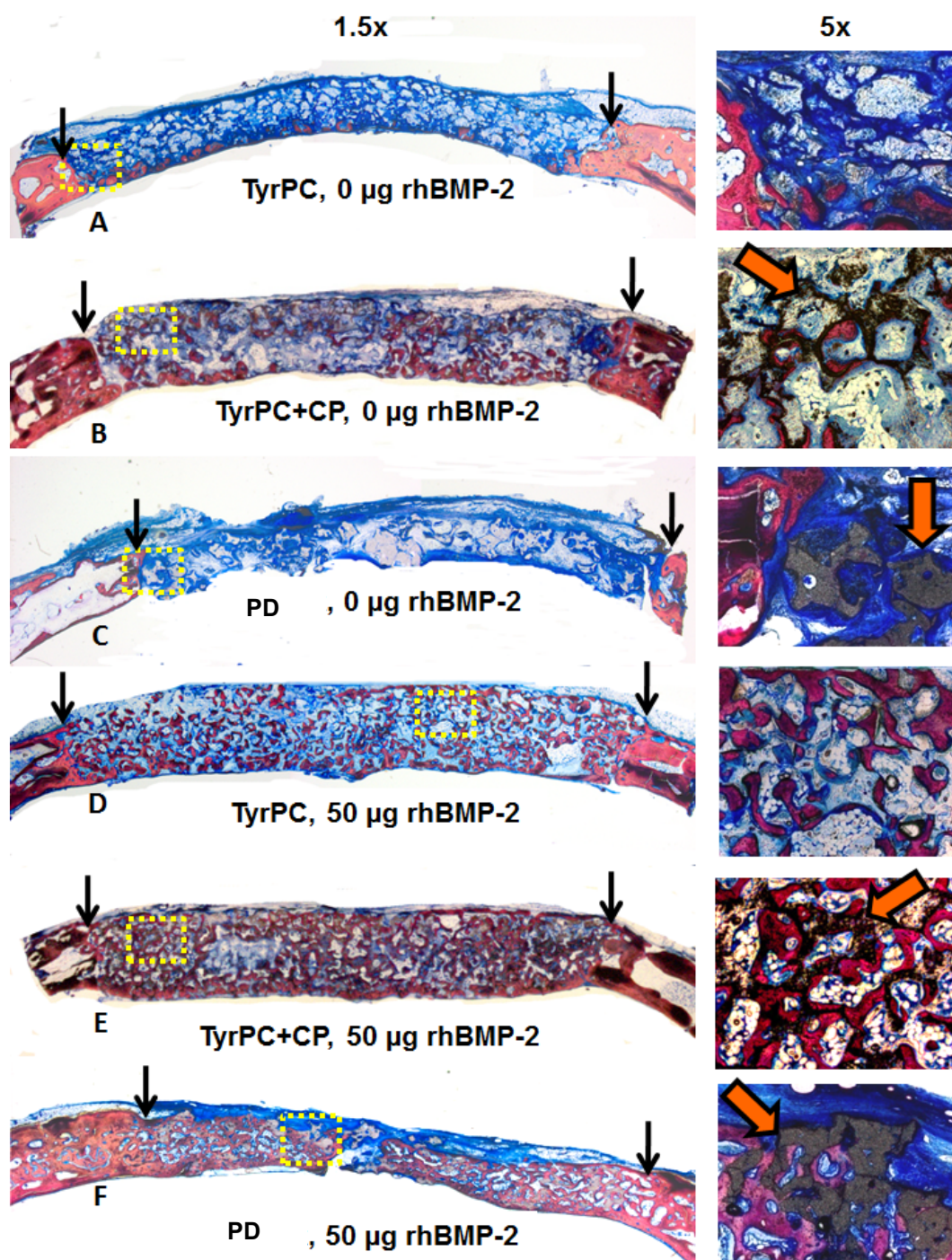
Figure 7.6. Representative histological images of the rabbit CSDs at 6 weeks post-implantation treated with (A) TyrPC, (B) TyrPC+CP, and (C) PD without rhBMP-2, (D) TyrPC, (E) TyrPC+CP, and (F) PD with rhBMP-2 (50 µg/scaffold). Black arrows outline the defect site and orange arrows indicate remaining calcium phosphate fragments. Histological sections were stained with Sanderson's Rapid Bone Stain and counterstained with van Gieson's picrofuchsin where bone was stained red, soft tissue blue and remaining implant fragments black.

Histomorphometric data (Figure 7.7) mirrored micro-CT data (figure 7.5A). The results suggested that TyrPC+CP had more bone area compared to TyrPC. The data also validated µCT analysis in that TyrPC and TyrPC+CP containing 50 µg rhBMP-2 had significantly greater bone area than the scaffolds without rhBMP-2.
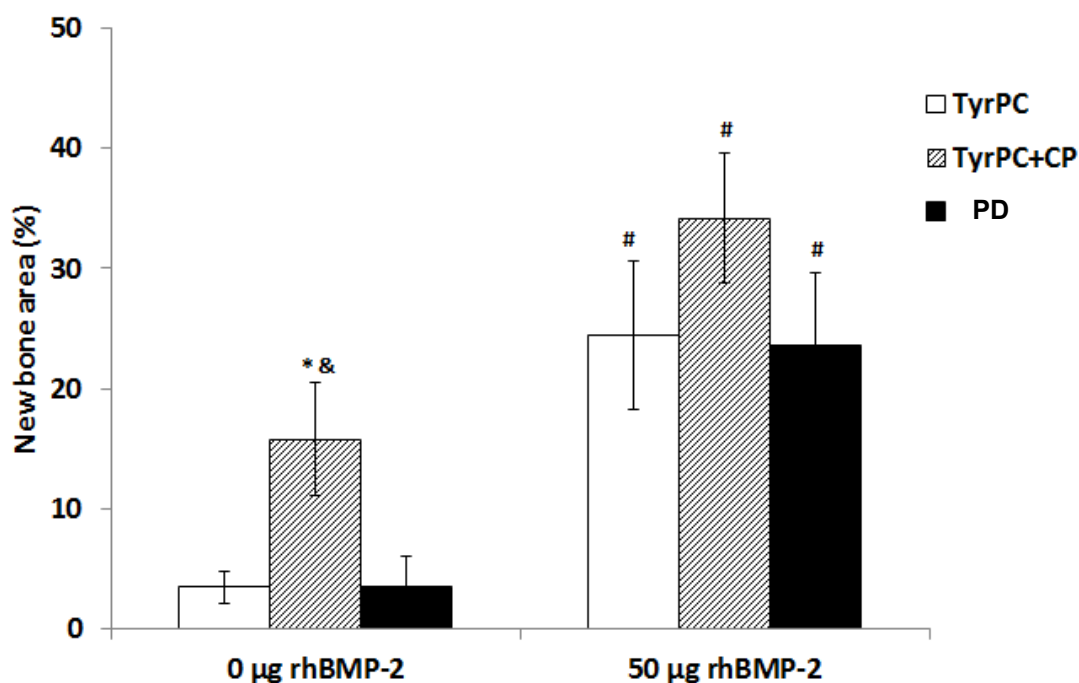
Figure 7.7. New bone area (%) in the defect site determined by histomorphometric image analysis. Data are reported as a mean ± standard deviation for n ≥ 4. * and & represent significant difference between TyrPC+CP vs. PD and TyrPC, respectively, and #: significant differences between each group without and with rhBMP-2 ($p < 0.05$).

Studies using the rabbit CSD calvarial model have reported rhBMP-2 dosing up to 290 µg/defect site delivered with a collagen sponge [108] and coral [109]. In this study, at 6 weeks we achieved remarkable bone regeneration in a stringent rabbit CSD model with either TyrPC+CP unsupplemented with rhBMP-2 or in conjunction with 50 µg rhBMP-2 /defect site. This is a greater than 20% decrease of the reported doses and could have

compelling clinical implications for rhBMP-2 devices. A possible explanation for the performance superiority of TyrPC-based scaffolds may be attributable to chemical and physical properties that promoted cell attachment, amplification and differentiation to an osteogenic phenotype and degradation in register with bone regeneration, thus improving regenerative outcome with a 50μg dose vs. traditional rhBMP-2 dosing that are 5 times greater[112].

The minimal dose of rhBMP-2 supplementation of TyrPC scaffolds significantly enhanced bone formation. There is a profound patient benefit when a delivery system (i.e., bone biomimetic substitute) provides a physiological, calibrated dose of rhBMP-2. A localized and physiological dose for therapeutic effect is safer and more economical than a supra-physiological dose of rhBMP-2. In addition, a localized effective dose of rhBMP-2 may mitigate against ectopic bone formation[110]. More importantly, we demonstrated that TyrPC+CP without rhBMP-2 may stimulate as much bone formation as a commercially available BGS supplemented with rhBMP-2. This compelling result is one of the most attractive features of the TyrPC family as bone-graft substitutes. Moreover, in contrast to potential immunogens used to deliver rhBMP-2, such as type I bovine collagen [107], we do not anticipate immunological sequelae from TyrPCs.

7.3   Conclusion

The *in vivo* performance of the polymers were evaluated using the rabbit cranial critical sized defect model, which has been well established and widely used as an *in vivo* model to evaluate bone formation as well as *in vivo* characteristics of tissue engineering scaffolds.[104, 105]

In general, the tissue response to the implants showed a normal wound healing response in spite of the fact that massive degradation of the test materials had occurred within 12 weeks post-implantation. There was only a minimal inflammatory response and only a thin fibrous capsule was observed. Since the fastest degrading terpolymer compositions had completely resorbed during the test period, the histological assessment of the *in vivo* tissue response is a strong indicator of the high degree of biocompatibility of the tested polycarbonate terpolymer compositions.

In the second *in vivo* study, scaffolds with optimized mechanical properties, and degradation and resorption rate (see Chapter 4) were fabricated using E1001(1K). The results revealed that porous 3D TyrPC scaffolds have good biocompatibility and maintained bio-mechanical properties upon degradation. Furthermore, at 6 weeks, in the rabbit CSD model, the following observations were noted:

1) The TyrPC scaffolds did not promote adverse systemic or localized tissue responses, had minimal new bone formation and significantly increased trabecular bone volume when supplemented with rhBMP-2.

2) TyrPC treated with rhBMP-2 produced a similar quantity of woven bone volume to a FDA-approved, commercially available bone graft substitute (BGS) with rhBMP-2.

3) TyrPC+CP alone had more trabecular bone formation than TyrPC and promoted similar new bone formation to BGS supplemented with rhBMP-2.

CHAPTER 8

Concluding remarks and on-going studies

The first comprehensive evaluation of tyrosine-derived polycarbonate (TyrPC) terpolymers as a new class of degradable biomaterials was presented. The evaluation included synthesis and chemical structure proof, a demonstration of the feasibility to fabricate bone regeneration scaffolds and modify scaffold properties post-fabrication, and a detailed study of *in vitro* cytotoxicity and osteogenic potential, and biocompatibility and osteogenic performance in a clinically relevant rabbit model, the rabbit calvarial critical size defect (CSD) model.

An important attribute of this class of polymers is the tunability of their degradation and resorption profiles. Our results indicate that variations in the molar fractions of either DT or PEG and changing the alkyl pendent chain on DTR within the polymer backbone can be used to tune the degradation and resorption profiles of these polymers. The focused library of TyrPC terpolymers that was investigated in this research is composed of polymers that may be beneficial for bone regeneration. To further illustrate the flexibility and tunability of this terpolymer system, other works showed the potential of using high DT or high PEG compositions for use as carriers for cortical neural probes[61] and as carriers of hydrophobic peptide molecules.[62]

The polymer composition E1001(1k) was determined as the optimal composition based on its *in vitro* degradation and erosion profile, *in vitro* osteogenic potential and *in vivo* biological performance in the rabbit calvarial critical-sized defect model for the fabrication of bone tissue engineering scaffolds.

Our results also show that TyrPC terpolymers exhibit minimal cytotoxicity and promote osteogenic differentiation and mineralization of MC3T3-E1 pre-osteoblasts and human-derived mesenchymal stem cells (hMSCs).

A normal wound healing response was observed *in vivo* associated with only minimal tissue inflammation. These results are particularly noteworthy since fast degrading implants were tested in the first set of *in vivo* studies, some of which resorbed completely over the course of the 12 week test period. This experimental design ensured that the implant sites were exposed to significant amounts of polymer degradation products.

In the second set of *in vivo* studies, micro-CT and histology/histomorphometric data clearly demonstrate significant bone repair from scaffold implants treated with rhBMP-2 as compared to non-treated scaffold implants within 6 weeks. Moreover, the dose of rhBMP-2 used in this study was ¼ of what is currently used clinically, indicating that TyrPC scaffolds may be an effective delivery vehicle for rhBMP-2. What is noteworthy in this study is that a slower degrading TyrPC terpolymer scaffold coated with calcium phosphate (TyrPC+CP) promoted the formation of significantly greater new trabecular bone than a commercially utilized and FDA-approved bone void filler, which is made from type-1 collagen and 80% β-TCP, in a critical-sized rabbit calvarial defect.

Overall, the results presented in this study illustrate the potential for this exciting class of polymers to the field of bone tissue engineering.

In relation to the studies and results presented in this thesis, several *in vivo* studies, in collaboration with Dr. Jeffrey O. Hollinger's group at Carnegie Mellon University and Dr. Pamela Brown-Baer's group at the United States Institute for Surgical

Research, are on-going. Specifically, *in vivo* studies using the critical-sized rabbit calvarial defect model will evaluate the following:

1. Effect of mineral coating on the quality of bone healing and healing rate at 2, 4, 6, 8, 12, and 16 weeks. Two coating compositions were used, specifically a calcium phosphate coating, as described in Chapter 5, and a synthetic bone mineral mix, which is a coating composition suggested by Dr. Raquel LeGeros of New York University. An FDA-approved non-load bearing bone void filler device made from poly(lactide-co-ε-caprolactone) and β-TCP was used as a control.

2. Effect of rhBMP-2 dose, by addition of 0, 10, 25 or 50 µg per scaffold, on bone regeneration at 4 weeks and 16 weeks.

REFERENCES

1.   Giannoudis, P. V.; Dinopoulos, H.; Tsiridis, E., Bone substitutes: An update. *Injury* **2005,** 36, (3, Supplement 1), S20-S27.

2.   Schieker, M.; Seitz, H.; Drosse, I.; Seitz, S.; Mutschler, W., Biomaterials as scaffold for tissue engineering. *European Journal of Trauma* **2006**, (2), 114-124.

3.   Muschler, G. F.; Raut, V. P.; Patterson, T. E.; Wenke, J. C.; Hollinger, J. O., The Design and Use of Animal Models for Translational Research in Bone Tissue Engineering and Regenerative Medicine. *Tissue Engineering Part B-Reviews* **2010,** 16, (1), 123-145.

4.   Doll, B.; Sfeir, C.; Azari, K.; Sarah, H.; Hollinger, J., Craniofacial repair. In *Bone regeneration and repair*, Lieberman, J.; Friedlaender, G., Eds. Humana Press: Totowa, New Jersey, 2005.

5.   Navarro, M.; Aparicio, C.; Charles-Harris, M.; Ginebra, M. P.; Engel, E.; Planell, J. A., Development of a biodegradable composite scaffold for bone tissue engineering: Physicochemical, topographical, mechanical, degradation, and biological properties. *Ordered Polymeric Nanostructures at Surfaces* **2006,** 200, 209-231.

6.   Burg, K. J. L.; Porter, S.; Kellam, J. F., Biomaterial developments for bone tissue engineering. *Biomaterials* **2000,** 21, (23), 2347-2359.

7.   LeGeros, R. Z., Properties of osteoconductive biomaterials: calcium phosphates. *Clin Orthop Relat Res* **2002**, (395), 81-98.

8.   LeGeros, R. Z., Calcium phosphate-based osteoinductive materials. *Chem Rev* **2008,** 108, (11), 4742-53.

9.   Salgado, A. J.; Coutinho, O. P.; Reis, R. L., Bone tissue engineering: State of the art and future trends. *Macromolecular Bioscience* **2004,** 4, (8), 743-765.

10.   Carano, R. A. D.; Filvaroff, E. H., Angiogenesis and bone repair. *Drug Discovery Today* **2003,** 8, (21), 980-989.

11.   Khan, Y.; Yaszemski, M. J.; Mikos, A. G.; Laurencin, C. T., Tissue Engineering of Bone: Material and Matrix Considerations
J Bone Joint Surg Am **2008,** 90 (Suppl 1), 36 -42.

12.   Laurencin, C.; Khan, Y.; El-Amin, S. F., Bone graft substitutes. *Expert Review of Medical Devices* **2006,** 3, (1), 49-57.

13.   Hutmacher, D. W.; Schantz, J. T.; Lam, C. X. F.; Tan, K. C.; Lim, T. C., State of the art and future directions of scaffold-based bone engineering from a biomaterials perspective. *Journal of Tissue Engineering and Regenerative Medicine* **2007,** 1, (4), 245-260.

14.   Orban, J. M.; Marra, K. G.; Hollinger, J. O., Composition options for tissue-engineered bone. *Tissue Engineering* **2002,** 8, (4), 529-539.

15.   Burkoth, A. K.; Burdick, J.; Anseth, K. S., Surface and bulk modifications to photocrosslinked polyanhydrides to control degradation behavior. *Journal of Biomedical Materials Research* **2000,** 51, (3), 352-359.

16.   Lee, K.-W.; Wang, S.; Lu, L.; Jabbari, E.; Currier, B. L.; Yaszemski, M. J., Fabrication and Characterization of Poly(Propylene Fumarate) Scaffolds with Controlled Pore Structures Using 3-Dimensional Printing and Injection Molding. *Tissue Engineering* **2006,** 12, (10), 2801-2811.

17.   Dean, D.; Wolfe, M. S.; Ahmad, Y.; Totonchi, A.; Chen, J. E.-K.; Fisher, J. P.; Cooke, M. N.; Rimnac, C. M.; Lennon, D. P.; Caplan, A. I.; Topham, N. S.; Mikos, A. G., Effect of Transforming Growth Factor β2 on Marrow-Infused Foam Poly(Propylene Fumarate) Tissue-Engineered Constructs for the Repair of Critical-Size Cranial Defects in Rabbits. *Tissue Engineering* **2005,** 11, (5-6), 923-939.

18.   Oh, S. H.; Park, I. K.; Kim, J. M.; Lee, J. H., In vitro and in vivo characteristics of PCL scaffolds with pore size gradient fabricated by a centrifugation method. *Biomaterials* **2007,** 28, (9), 1664-1671.

19.   Laurencin, C. T.; Norman, M. E.; Elgendy, H. M.; El-Amin, S. F.; Allcock, H. R.; Pucher, S. R.; Ambrosio, A. A., Use of polyphosphazenes for skeletal tissue regeneration. *Journal of Biomedical Materials Research* **1993,** 27, (7), 963-973.

20.   Borden, M.; Attawia, M.; Khan, Y.; Laurencin, C. T., Tissue engineered microsphere-based matrices for bone repair: : design and evaluation. *Biomaterials* **2002,** 23, (2), 551-559.

21.   Laurencin, C. T.; Attawia, M. A.; Elgendy, H. E.; Herbert, K. M., Tissue engineered bone-regeneration using degradable polymers: The formation of mineralized matrices. *Bone* **1996,** 19, (1, Supplement 1), S93-S99.

22. Bergsma, E. J.; Rozema, F. R.; Bos, R. R. M.; Debruijn, W. C., Foreign-Body Reactions to Resorbable Poly(L-Lactide) Bone Plates and Screws Used for the Fixation of Unstable Zygomatic Fractures. *Journal of Oral and Maxillofacial Surgery* **1993,** 51, (6), 666-670.

23. Martin, C.; Winet, H.; Bao, J. Y., Acidity near eroding polylactide-polyglycolide in vitro and in vivo in rabbit tibial bone chambers. *Biomaterials* **1996,** 17, (24), 2373-2380.

24. Hutmacher, D. W., Scaffolds in tissue engineering bone and cartilage. *Biomaterials* **2000,** 21, (24), 2529-2543.

25. Rezwan, K.; Chen, Q. Z.; Blaker, J. J.; Boccaccini, A. R., Biodegradable and bioactive porous polymer/inorganic composite scaffolds for bone tissue engineering. *Biomaterials* **2006,** 27, (18), 3413-3431.

26. Guarino, V.; Causa, F.; Netti, P. A.; Ciapetti, G.; Pagani, S.; Martini, D.; Baldini, N.; Ambrosio, L., The role of hydroxyapatite as solid signal on performance of PCL porous scaffolds for bone tissue regeneration. *J Biomed Mater Res B Appl Biomater* **2008,** 86B, (2), 548-57.

27. Daniels, A. U.; Chang, M.; Andrianø, K. P.; Heller, J., Mechanical Properties of Biodegradable Polymers and Composites Proposed for Internal Fixation of Bone. *Journal of Applied Biomaterials* **1990,** 1, 57-78.

28. Tomsia, A. P.; Saiz, E.; Song, J.; Bertozzi, C. R., Biomimetic Bonelike Composites and Novel Bioactive Glass Coatings. *Advanced Engineering Materials* **2005,** 7, (11), 999-1004.

29. Salinas, C. N.; Anseth, K. S., Mesenchymal Stem Cells for Craniofacial Tissue Regeneration: Designing Hydrogel Delivery Vehicles. *Journal of Dental Research* **2009,** 88, (8), 681-692.

30. Haidar, Z.; Hamdy, R.; Tabrizian, M., Delivery of recombinant bone morphogenetic proteins for bone regeneration and repair. Part A: Current challenges in BMP delivery. *Biotechnology Letters* **2009,** 31, (12), 1817-1824.

31. Haidar, Z.; Hamdy, R.; Tabrizian, M., Delivery of recombinant bone morphogenetic proteins for bone regeneration and repair. Part B: Delivery systems for BMPs in orthopaedic and craniofacial tissue engineering. *Biotechnology Letters* **2009,** 31, (12), 1825-1835.

32.   Pelled, G.; Ben-Arav, A.; Hock, C.; Reynolds, D. G.; Yazici, C.; Zilberman, Y.; Gazit, Z.; Awad, H.; Gazit, D.; Schwarz, E. M., Direct Gene Therapy for Bone Regeneration: Gene Delivery, Animal Models, and Outcome Measures. *Tissue Engineering Part B: Reviews* 16, (1), 13-20.

33.   Hooper, K. A.; Macon, N. D.; Kohn, J., Comparative histological evaluation of new tyrosine-derived polymers and poly (L-lactic acid) as a function of polymer degradation. *Journal of Biomedical Materials Research* **1998,** 41, (3), 443-454.

34.   Ertel, S. I.; Kohn, J., Evaluation of a Series of Tyrosine-Derived Polycarbonates as Degradable Biomaterials. *Journal of Biomedical Materials Research* **1994,** 28, (8), 919-930.

35.   Tangpasuthadol, V.; Shefer, A.; Hooper, K. A.; Kohn, J., Thermal properties and physical ageing behaviour of tyrosine-derived polycarbonates. *Biomaterials* **1996,** 17, (4), 463-468.

36.   Choueka, J.; Charvet, J. L.; Koval, K. J.; Alexander, H.; James, K. S.; Hooper, K. A.; Kohn, J., Canine bone response to tyrosine-derived polycarbonates and poly(L-lactic acid). *Journal of Biomedical Materials Research* **1996,** 31, (1), 35-41.

37.   James, K.; Levene, H.; Parsons, J. R.; Kohn, J., Small changes in polymer chemistry have a large effect on the bone-implant interface: evaluation of a series of degradable tyrosine-derived polycarbonates in bone defects. *Biomaterials* **1999,** 20, (23-24), 2203-12.

38.   Abramson, S. D.; Bolikal, D.; Levene, H.; Simon, J.; Kohn, J. In *Small changes in polymer structure can dramatically increase degradation rates: the effect of free carboxylate groups on the properties of tyrosine-derived polycarbonates*, Sixth World Biomaterials Congress, Kamuela, HI, 2000; Lucas, L. C.; Anderson, J. M.; Howlett, C. R.; Kim, Y. H.; Kirkpatrick, C. J.; Okano, T.; Pilliar, R.; Zhang, X., Eds. Society for Biomaterials: Kamuela, HI, 2000; p 1164.

39.   Yu, C.; Kohn, J., Tyrosine-PEG-derived poly(ether carbonate)s as new biomaterials - Part I: Synthesis and evaluation. *Biomaterials* **1999,** 20, (3), 253-264.

40.   Yu, C.; Mielewczyk, S. S.; Breslauer, K. J.; Kohn, J., Tyrosine-PEG-derived poly(ether carbonate)s as new biomaterials - Part II: Study of inverse temperature transitions. *Biomaterials* **1999,** 20, (3), 265-272.

41.   Tziampazis, E.; Kohn, J.; Moghe, P. V., PEG-variant biomaterials as selectively adhesive protein templates: model surfaces for controlled cell adhesion and migration. *Biomaterials* **2000,** 21, (5), 511-520.

42.   Karageorgiou, V.; Kaplan, D., Porosity of 3D biornaterial scaffolds and osteogenesis. *Biomaterials* **2005,** 26, (27), 5474-5491.

43.   Levene, H.; Lhommeau, C.; Kohn, J. Porous polymer scaffolds for tissue engineering. 2000.

44.   Magno, M. H. R.; Kim, J.; Srinivasan, A.; McBride, S.; Bolikal, D.; Darr, A.; Hollinger, J. O.; Kohn, J., Synthesis, degradation and biocompatibility of tyrosine-derived polycarbonate scaffolds. *Journal of Materials Chemistry* **2010,** 20, (40), 8885-8893.

45.   Hooper, K. A.; Kohn, J., Diphenolic monomers derived from the natural amino acid alpha-L-tyrosine: An evaluation of peptide coupling techniques. *Journal of Bioactive and Compatible Polymers* **1995,** 10, (4), 327-340.

46.   Pulapura, S.; Kohn, J., Tyrosine-derived polycarbonates: Backbone-modified "pseudo"-poly(amino acids) designed for biomedical applications. *Biopolymers* **1992,** 32, (4), 411-417.

47.   Hooper, K. A.; Cox, J. D.; Kohn, J., Comparison of the effect of ethylene oxide and gamma-irradiation on selected tyrosine-derived polycarbonates and poly(L-lactic acid). *Journal of Applied Polymer Science* **1997,** 63, (11), 1499-1510.

48.   Levene, H. Analysis of tyrosine-derived novel synthetic polymer scaffolds for tissue engineering and guided tissue regeneration. Rutgers University, 1999.

49.   Wu, L.; Ding, J., In vitro degradation of three-dimensional porous poly(,-lactide-co-glycolide) scaffolds for tissue engineering. *Biomaterials* **2004,** 25, (27), 5821-5830.

50.   Seeherman, H. J.; Azari, K.; Bidic, S.; Rogers, L.; Li, X. J.; Hollinger, J. O.; Wozney, J. M., rhBMP-2 delivered in a calcium phosphate cement accelerates bridging of critical-sized defects in rabbit radii. *Journal of Bone and Joint Surgery-American Volume* **2006,** 88A, (7), 1553-1565.

51.   Schieker, M.; Heiss, C.; Mutschler, W., [Bone substitutes.]. *Unfallchirurg* **2008,** 111, (8), 613-20.

52.   Takigami, H.; Kumagai, K.; Latson, L.; Togawa, D.; Bauer, T.; Powell, K.; Butler, R. S.; Muschler, G. F., Bone formation following OP-1 implantation is improved by addition of autogenous bone marrow cells in a canine femur defect model. *J Orthop Res* **2007,** 25, (10), 1333-42.

53.   Hollinger, J. O., *Biomedical applications of synthetic biodegradable polymers*. CRC Press: Boca Raton, 1995; p 247 p.

54.   Zhu, G. Z.; Mallery, S. R.; Schwendeman, S. P., Stabilization of proteins encapsulated in injectable poly (lactide-co-glycolide). *Nature Biotechnology* **2000,** 18, (1), 52-57.

55.   Bourke, S. L.; Kohn, J., Polymers derived from the amino acid L-tyrosine: polycarbonates, polyarylates and copolymers with poly(ethylene glycol). *Advanced Drug Delivery Reviews* **2003,** 55, (4), 447-466.

56.   Engelberg, I.; Kohn, J., Physico-mechanical properties of degradable polymers used in medical applications: a comparative study. *Biomater* **1991,** 12, 292-304.

57.   Tschopp, J. F.; Tolley, J. O.; Malaney, T.; Mazur, C.; Bellantoni, R.; Abramson, S. D.; Kohn, J.; Wang, B.; Kemnitzer, J. E. In *In vivo resorption profile of matrices from tyrosine-derived polycarbonates with variation in free carboxylate content*, Sixth World Biomaterials Congress Society for Biomaterials, Kamuela, HI, 2000; Lucas, L. C.; Anderson, J. M.; Howlett, C. R.; Kim, Y. H.; Kirkpatrick, C. J.; Okano, T.; Pilliar, R.; Zhang, X., Eds. Society for Biomaterials: Kamuela, HI, 2000; p 1334.

58.   Sharma, R. I.; Kohn, J.; Moghe, P. V., Poly(ethylene glycol) enhances cell motility on protein-based poly(ethylene glycol)-polycarbonate substrates: A mechanism for cell-guided ligand remodeling. *Journal of Biomedical Materials Research Part A* **2004,** 69A, (1), 114-123.

59.   Briggs, T.; Treiser, M. D.; Holmes, P. F.; Kohn, J.; Moghe, P. V.; Arinzeh, T. L., Osteogenic differentiation of human mesenchymal stem cells on poly(ethylene glycol)-variant biomaterials. *Journal of Biomedical Materials Research Part A* **2009,** 91A, (4), 975-984.

60.   Abramson, S. D. Selected bulk and surface properties and biocompatibility of a new class of tyrosine-derived polycarbonates. Rutgers University, 2002.

61.   Lewitus, D.; Smith, K. L.; Shain, W.; Kohn, J., Ultrafast resorbing polymers for use as carriers for cortical neural probes. *Acta Biomaterialia* **2011,** 7, (6), 2483-2491.

62.   Khan, I. J. The utility of L-Tyrosine based polycarbonate copolymers containing poly(ethylene glycol) as a degradable carrier for the release of a hydrophobic peptide molecule. Rutgers University, New Brunswick, 2009.

63.   Murthy, N. S.; Wang, W.; Kohn, J., Microphase separation in copolymers of hydrophilic PEG blocks and hydrophobic tyrosine-derived segments using simultaneous SAXS/WAXS/DSC. *Polymer* **2010,** 51, (17), 3978-3988.

64.   Pesnell, A. A focused library of tyrosine-derived polycarbonates for the discovery of optimal polymers for use in resorbable stents. Rutgers, The State University of New Jersey, New Brunswick, 2006.

65.   Krogman, N. R.; Singh, A.; Nair, L. S.; Laurencin, C. T.; Allcock, H. R., Miscibility of Bioerodible Polyphosphazene/Poly(lactide-co-glycolide) Blends. *Biomacromolecules* **2007,** 8, (4), 1306-1312.

66.   Vert, M.; Li, S. M.; Spenlehauer, G.; Guerin, P., Bioresorbability and Biocompatibility of Aliphatic Polyesters. *Journal of Materials Science-Materials in Medicine* **1992,** 3, (6), 432-446.

67.   Griffith, L. G., Emerging design principles in biomaterials and scaffolds for tissue engineering. *Ann N Y Acad Sci* **2002,** 961, 83-95.

68.   Wu, L. B.; Ding, J. D., In vitro degradation of three-dimensional porous poly(D,L-lactide-co-glycolide) scaffolds for tissue engineering. *Biomaterials* **2004,** 25, (27), 5821-5830.

69.   Zhu, K. J.; Hendren, R. W.; Jensen, K.; Pitt, C. G., Synthesis, properties, and biodegradation of poly(1,3-trimethylene carbonate). *Macromolecules* **1991,** 24, (8), 1736-1740.

70.   Tangpasuthadol, V.; Pendharkar, S. M.; Kohn, J., Hydrolytic degradation of tyrosine-derived polycarbonates, a class of new biomaterials. Part I: Study of model compounds. *Biomaterials* **2000,** 21, (23), 2371-2378.

71.   Tangpasuthadol, V.; Pendharkar, S. M.; Peterson, R. C.; Kohn, J., Hydrolytic degradation of tyrosine-derived polycarbonates, a class of new biomaterials. Part II: 3-yr study of polymeric devices. *Biomaterials* **2000,** 21, (23), 2379-2387.

72.   Hollinger, J. O., Bone Dynamics. In *Biology and Clinical Applications*, Lieberman, J. R.; Friedlaender, G. E., Eds. Humana Press Inc.: Totowa, NJ, 2005; pp 1-19.

73.   Baker, S. C.; Rohman, G.; Southgate, J.; Cameron, N. R., The relationship between the mechanical properties and cell behaviour on PLGA and PCL scaffolds for bladder tissue engineering. *Biomaterials* **2009,** 30, (7), 1321-1328.

74.   Gomes, M. E.; Ribeiro, A. S.; Malafaya, P. B.; Reis, R. L.; Cunha, A. M., A new approach based on injection moulding to produce biodegradable starch-based polymeric scaffolds: morphology, mechanical and degradation behaviour. *Biomaterials* **2001,** 22, (9), 883-889.

75.   Li, X.; Xie, J.; Yuan, X.; Xia, Y., Coating Electrospun Poly(Îμ-caprolactone) Fibers with Gelatin and Calcium Phosphate and Their Use as Biomimetic Scaffolds for Bone Tissue Engineering. *Langmuir* **2008,** 24, (24), 14145-14150.

76.   Chikara, O.; Masanobu, K.; Toshiki, M., Coating bone-like apatite onto organic substrates using solutions mimicking body fluid. *Journal of Tissue Engineering and Regenerative Medicine* **2007,** 1, (1), 33-38.

77.   Costa, H. d. S.; Pereira, M. M.; Andrade, G. I.; Stancioli, E. F. B.; Mansur, H. S., Characterization of calcium phosphate coating and zinc incorporation on the porous alumina scaffolds. *Materials Research* **2007,** 10, 27-29.

78.   Fernandes, H.; Dechering, K.; Van Someren, E.; Steeghs, I.; Apotheker, M.; Leusink, A.; Bank, R.; Janeczek, K.; Van Blitterswijk, C.; de Boer, J., The Role of Collagen Crosslinking in Differentiation of Human Mesenchymal Stem Cells and MC3T3-E1 Cells. *Tissue Engineering Part A* **2009,** 15, (12), 3857-3867.

79.   Timmer, M. D.; Shin, H.; Horch, R. A.; Ambrose, C. G.; Mikos, A. G., In vitro cytotoxicity of injectable and biodegradable poly(propylene fumarate)-based networks: Unreacted macromers, cross-linked networks, and degradation products. *Biomacromolecules* **2003,** 4, (4), 1026-1033.

80.   Kim, J.; Lee, K. W.; Hefferan, T. E.; Currier, B. L.; Yaszemski, M. J.; Lu, L., Synthesis and evaluation of novel biodegradable hydrogels based on poly(ethylene glycol) and sebacic acid as tissue engineering scaffolds. *Biomacromolecules* **2008,** 9, (1), 149-157.

81.   Sung, H. J.; Chandra, P.; Treiser, M. D.; Liu, E.; Iovine, C. P.; Moghe, P. V.; Kohn, J., Synthetic polymeric substrates as potent pro-oxidant versus anti-oxidant regulators of cytoskeletal remodeling and cell apoptosis. *J Cell Physiol* **2009,** 218, (3), 549-57.

82.   Hynes, R. O., Integrins - a Family of Cell-Surface Receptors. *Cell* **1987,** 48, (4), 549-554.

83.   Wilson, C. J.; Clegg, R. E.; Leavesley, D. I.; Pearcy, M. J., Mediation of biomaterial-cell interactions by adsorbed proteins: A review. *Tissue Engineering* **2005,** 11, (1-2), 1-18.

84.   Garcia, A. J.; Vega, M. D.; Boettiger, D., Modulation of cell proliferation and differentiation through substrate-dependent changes in fibronectin conformation. *Molecular Biology of the Cell* **1999,** 10, (3), 785-798.

85.   Kim, J.; Hefferan, T. E.; Yaszemski, M. J.; Lu, L., Potential of Hydrogels Based on Poly(ethylene glycol) and Sebacic Acid as Orthopedic Tissue Engineering Scaffolds. *Tissue Engineering* **2009,** 15, (8), 2299-2307.

86.   Huang, W. B.; Carlsen, B.; Wulur, I.; Rudkin, G.; Ishida, K.; Wu, B.; Yamaguchi, D. T.; Miller, T. A., BMP-2 exerts differential effects on differentiation of rabbit bone marrow stromal cells grown in two-dimensional and three-dimensional systems and is required for in vitro bone formation in a PLGA scaffold. *Experimental Cell Research* **2004,** 299, (2), 325-334.

87.   Greenwald, A. S.; Boden, S. D.; Goldberg, V. M.; Khan, Y.; Laurencin, C. T.; Rosier, R. N.; Implants, C. B., Bone-graft substitutes: Facts, fictions, and applications. *Journal of Bone and Joint Surgery-American Volume* **2001,** 83A, (Supplement 2), 98-103.

88.   Langer, R.; Vacanti, J. P., Tissue Engineering. *Science* **1993,** 260, (5110), 920-926.

89.   Habibovic, P.; de Groot, K., Osteoinductive biomaterials—properties and relevance in bone repair. *Journal of Tissue Engineering and Regenerative Medicine* **2007,** 1, (1), 25-32.

90.   Albrektsson, T.; Johansson, C., Osteoinduction, osteoconduction and osseointegration. *European Spine Journal* **2001,** 10, S96-S101.

91.   Seeherman, H.; Wozney, J. M., Delivery of bone morphogenetic proteins for orthopedic tissue regeneration. *Cytokine & Growth Factor Reviews* **2005,** 16, (3), 329-345.

92.   Muschler, G. E.; Nakamoto, C.; Griffith, L. G., Engineering principles of clinical cell-based tissue engineering. *Journal of Bone and Joint Surgery-American Volume* **2004,** 86A, (7), 1541-1558.

93.   Urist, M. R., Bone: Formation by Autoinduction. *Science* **1965,** 150, (3698), 893-899.

94.   Goldberg, C. S.; Antonyshyn, O.; Midha, R.; Fialkov, J. A., Measuring pulsatile forces on the human cranium. *Journal of Craniofacial Surgery* **2005,** 16, (1), 134-139.

95.   Saito, N.; Okada, T.; Horiuchi, H.; Murakami, N.; Takahashi, J.; Nawata, M.; Ota, H.; Nozaki, K.; Takaoka, K., A biodegradable polymer as a cytokine delivery system for inducing bone formation. *Nature Biotechnology* **2001,** 19, (4), 332-5.

96.   Lutolf, M. P.; Weber, F. E.; Schmoekel, H. G.; Schense, J. C.; Kohler, T.; Muller, R.; Hubbell, J. A., Repair of bone defects using synthetic mimetics of collagenous extracellular matrices. *Nature Biotechnology* **2003,** 21, (5), 513-8.

97.   Ertel, S. I.; Kohn, J.; Zimmerman, M. C.; Parsons, J. R., Evaluation of Poly(Dth Carbonate), a Tyrosine-Derived Degradable Polymer, for Orthopedic Applications. *Journal of Biomedical Materials Research* **1995,** 29, (11), 1337-1348.

98.   Asikainen, A. J.; Noponen, J.; Mesimaki, K.; Laitinen, O.; Peltola, J.; Pelto, M.; Kellomaki, M.; Ashammakhi, N.; Lindqvist, C.; Suuronen, R., Tyrosine derived polycarbonate membrane is useful for guided bone regeneration in rabbit mandibular defects. *J Mater Sci Mater Med* **2005,** 16, (8), 753-8.

99.   Asikainen, A. J.; Noponen, J.; Lindqvist, C.; Pelto, M.; Kellomaki, M.; Juuti, H.; Pihlajamaki, H.; Suuronen, R., Tyrosine-derived polycarbonate membrane in treating mandibular bone defects. An experimental study. *J R Soc Interface* **2006,** 3, (10), 629-35.

100.   Li, P.; Bakker, D.; vanBlitterswijk, C. A., The bone-bonding polymer Polyactive(R) 80/20 induces hydroxycarbonate apatite formation in vitro. *Journal of Biomedical Materials Research* **1997,** 34, (1), 79-86.

101.   Du, C.; Meijer, G. J.; van de Valk, C.; Haan, R. E.; Bezemer, J. M.; Hesseling, S. C.; Cui, F. Z.; de Groot, K.; Layrolle, P., Bone growth in biomimetic apatite coated porous Polyactive 1000PEGT70PBT30 implants. *Biomaterials* **2002,** 23, (23), 4649-56.

102.   Nandakumar, A.; Yang, L.; Habibovic, P.; van Blitterswijk, C., Calcium phosphate coated electrospun fiber matrices as scaffolds for bone tissue engineering. *Langmuir : the ACS journal of surfaces and colloids* **2010,** 26, (10), 7380-7.

103.   Kim, H. J.; Kim, U. J.; Kim, H. S.; Li, C.; Wada, M.; Leisk, G. G.; Kaplan, D. L., Bone tissue engineering with premineralized silk scaffolds. *Bone* **2008,** 42, (6), 1226-34.

104.   Robinson, B. P.; Hollinger, J. O.; Szachowicz, E. H.; Brekke, J., Calvarial Bone Repair with Porous D,L-Polylactide. *Otolaryngology-Head and Neck Surgery* **1995,** 112, (6), 707-713.

105.   Shin, H.; Ruhe, P. Q.; Mikos, A. G.; Jansen, J. A., In vivo bone and soft tissue response to injectable, biodegradable oligo(poly(ethylene glycol) fumarate) hydrogels. *Biomaterials* **2003,** 24, (19), 3201-3211.

106.   Davies, J. E.; Matta, R.; Mendes, V. C.; Perri de Carvalho, P. S., Development, characterization and clinical use of a biodegradable composite scaffold for bone engineering in oro-maxillo-facial surgery. *Organogenesis* **2010,** 6, (3), 161-166.

107.   DeLustro, F.; Dasch, J.; Keefe, J.; Ellingsworth, L., Immune responses to allogeneic and xenogeneic implants of collagen and collagen derivatives. *Clin Orthop Relat Res* **1990**, (260), 263-79.

108.   Smith, D. M.; Afifi, A. M.; Cooper, G. M.; Mooney, M. P.; Marra, K. G.; Losee, J. E., BMP-2-based repair of large-scale calvarial defects in an experimental model: Regenerative surgery in cranioplasty. *Journal of Craniofacial Surgery* **2008,** 19, (5), 1315-1322.

109.   Hou, R.; Chen, F. L.; Yang, Y. W.; Cheng, X. B.; Gao, Z.; Yang, H. W. O.; Wu, W.; Mao, T. Q., Comparative study between coral-mesenchymal stem cells-rhBMP-2 composite and auto-bone-graft in rabbit critical-sized cranial defect model. *Journal of Biomedical Materials Research Part A* **2007,** 80A, (1), 85-93.

110.   Weber, F. E.; Eyrich, G.; Gratz, K. W.; Thomas, R. M.; Maly, F. E.; Sailer, H. F., Disulfide bridge conformers of mature BMP are inhibitors for heterotopic ossification. *Biochemical and Biophysical Research Communications* **2001,** 286, (3), 554-558.

111.   Lu, L.; Peter, S. J.; Lyman, M. D.; Lai, H. L.; Leite, S. M.; Tamada, J. A.; Uyama, S.; Vacanti, J. P.; Langer, R.; Mikos, A. G., In vitro and in vivo degradation of porous poly(DL-lactic-co-glycolic acid) foams. *Biomaterials* **2000,** 21, (18), 1837-1845.

112.   Kim, J.; Magno, H. M.; Alvarez, P.; Darr, A.; Kohn, J.; Hollinger, J. O., Osteogenic Differentiation of Pre-Osteoblasts on Biomimetic Tyrosine-Derived Polycarbonate Scaffolds *Biomacromolecules* **2011,** In press.

APPENDIX 1

"Synthesis, degradation and biocompatibility of tyrosine-derived polycarbonate scaffolds"

Preface

M. H. R. Magno, J. Kim, A. Srinivasan, S. McBride, D. Bolikal, A. Darr, J. O. Hollinger and J. Kohn, Synthesis, degradation and biocompatibility of tyrosine-derived polycarbonate scaffolds. *Journal of Materials Chemistry*, 2010, **20**, 8885-8893 – Reproduced by permission of the Royal Society of Chemistry

Abstract

Polycarbonate terpolymers consisting of desaminotyrosyl-tyrosine alkyl esters (DTR), desaminotyrosyl-tyrosine (DT), and low molecular weight blocks of poly(ethylene glycol) (PEG) are a new class of polymers that have good engineering properties while also being resorbable *in vivo*. This study is the first evaluation of their (i) degradation behavior, (ii) *in vitro* cytotoxicity, and (iii) *in vivo* biocompatibility. Porous, tissue engineering scaffolds were prepared by a combination of solvent casting, porogen leaching and phase separation techniques. The scaffolds (>90% porosity) displayed (i) a bimodal pore distribution with micropores of less than 20 μm and macropores between 200 and 400 μm, (ii) a highly interconnected and open pore architecture, and (iii) a highly organized microstructure where the micropores are oriented and aligned along the walls of the macropores. Molecular weight (number average, Mn) and mass loss were determined in vitro (PBS at 37 $^{\circ}$C) for up to 28 days. All three terpolymer compositions were fast degrading and retained only 10% of their initial molecular weight after 21 days, while mass loss during the 28 days was polymer composition-dependent. *In vitro* biocompatibility of the polymer scaffolds was determined up to 14 days by measuring metabolic activity of MC3T3.E1 (subclone 4) pre-osteoblasts. The outcome showed no statistical difference between cells cultured in monolayer and all tested polymer scaffolds. Robust cell attachment throughout the scaffold volume was observed by confocal microscopy and SEM. The biocompatibility of resorbing scaffolds was evaluated at 12 weeks in a critical sized defect (CSD) rabbit calvaria model and showed only a minimal inflammatory response. Overall, the results reported here illustrate the

potential utility of tyrosine-derived polycarbonate terpolymers in the design of tissue engineering scaffolds.

Introduction

The use of degradable polymers as tissue engineering scaffolds is widely investigated. Within this area of research, a significant need exists for the development of tissue scaffolds for bone regeneration.[1, 2] However, they have drawbacks including the production of a local acidic environment upon degradation. This property has limited the potential utility of aliphatic polyesters in bone tissue engineering. [3, 4] The tyrosine-derived terpolymers being introduced in this study are a potential alternative to poly(α-hydroxyester)s. The monomeric unit for all tyrosine-derived polycarbonates is desaminotyrosyl-tyrosine alkyl ester (DTR), a derivative of naturally occurring tyrosine dipeptide. This particular structure gives rise to a family of non-toxic diphenolic monomers. [5-8]

A series of previous studies highlighted the potential of a specific tyrosine-derived polycarbonate, poly(DTE carbonate), for use in orthopedic applications due to its *in vivo* bone biocompatibility and physical properties.[9] The strength of poly(DTE carbonate) exceeds that of other degradable polymers including poly(ε-caprolactone) and poly(ortho ester)s. Poly-(DTE carbonate) exhibits a tensile modulus comparable to that of high molecular weight poly(L-lactic acid) (2.4–10 GPa).[10, 11]

Poly(DTE carbonate) has been explored in several biomedical applications, including low or minimally load-bearing orthopedic implants. Poly(DTE carbonate) pins were found to degrade at about the same rate as high molecular weight PLLA pins [12]

while erosion and complete resorption of poly(DTE carbonate) implants were too slow for most practical applications.[13] Previous efforts to accelerate the degradation rates of tyrosine-derived polycarbonates focused on the synthesis of copolymers of poly(ethylene glycol) (PEG) and DTE, such as poly(DTE-*co*-PEG carbonate)s.[14, 15] As an alternative approach, copolymers of DTR and desaminotyrosyl-tyrosine (DT), such as poly(DTR-*co*-DT carbonate) were also synthesized and tested. [16, 17]

Yu and Kohn [14] showed that poly(DTE-*co*-PEG carbonate)s undergo backbone degradation at a rate much faster than poly(DTE carbonate). However, the incorporation of PEG into the backbone of poly(DTE carbonate) also affected the mechanical and biological properties of the resulting polymers. The presence of PEG in the polymer backbone was associated with an increased tendency to absorb water and a significant reduction of mechanical strength.[14] The biological properties were also affected: the amount of adsorbed protein, *e.g.*, human fibronectin, on the polymers and its bioactivity decreased at PEG(MW1000) molar fractions greater than 6%.[18] Additionally, cell motility of L929 mouse fibroblast cells had a biphasic response: cell motility increased with increasing molar fraction of PEG in the copolymer up to about 4 mol%, and then decreased at higher PEG molar fractions.[19] A study also evaluated the potential of PEG containing tyrosine-derived polycarbonates to influence the osteogenic differentiation of human mesenchymal stem cells.[20] Thus, incorporation of PEG into the polymer backbone allows for modification of bulk and surface properties.[14, 15, 18]

The study of poly(DTR-*co*-DT carbonate)s by Abramson[21] provided an alternative approach to accelerate the rate of polymer degradation of poly(DTR carbonate)s: copolymers of DTR and DT degraded faster *in vitro* with increasing molar

fraction of DT in the polymer backbone. Levene [22] showed a similar increase in the rate of polymer degradation *in vivo*, and demonstrated the potential of DT containing copolymers in bone tissue engineering. Based on these prior studies, DTR, DT, and PEG were combined to create a new terpolymer system, referred to as tyrosine-derived polycarbonate terpolymers (Figure A1.1). These terpolymers may preserve the excellent bone biocompatibility of poly(DTE carbonate) while providing for precise control of (i) the rate of degradation and resorption, (ii) the bulk and surface properties, and (iii) the biological interactions of these polymers with cells and tissues. Therefore, the objective of the current study was to determine the effects of the terpolymer composition on physical properties, degradation behavior, and biological responses.

Materials and methods

Materials

All chemicals used were reagent grade, HPLC grade and high purity. These chemicals were used as received except desaminotyrosyl-tyrosine ethyl ester (DTE, Integra Life Sciences, Plainsboro, NJ) which was purified further by washing with dichloromethane (DCM). Tyrosine *tert*-butyl ester (TtBu) was purchased from Bachem (Torrance, CA). Desaminotyrosine or 3-(4'-hydroxyphenyl) propionic acid (Dat) was purchased from Apin Chemicals (UK). Hydroxybenzotriazole (HOBt), bis(trichloromethyl)carbonate (triphosgene) and poly(ethylene glycol), M_w 1000 (PEG$_{1K}$) were obtained from Fluka (Switzerland). 1-Ethyl-3-(3-dimethylaminopropyl) carbodiimide hydrochloride (EDCI) was purchased from Kawaguchi Chemical Industry (Japan). Poly(ethylene glycol) M_w 2000 (PEG$_{2K}$) was purchased from Clariant Corporation (Charlotte, NC). Tetrahydrofuran (THF) and *N,N*-dimethylformamide (DMF) were obtained from EMD (Germany). Pyridine, dichloromethane (DCM), methanol (MeOH), 1,4-dioxane and isopropyl alcohol (IPA) were obtained from Fisher Scientific (Pittsburgh, PA). Dimethylsulfoxide-d$_6$ (DMSO-d$_6$), deuterated chloroform (CDCl$_3$), trifluoroacetic acid (TFA), HPLC water with 0.1% TFA, sodium chloride (NaCl) and Dulbecco's phosphate buffered saline, modified, without calcium chloride and magnesium chloride, (PBS) were obtained from Sigma-Aldrich Chemical Co. (St Louis, MO).

Synthesis and characterization

Tyrosine-derived polycarbonate terpolymers were synthesized by condensation reaction of triphosgene and tyrosine-derived diphenol.[5, 6, 14] The preparation of E2502(2K) described here serves as a typical example. A mixture of DTE (15 g, 0.04 mol), desaminotyrosyl-tyrosine tert-butyl ester (DTtBu) (5.5 g, 0.01 mol) and PEG2K (2.3 g, 10 mmol) was dissolved in 140 mL of DCM and 18 mL of pyridine in a round bottom flask that was continuously purged with N_2 gas. A solution of 6.3 g (60 mmol) of triphosgene in 20 mL of DCM was added to the reaction mixture with stirring over a two-hour period at room temperature. After the desired molecular weight was reached (around 200 kDa polystyrene equivalent MW by GPC using DMF as mobile phase), TFA (90 mL) was added to the reaction mixture. The polymer was precipitated using isopropyl alcohol (IPA, 400 mL) and then successively washed with IPA, IPA : H_2O (1:1) and H_2O. The precipitation and washings were carried out in a 4 L industrial blender. The polymer was allowed to dry by blowing N_2 gas overnight and then in a vacuum oven at 40 $^{\circ}$C for 48 hours. The polymer composition was determined by ^{1}H NMR in DMSO-d_6 or CDCl$_3$ (Varian 400 or 500 MHz). By integration of the ^{1}H NMR peaks, the molar ratio of DTR, DT and PEG was calculated. Molecular weights (number average, M_n) and polydispersity index (PDI) were determined using GPC relative to polystyrene standards. The GPC system consisted of a 515 HPLC pump, 717plus auto sampler, a 2414 RI detector and Empower Pro® Software (Waters Corporation, Milford, MA). Two PL gel columns (Polymer Laboratories, Amherst, MA), 1,000 and 100,000 Å , were used in series. DMF containing 0.1% TFA at a flow rate of 0.8 mL min^{-1} was used as the mobile phase. The molecular weights were computed against polystyrene standards.

The glass transition temperatures (T_g) of the polymers were determined in the second heat cycle as the midpoint of the transition using differential scanning calorimetry (DSC) (DSC2920, TA Instruments, New Castle, DE) with a heating rate of 10 ^{o}C min^{-1}.

To simplify the naming of the tyrosine-derived terpolymers, the notation RXXYY(MW) is used to name poly(DTR-*co*-XX%-DT-*co*-YY%-PEGMW carbonate) where R is the alkyl pendent chain, XX is the mole percent of DT, YY is the mole percent of PEG and MW is the weight average molecular weight of PEG. As an example, poly(DTE carbonate) will be designated as E0000 where E stands for ethyl while poly(DTE-*co*-25%-DT-*co*-02%-PEG$_{2K}$ carbonate) will have a notation of E2502(2K).

Scaffold fabrication

Scaffolds were fabricated using a combination of solvent casting/porogen leaching/phase separation techniques.[23] Briefly, 300 mg of polymer were dissolved in 300 mL of DI water and 3 mL of 1,4-dioxane. Sodium chloride (NaCl) which was sieved to 212–425 μm particle size was weighed into a Teflon dish (11 g). The polymer solution was slowly poured over NaCl and was allowed to diffuse undisturbed for 1 hour. The Teflon dish was covered to prevent evaporation of solvent. After 1 hour, the mold was frozen in liquid nitrogen for 5–10 minutes and then freeze-dried for 48 hours. Dried scaffolds were cut to size using custom-made stainless steel punchers with inner diameter of 16.2 mm or 10.4 mm and incubated in DI water at room temperature to leach out NaCl. The presence of Cl$^-$ ions was determined by addition of AgNO$_3$ (silver nitrate) solution to the wash. The formation of a white precipitate (AgCl) upon addition of the AgNO$_3$ solution indicated that NaCl was still leaching out from the scaffold. When no

further precipitate could be detected, the leached scaffolds were removed from DI water, blotted dry and dried for 48 hours under vacuum at room temperature. Scaffolds for *in vitro* cell studies and *in vivo* rabbit calvaria experiments were sterilized using a 12 hour cycle of ethylene oxide (EtO) at room temperature (AN74i, Andersen Products, Haw River, NC). Sterility was verified using a Steritest® (AN-80, Andersen Products, Haw River, NC). The samples were subsequently degassed in a vacuum oven (-101.6 kPa) at room temperature and the absence of residual EtO was verified by ^{1}H NMR. Pore architecture of sputter coated scaffolds (SCD 004, 30 milliAmps for 120 seconds with Au/Pd) was evaluated using a scanning electron microscope (SEM, Amray 1830I, 20 kV). A 75x magnification was used to determine the gross structure and a 250x magnification was used to evaluate the microporous structure of the scaffolds.

In vitro degradation and erosion

The degradation and erosion profiles of tyrosine-derived polycarbonate scaffolds were measured by incubating scaffold discs in PBS (phosphate buffered saline, 10 mL) in scintillation vials with one scaffold per vial at 37 °C. Aliquots of the buffer and the scaffold were collected at predetermined intervals up to 28 days. To allow PBS to permeate into the scaffolds, the vial containing the scaffold and the PBS was subjected to several cycles of atmospheric and vacuum pressure before incubation.[22, 24] Scaffolds at t=0 were subjected to the same conditions except they were not incubated. The retrieved scaffolds were rinsed three times with DI water, blotted dry, and freeze-dried. GPC analysis of freeze-dried scaffold dissolved in 1 mL DMF with 0.1% TFA was used to determine the molecular weight loss. To measure mass loss, aliquots from the supernatant

were treated with 1 N NaOH to hydrolyze the terpolymer fragments to DT and PEG_{MW}. Acidification with 12 N HCl followed by HPLC analysis gave the amount of DT in the supernatant.

The HPLC system consisted of a Waters Alliance 2695 Module, Waters 2487 Dual l Absorbance Ultraviolet (UV) Detector and Empower Pro® Software (Waters Corporation, Milford, MA). The column was a Perkin-Elmer Pecosphere C18 (33 x 4.6 mm; 3 μm particle size; cat. # 0258-1064, Waltham, MA). The mobile phase was a mixture of water and methanol both containing 0.1% TFA with a gradient of 80:20 to 40:60 in 6 minutes. The column temperature was set at 25 ^{o}C. The injection volume was 5 μL. The concentration of DT in the hydrolyzed aliquot was determined from a DT standard calibration curve. The amount of DT that has leached into the buffer was a good approximation of the extent of erosion of the polymer. All analyses were done in triplicate. Samples were collected weekly except for E2502(2K) where samples were collected for days 1 and 2 and weekly thereafter.

In vitro cytotoxicity of the scaffolds

To determine the cytotoxicity of the polymer scaffolds, MC3T3-E1 (subclone 4) cells (ATCC, Manassa, VA) were seeded at a density of 5000 cells cm^{-2} on the bottom of a tissue culture plate and incubated for 24 h. The scaffolds were then placed into the inserts of the transwell (Costar, membrane pore size: 3.0 μm, Pittsburgh, PA) and the cells were further cultured for up to 14 days. Transwell inserts without the polymer scaffolds were also transferred to the culture plates containing the cells and used as a control. On days 1, 7 and 14, the cell viability was determined using a colorimetric cell

metabolic assay (CellTiter 96 Aqueous One Solution, Promega, Madison, WI), based on the MTS tetrazolium compound, 3-(4,5-dimethyl-2-yl)-5-(3-carboxymethoxyphenyl)-2-(4-sulfophenyl)-2*H*-tetrazolium. The reagent solution was added to each well and incubated for 1 h at 37 $^\circ$C. The supernatant from each well was transferred to a 96-well plate. The absorbance at 490 nm was measured using a plate reader (Tecan, Männedorf, Switzerland), which is directly correlated to the viable cell number, and inversely correlated to the toxicity of the polymer scaffolds. For each time period, the metabolic activity of the cells cultured was normalized to the control and the initial number of cells.

Cell attachment and characterization

To determine cell attachment on the 3D scaffolds, murine calvaria derived pre-osteoblasts, MC3T3-E1 (subclone 4) were used (ATCC, Manassa, VA). Before cell seeding, the sterile scaffolds were hydrated[25] for one hour in a α-MEM medium (Gibco, Carlsbad, CA) supplemented with 10% fetal bovine serum (ATCC), 100 U mL^{-1} penicillin, and 100 μg mL^{-1} streptomycin. The cells were then seeded on each scaffold at a density of 2 x 10^5 cells and cultured in the medium for up to 4 days at 37 $^\circ$C in a 5% CO_2 atmosphere. At days 1 and 4, the cell viability and attachment were assessed using a Live/Dead staining method and SEM. For Live/Dead staining, the scaffold was washed with PBS and incubated in 0.5 mL of the Live/Dead dye solution (5 μL of Calcein AM and 20 μL of Ethidium homodimer dye in 10 mL of PBS) for 30 min. The cell construct was subjected to a confocal laser scanning microscopy (Fluoview 1000, Olympus, Center Valley, PA) to visualize relative cell viability over time. The percentage of live cells was quantified using the image analysis program (Optimas version 6.5, Media Cybernetics,

Bethesda, MD) by measuring the percentage of live and dead cell areas in at least three randomly chosen microscopy images. To further assess the morphology of adherent cells on the scaffolds, each cell construct was fixed in 2.5% glutaraldehyde and post-fixed with 1% osmium tetroxide in 0.1 M sodium cacodylate buffer (pH 7.2). Scaffolds were then dehydrated in ascending grades of ethanol (50–100%) and critical point dried. Samples were bisected sagittally to expose the inner core of the foam, attached to an SEM stub with double-sided tape, and sputter coated with gold at different angles using a Pelco SC-6 Sputter Coater (Redding, CA). Samples were then examined with a Hitachi 2460N scanning electron microscope (Tokyo, Japan). Digital images were obtained using Quartz PCI image management software (Hitachi, Pleasanton, CA).

In vivo biocompatibility assessment in rabbit critical-sized calvarial defect

All surgical procedures involving animals were approved by the Institutional Animal Care and Use Committee (IACUC) at Rutgers University. The NIH Guide for Care and Use of Laboratory Animals was observed in the treatment of all experimental animals. Research was conducted in compliance with the Animal Welfare Act and other Federal statutes relating to animals and experiments involving animals. The research adheres to the principles set forth in the Guide for Care and Use of Laboratory Animals, National Research Council, 1996.

Skeletally mature New Zealand White male rabbits were used to assess *in vivo* biocompatibility. Following standard practices for aseptic surgery, a critical sized defect (CSD) in the calvaria was created in the parietal bone using a 15 mm surgical trephine as

described previously.[26] A semilunar coronal incision was prepared through soft tissues with sharp dissection and the parietal bones were visualized. Using a surgical drill with a trephine supplemented with physiological saline for irrigation, a craniotomy (15 mm diameter) was prepared midway between the supraorbital ridge and across the mid-sagittal sinus. A tyrosine-derived polycarbonate scaffold was inserted into the single craniotomy and soft tissues were closed in layers with resorbable 4-0 Dexon sutures. The skin was closed with surgical staples.

After 12 weeks, rabbits were sacrificed humanely according to NIH and University guidelines with an intravenous (*i.v.*) overdose of barbiturate (200 mg kg^{-1} body weight). Selected tissues were placed immediately into formalin for histological processing and analysis.

Histology

The specimens were dehydrated in ascending grades of alcohol, cleared in xylene at 4 $^{\circ}$C to minimize implant solvation during processing and embedded (undecalcified) in poly(methyl methacrylate). The specimens were cut and ground to 30 μm thick sections with an Exakt diamond bandsaw and MicroGrinder (Exakt Technologies, Oklahoma City, OK). Slides were acid etched with 1% formic acid for three and a half minutes, sonicated with 50% ethyl alcohol for two minutes and then air dried. The slides were stained with Sanderson's Rapid Bone Stain and counterstained with van Gieson's picrofuchsin, which resulted in soft tissue staining blue and bone staining pink/red.

Statistical analysis

All data are represented as means ± standard deviations. Statistical analysis was performed using single factor analysis of variance (ANOVA) with Tukey–Kramer's *post hoc* test at a significance level of $\rho \leq 0.05$.

Results

To simplify the naming of the tyrosine-derived terpolymers, the notation RXXYY(MW) is used to name poly(DTR-*co*-XX%-DT-*co*-YY%-PEGMW carbonate)s. See the Methods section for a detailed explanation of this nomenclature.

Polymer synthesis and fabrication

Using the procedure described, the following tyrosine-derived polycarbonates were synthesized: E1501(2K), E2002(1K), and E2502(2K). The GPC-molecular weight (M_n), polydispersity index (PDI), T_g and composition by ^{1}H NMR are given in Table A1.1.

Table A1.1. Characterization of tyrosine-derived polycarbonates

Polymer	M_n (kDa)/ PDI	T_g (°C)	Composition (mol%)		
			DTE	DT	PEG
E1501(2K)	172/1.44	91	84	15	1
E2002(1K)	255/1.33	83	78	20	2
E2502 (2K)	217/1.28	83	74	24	2

The structure of E2502(2K) and chemical shifts of a typical ^{1}H NMR spectrum of the polymer are listed in Figure A1.1.

These polymers were fabricated into 3D porous scaffolds and pore architecture was assessed by SEM. The scaffold dimensions were 9 mm (diameter) x 2 mm (thickness) and the average mass of E1501(2K) scaffolds was 4.2 ± 0.8 mg (n = 66), of E2002(1K) scaffolds was 5.0 ± 0.7 mg (n = 15) and of E2502(2K) scaffolds was 5.6 ± 0.9 mg (n = 36). Each scaffold possessed (i) a bimodal pore distribution, with micropores that are less than 20 μm and macropores between 200 and 400 μm, (ii) a highly interconnected and open pore architecture, and (iii) micropores that are oriented and aligned along the sides of the macropores (Figure A1.2).

In vitro degradation of the scaffolds

The *in vitro* degradation and erosion of E1501(2K), E2002(1K) and E2502(2K) scaffolds in PBS at 37 ^{o}C were determined up to 4 weeks by molecular weight (MW) retention and mass retention. After a week of incubation in PBS at 37 ^{o}C, E1501(2K) and E2002(1K) scaffolds retained only 20% of their MW while E2502(2K) scaffolds had eroded completely (Figure A1.3A). E2502(2K) degradation was evident as early as day 1 with only 50% MW retained and with less than 40% MW after day 2. These results indicate that for all scaffold compositions, rapid degradation of the polymer backbone occurred within 7 days of incubation in PBS at 37 ^{o}C. Although substantial loss in MW was observed, mass loss was not as drastic. At day 7, E2502(2K) was completely eroded in PBS while only approximately 10% of E1501(2K) and E2002(1K) eroded (Figure

A1.3B). Overall, the rate of *in vitro* degradation and erosion increased with increase of DT and PEG mole fractions in the polymer backbone.

In vitro cytotoxicity of the scaffolds

The *in vitro* cytotoxicity of the polymer scaffolds was determined using MC3T3-E1.4 pre-osteoblasts cultured in the presence of the scaffolds. The percent metabolic activity of the cells was normalized to that of the cells cultured on tissue culture polystyrene (TCPS) without the scaffolds (Figure A1.4A). The metabolic activity of the MC3T3-E1.4 pre-osteoblasts with tyrosine-derived polycarbonate scaffolds was similar to the control throughout the tested time periods. Although a statistical difference was detected at day 7 between E2502(2K) and the control, the metabolic activity of the cells with the tyrosine-derived polycarbonate scaffolds was over 98% at any given time period. These results indicate that the tyrosine-derived polycarbonate based scaffolds have no detrimental effect on the metabolic activity of MC3T3-E1.4 pre-osteoblasts when compared to the control. The number of cells at each time period was measured and normalized to the amount initially seeded (Figure A1.4B). There was no statistical difference in the number of cells cultured. The number of cells increased over time, indicating that the cells proliferated in the presence of the tyrosine-derived polycarbonate scaffolds.

Cell attachment

MC3T3-E1.4 pre-osteoblasts were seeded on the tyrosine-derived polycarbonate scaffolds and cell attachment was determined. The confocal microscopic images showed that after 24 h of cell culture, almost all attached cells were viable and there were few dead cells (Figure A1.5). There was no statistical difference in the cell viability between the samples ($\rho > 0.05$), indicating that most of the attached MC3T3-E1.4 pre-osteoblasts were viable.

The MC3T3-E1.4 cells on the scaffolds after 24 h had attached and spread on the surface and throughout the pores of the tyrosine-derived polycarbonate scaffolds, regardless of polymer composition (Figure A1.6). These results indicate that the bimodal pore structured tyrosine-derived polycarbonates avidly support cell attachment as well as spreading on the surface without any further modification.

Effect of degassing time on cytotoxicity

The effect of degassing time after EtO sterilization of the scaffolds on cell viability was also determined using Live/Dead staining (Figure A1.7). Most of the MC3T3-E1.4 pre-osteoblasts were viable on scaffolds with no macroscopic and statistical difference ($p > 0.05$) in the cell viability between the samples after 4 days of culture at 37$^{\text{o}}$C. Moreover, the ^{1}HNMR (in CDCl$_3$) spectra of the scaffolds degassed for 48 h and 14 days did not reveal a detectable peak at 2.54 ppm (methylene protons of EtO), indicating that 2 day degassing of EtO sterilized scaffolds may be enough to completely remove residual EtO.

In vivo biocompatibility

A critical sized defect in a rabbit skull (15 mm diameter) was created to assess *in vivo* biological performance of tyrosine-derived polycarbonate scaffolds. The critical sized bone defect showed some soft tissue healing in the specimens at 12 weeks post-implantation (Figure A1.8A). The host implant bones were bridged by extensive fibrous connective tissue (Figure A1.8A and D) and the degradation of the polymer was quite marked, >90% of the implant degraded by 12 weeks (Figure A1.8D and E). Neither osteolysis nor any severe inflammatory response was observed within the specimens as a consequence of the implanted material.

New cancellous bone formation was limited to small areas along the implant/host calvaria tissue interface and only to the degree that is anticipated in the normal sequence of wound healing (Figure A1.8B). There was no evidence of either pericranial or dural bone growth. Likewise, there was no evidence of bulk new bone formation within the implant as a result of the rapid degradation profile of the polymer. Within the medullary cavity of the calvaria, there was evidence of osteoblast activity, regions of newly formed osteoid and the presence of erythrocytes, all of which suggest a normal wound healing response (Figure A1.8C and F). Overall, the implant materials were found to be biocompatible, although histological assessment of their performance was not possible due to their rapid degradation profile.

Discussion

The optimized synthesis conditions described above yielded off-white high molecular weight polymers (around 200,000 Daltons) with a narrow molecular weight distribution (Table A1.1). Chemical structure of these polymers was determined by ^{1}H NMR. The mole fractions of DTE, DT and PEG$_{MW}$ were estimated from the integration of the proton peaks. These values were very close to theoretical values. In previous studies, Yu and Kohn[14] have shown that poly(DTR-*co*-PEG carbonate)s are random copolymers based on the integration of six carbonate peaks from ^{13}C NMR. These observations were confirmed by Pesnell[27] who showed that the iodinated versions of the polymers described here, poly(I$_2$DTR-*co*-I$_2$DT-*co*-PEG carbonate)s, also appear to be random copolymers. The terpolymers described in this study were synthesized using a similar polycondensation reaction, and are expected to possess random copolymer structure as well. Further, Yu and Kohn[14] observed that the dry T_g of poly(DTR-*co*-PEG carbonate)s decreased with increasing mole fraction of PEG while Abramson[21] observed that T_g increased with increasing mole fraction of DT in poly(DTR-*co*-DT carbonate)s. In this current study, an increase in the mole fraction of PEG$_{2K}$ resulted in a decrease in the T_g, as in the case of E1501(2K) and E2502(2K) (Table A1.1) indicating that the effect of increasing PEG mole fraction had a more significant effect on the T_g than the DT mole fraction. For E1501(2K) and E2002(1K) where PEG weight% was the same, 2.6%, one would expect a higher T_g for the latter because of an increase in DT, but this was not seen.

3D porous scaffolds having bimodal and interconnected pore architecture were obtained. Macropores (pore diameter between 200 and 400 μm) were created from

casting on NaCl crystals that were eventually leached out. Micropores (less than 20 μm) were formed when phase separation of the polymer solution occurred during rapid cooling in liquid N_2. The porosity of similar 3D tyrosine-derived polycarbonate scaffolds, fabricated in previous studies using this technique, was found to be approximately 95% by mercury porosimetry.[22] The macropores were highly interconnected and the micropores that were oriented and formed channels around the bigger pores enhanced this interconnectivity as seen in SEM images (Figure A1.2).

The rate of *in vitro* degradation of tyrosine-derived polycarbonates is affected by the composition of the polymer backbone. It has been shown that compression molded films of poly(DTE carbonate) degraded more slowly than films of poly(DTE-*co*-PEG carbonate)s and that increasing amount of PEG resulted in faster degradation, likely due to an increase in water uptake.[14] Abramson[21] has shown the same effect for films of poly(DTE-*co*-DTcarbonate)s: the rate of degradation increased as the mole fraction of DT was increased. Our studies indicate that the simultaneous presence of PEG and DT within the terpolymer structure has a synergistic effect on accelerating both the *rate* of degradation (*i.e.*, molecular weight loss, Figure A1.3A) and the rate of resorption (*i.e.*, mass loss, Figure A1.3B).

Dry scaffolds were sufficiently strong for surgical implantation; but, when scaffolds were incubated in PBS, mechanical strength decreased quickly over time. Because the polymers used in the current study had degraded significantly within 7 days, mechanical strength could not be appropriately measured for a meaningful length of time. For this study, the test polymers were intentionally designed to be fast degrading. For initial biocompatibility studies, the use of fast degrading test articles ensures that the

implant sites are exposed to high concentrations of degradation products, increasing the sensitivity of the biocompatibility assays. Obviously, for use in medical applications, further optimization of the terpolymer composition is needed to ensure that scaffolds have sufficient strength retention over the time required for tissue regeneration to occur.

The use of transwell inserts was an effective method to evaluate the *in vitro* cytotoxicity of the scaffolds as a function of incubation time since degradation products such as monomers or oligomers effectively go through the membrane of a transwell (pore size: 3.0 μm) while polymers stay in the transwell without directly having contact with cells.[28, 29] MC3T3-E1.4 pre-osteoblast viability in the presence of tyrosine-derived polycarbonate scaffolds revealed cyto-compatibility when compared to polymer-free tissue culture medium over 14 days. In addition, there was no significant pH change in the media throughout the test period between the test groups and the polymer-free medium.

Poly(hydroxyethyl methacrylate) (HEMA) and glycosaminoglycan containing hydrogels contain free carboxylic groups such as the ones found in DT. These hydrogels inhibit macrophage adhesion and complement activation.[30] DT-containing polycarbonates may exhibit similar cellular responses. In contrast, the degradation products released from poly(α-hydroxyester)s can be cytotoxic due to their inherent acidity.[3]

The MC3T3-E1.4 pre-osteoblast attachment on all 3D tyrosine-derived polycarbonate scaffolds was robust at 24 h following seeding (Figure A1.6). Cell attachment behavior was not studied beyond 24 hours on E2502(2K) due to significant disintegration of the scaffold.

Ethylene oxide (EtO) sterilization is widely used to sterilize degradable, polymeric biomaterials, which are usually not compatible with high temperature sterilization process such as autoclaving.[31] However, one of the main concerns is residual EtO due to its potential toxicity and/or carcinogenicity.[31, 32] To completely remove EtO from the materials, scaffolds were degassed in vacuum at room temperature for 14 days[33], although the characteristic EtO peak in the ^{1}H NMR spectrum of samples was no longer detectable after as little as 2 days of degassing. To further assess *in vitro* cytocompatibility, a Live/Dead assay was utilized to ensure that the degassing period was sufficient to ensure the viability of cells attached to test scaffolds (Figure A1.7). No difference in cell viability was noted.

To assess *in vivo* performance of the polymers, we chose the rabbit cranial critical sized defect model, which has been well established and widely used as an *in vivo* model to evaluate bone formation as well as *in vivo* characteristics of tissue engineering scaffolds.[34-36] In general, the tissue response to the implants showed a normal wound healing response in spite of the fact that massive degradation of the test materials had occurred within 12 weeks post-implantation (Figure A1.8). There was only a minimal inflammatory response and a thin fibrous capsule observed. Since the fastest degrading terpolymer compositions had completely resorbed during the test period, the histological assessment of the *in vivo* tissue response is a strong indicator of the biocompatibility of the tested polycarbonate terpolymer compositions.

Conclusions

Here we present the first comprehensive evaluation of tyrosine-derived polycarbonate terpolymers as a new class of degradable biomaterials. The evaluation included synthesis and chemical structure proof, a demonstration of the feasibility to fabricate tissue scaffolds, and a detailed study of *in vitro* cytotoxicity and biocompatibility in a clinically relevant rabbit model. Our results indicate that tyrosine-derived polycarbonate terpolymers exhibit minimal cytotoxicity and a normal wound healing response *in vivo* associated with only minimal tissue inflammation. These results are particularly noteworthy since fast degrading implants were tested, some of which resorbed completely over the course of the 12 week test period. This experimental design ensured that the implant sites were exposed to significant amounts of polymer degradation products. Another important attribute of this class of polymers is the apparent tunability of their degradation and resorption profiles. While only a small subset of the entire range of terpolymer compositions were explored here, our results indicate that variations in the molar fractions of either DT or PEG within the polymer backbone can be used to tune the degradation and resorption profiles of these polymers. Overall, the results presented in this study illustrate the potential for this exciting class of polymers to the field of tissue engineering.

Acknowledgements

References

1.   M. Schieker, C. Heiss and W. Mutschler, *Unfallchirurg*, 2008, **111**, 613-620.

2.   H. Takigami, K. Kumagai, L. Latson, D. Togawa, T. Bauer, K. Powell, R. S. Butler and G. F. Muschler, *J Orthop Res*, 2007, **25**, 1333-1342.

3.   J. O. Hollinger, *Biomedical applications of synthetic biodegradable polymers*, CRC Press, Boca Raton, 1995.

4.   G. Z. Zhu, S. R. Mallery and S. P. Schwendeman, *Nature Biotechnology*, 2000, **18**, 52-57.

5.   S. Pulapura and J. Kohn, *Biopolymers*, 1992, **32**, 411-417.

6.   S. I. Ertel and J. Kohn, *Journal of Biomedical Materials Research*, 1994, **28**, 919-930.

7.   K. A. Hooper and J. Kohn, *Journal of Bioactive and Compatible Polymers*, 1995, **10**, 327-340.

8.   S. L. Bourke and J. Kohn, *Advanced Drug Delivery Reviews*, 2003, **55**, 447-466.

9.   J. Choueka, J. L. Charvet, K. J. Koval, H. Alexander, K. S. James, K. A. Hooper and J. Kohn, *Journal of Biomedical Materials Research*, 1996, **31**, 35-41.

10.   A. U. Daniels, M. Chang, K. P. Andrianø and J. Heller, *Journal of Applied Biomaterials*, 1990, **1**, 57-78.

11.   I. Engelberg and J. Kohn, *Biomater*, 1991, **12**, 292-304.

12.   K. A. Hooper, N. D. Macon and J. Kohn, *Journal of Biomedical Materials Research*, 1998, **41**, 443-454.

13.   K. James, H. Levene, J. R. Parsons and J. Kohn, *Biomaterials*, 1999, **20**, 2203-2212.

14.   C. Yu and J. Kohn, *Biomaterials*, 1999, **20**, 253-264.

15. C. Yu, S. S. Mielewczyk, K. J. Breslauer and J. Kohn, *Biomaterials*, 1999, **20**, 265-272.

16. S. D. Abramson, D. Bolikal, H. Levene, J. Simon and J. Kohn, in *Sixth World Biomaterials Congress*, eds. L. C. Lucas, J. M. Anderson, C. R. Howlett, Y. H. Kim, C. J. Kirkpatrick, T. Okano, R. Pilliar and X. Zhang, Society for Biomaterials, Kamuela, HI, 2000, p. 1164.

17. J. F. Tschopp, J. O. Tolley, T. Malaney, C. Mazur, R. Bellantoni, S. D. Abramson, J. Kohn, B. Wang and J. E. Kemnitzer, in *Sixth World Biomaterials Congress Society for Biomaterials*, eds. L. C. Lucas, J. M. Anderson, C. R. Howlett, Y. H. Kim, C. J. Kirkpatrick, T. Okano, R. Pilliar and X. Zhang, Society for Biomaterials, Kamuela, HI, 2000, p. 1334.

18. E. Tziampazis, J. Kohn and P. V. Moghe, *Biomaterials*, 2000, **21**, 511-520.

19. R. I. Sharma, J. Kohn and P. V. Moghe, *J Biomed Mater Res A*, 2004, **69A**, 114-123.

20. T. Briggs, M. D. Treiser, P. F. Holmes, J. Kohn, P. V. Moghe and T. L. Arinzeh, *J Biomed Mater Res A*, 2009, **91A**, 975-984.

21. S. D. Abramson, in *Biomedical Engineering*, Rutgers University, 2002, p. 163.

22. H. Levene, Rutgers University, 1999.

23. H. Levene, C. Lhommeau and J. Kohn, ed. U. States, Rutgers, The State University of New Jersey (New Brunswick, NJ), US, 2000.

24. L. Wu and J. Ding, *Biomaterials*, 2004, **25**, 5821-5830.

25. G. A. Silva, O. P. Coutinho, P. Ducheyne, I. M. Shapiro and R. L. Reis, *Biomaterials*, 2007, **28**, 326-334.

26. H. J. Seeherman, K. Azari, S. Bidic, L. Rogers, X. J. Li, J. O. Hollinger and J. M. Wozney, *J Bone Joint Surg Am*, 2006, **88A**, 1553-1565.

27. A. Pesnell, Rutgers, The State University of New Jersey, New Brunswick, 2006.

28. M. D. Timmer, H. Shin, R. A. Horch, C. G. Ambrose and A. G. Mikos, *Biomacromolecules*, 2003, **4**, 1026-1033.

29.   J. Kim, K. W. Lee, T. E. Hefferan, B. L. Currier, M. J. Yaszemski and L. Lu, *Biomacromolecules*, 2008, **9**, 149-157.

30.   H. J. Sung, P. Chandra, M. D. Treiser, E. Liu, C. P. Iovine, P. V. Moghe and J. Kohn, *J Cell Physiol*, 2009, **218**, 549-557.

31.   B. D. Ratner, *Biomaterials science : an introduction to materials in medicine*, Elsevier Academic Press, Amsterdam ; Boston, 2004.

32.   V. Handlos, *Biomaterials*, 1984, **5**, 86-88.

33.   K. A. Hooper, J. D. Cox and J. Kohn, *Journal of Applied Polymer Science*, 1997, **63**, 1499-1510.

34.   J. Hollinger, *Bone*, 1993, **14**, 575-580.

35.   B. P. Robinson, J. O. Hollinger, E. H. Szachowicz and J. Brekke, *Otolaryng Head Neck*, 1995, **112**, 707-713.

36.   H. Shin, P. Q. Ruhe, A. G. Mikos and J. A. Jansen, *Biomaterials*, 2003, **24**, 3201-3211.
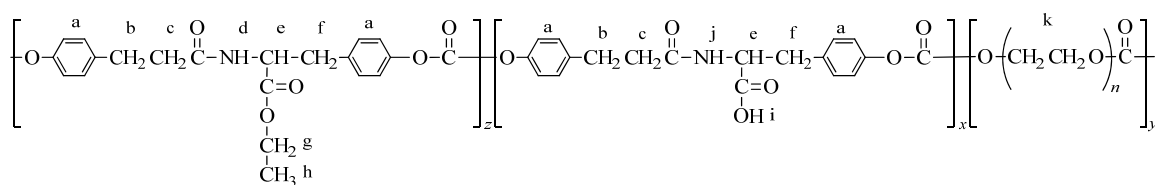
Hydrogen	Chemical shift (ppm)	Hydrogen	Chemical shift (ppm)
a	7.3	b	2.4
c	2.7	d	8.4
e	4.4	f	2.8, 3.0
g	4.0	h	1.1
i	12.8	j	8.3
k	3.5, 3.6, 4.1		

Figure A1.1. Chemical structure and ^{1}H-NMR chemical shift assignment for poly(DTR-co-x%DT-co-y%PEG$_{MW}$ carbonate). The % mole composition of each monomer component was calculated based on the integration of amide protons (d, j) at ~8.3 and ~8.4 ppm, aromatic protons (a) at ~7.2 ppm and PEG methylene protons (k) at ~4.1, ~3.6 and ~3.5 ppm. x and y are mole fractions of DT and PEG, respectively, z, the mole fraction of DTR, equals 1- x-y and n is the number of ethylene glycol repeat units in PEG. By varying the length of the respective pendent chain (R), different DTR diphenols are obtained.
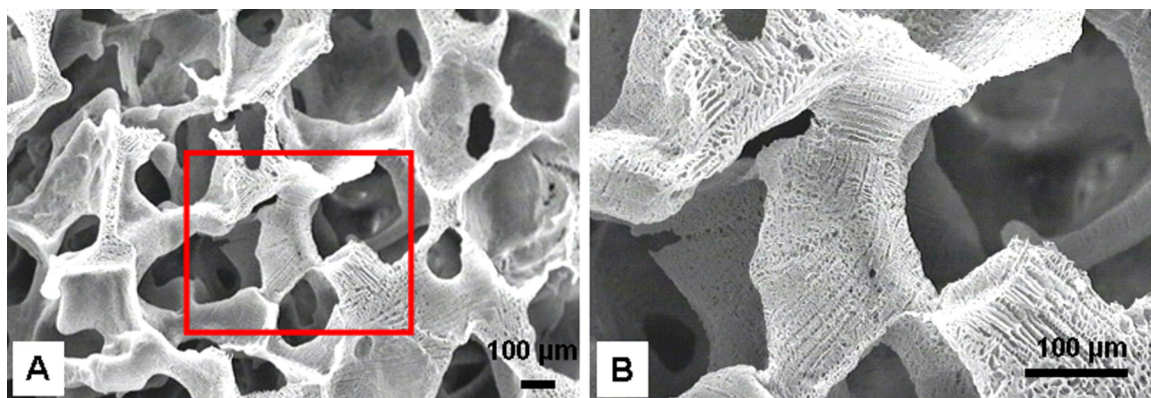
Figure A1.2. SEM images of E2502(2K) scaffolds fabricated using the combined solvent casting/porogen leaching/phase separation techniques. (A) Low and (B) high magnification, respectively.
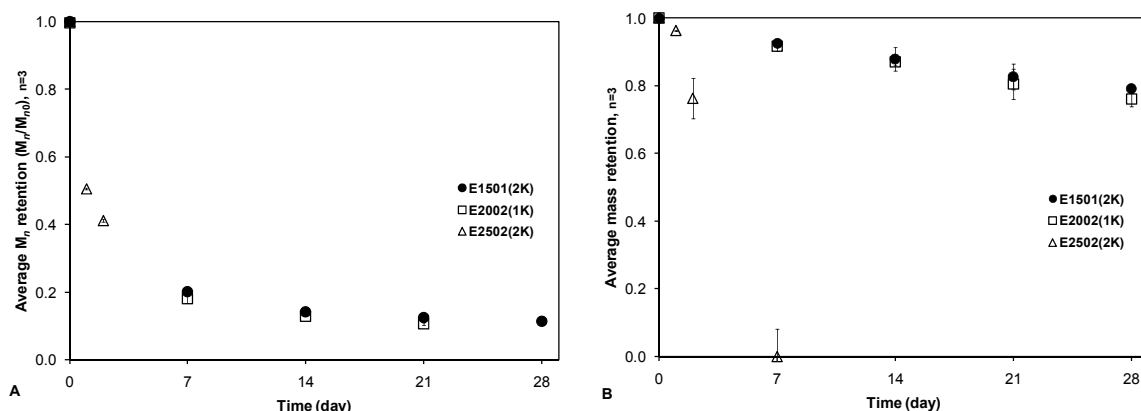
Figure A1.3. *In vitro* degradation and erosion profiles of tyrosine-derived polycarbonate scaffolds at various time points in PBS at 37 °C. (A) Fraction of molecular weight (MW) remaining determined from GPC (in DMF containing 0.1% TFA) relative to polystyrene calibration standards and (B) fraction of mass remaining determined by HPLC relative to DT calibration standards. Error bars represent means ± standard deviation for n=3.
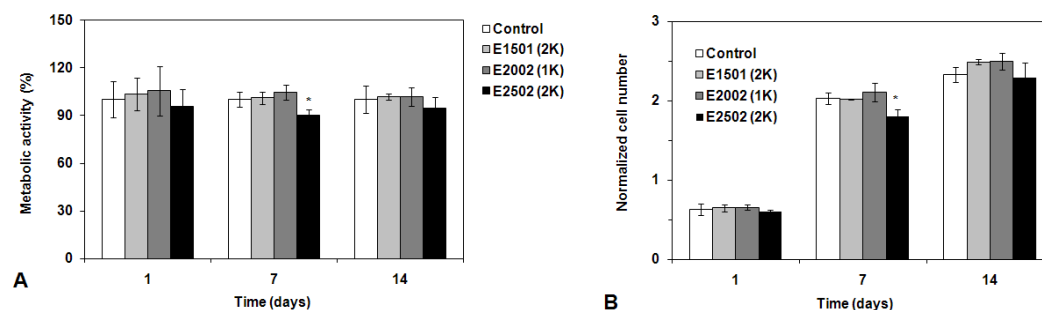
Figure A1.4. (A) The percent metabolic activity and (B) the normalized cell number of MC3T3-E1 cells cultured in the presence of various tyrosine-derived polycarbonate scaffolds up to 14 days of incubation at 37 °C. Error bars represent means ± standard deviation for n=3. * indicates significant ($\rho < 0.05$) difference from the control which is MC3T3-E1 cells cultured without the scaffolds.
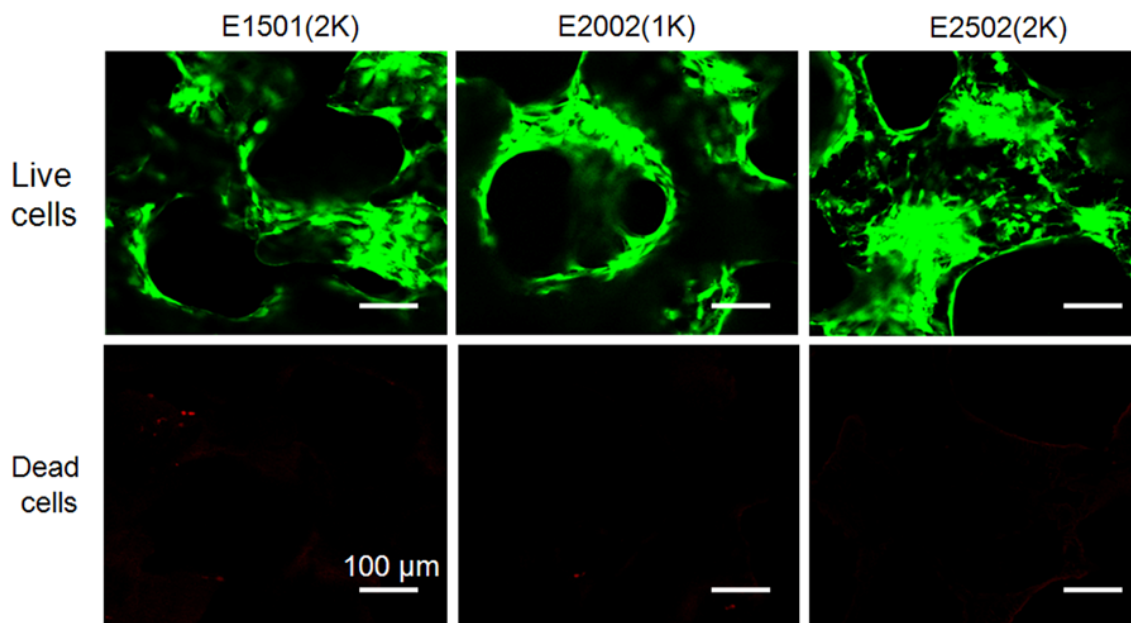
Figure A1.5. Confocal microscopic images of MC3T3-E1 cells on different tyrosine-derived polycarbonate scaffolds after 1 day of culture. Live cells fluoresce green and dead cells red.
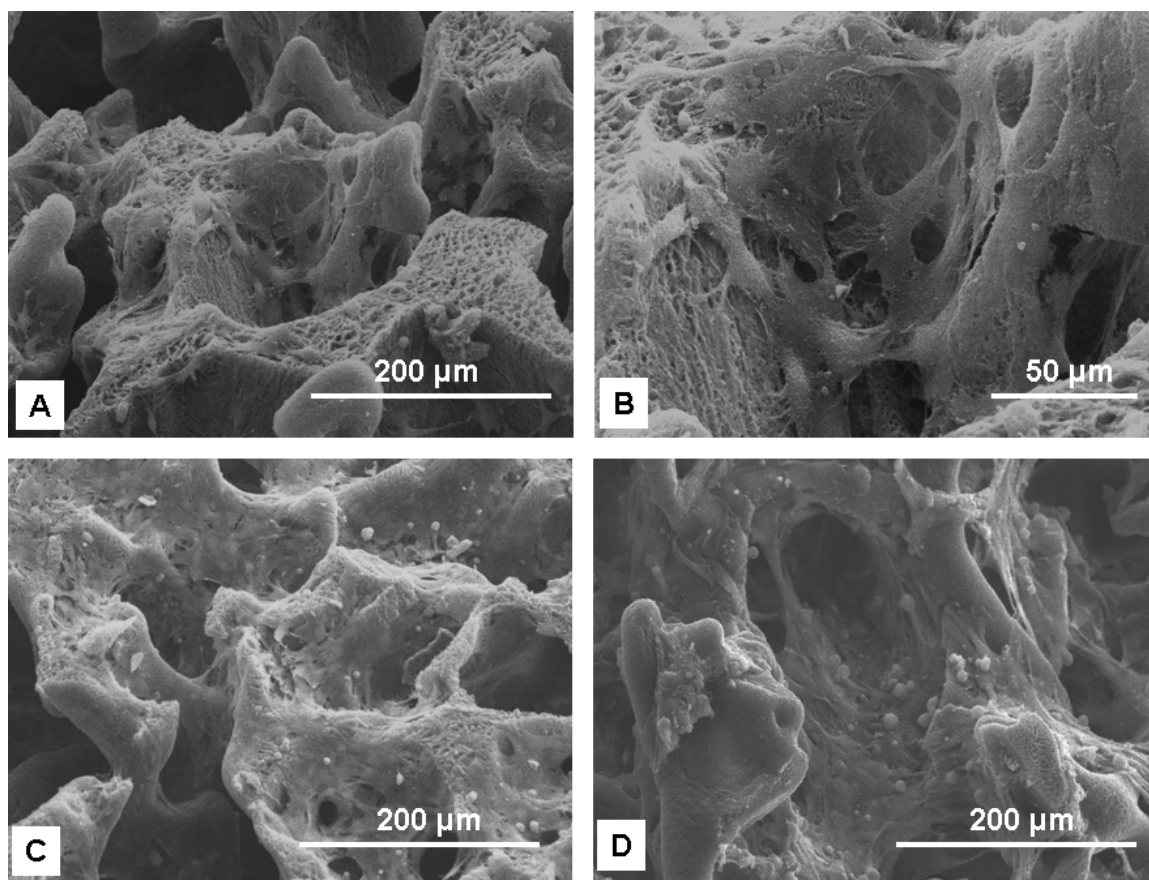
Figure A1.6. SEM images of MC3T3-E1 cells after 24 hrs of culture on different tyrosine-derived polycarbonate scaffolds. (A) E1501(2K) with low and (B) high magnification, respectively, (C) E2002(1K), and (D) E2502(2K) scaffolds.
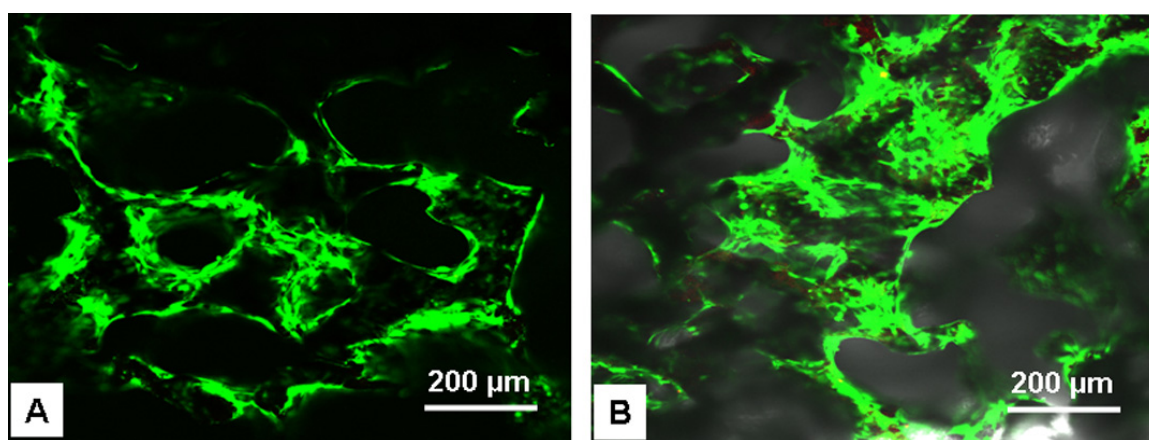
Figure A1.7. Confocal microscopic images of MC3T3-E1 cells after 4 days of culture on tyrosine derived polycarbonate scaffold, E1501(2K) degassed for (A) 48 hrs and (B) 14 days after EtO sterilization.
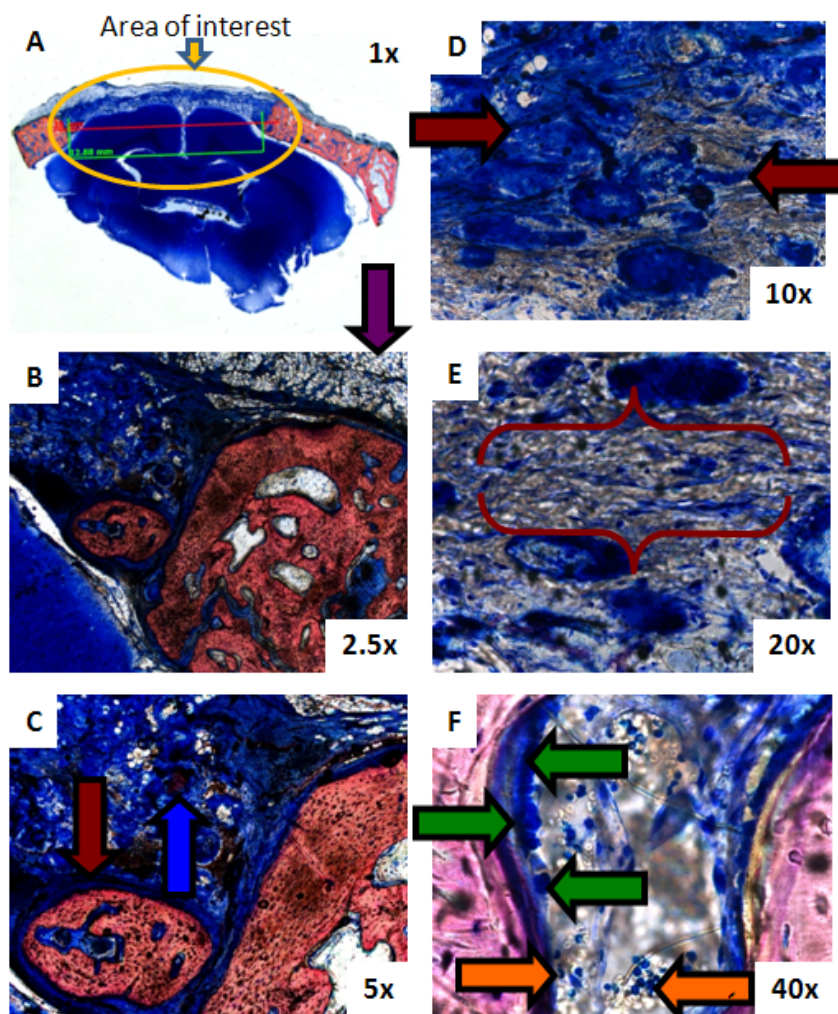
Figure A1.8. A typical section of the implanted tyrosine-derived polycarbonate (E1501(2K)) after 12 weeks of implantation. The specimens were cut and grounded to 30 μm thick sections and stained with Sanderson's Rapid Bone Stain and counterstained with van Gieson's picrofuchsin. Soft tissue was stained blue and bone was pink/red. Fat cells were filling the pericranial region of the defect (purple arrow) and a few islands of new cancellous bone formation were seen (blue arrows) surrounded by fibrous tissue (dark red arrow). Defect area was pervaded by fibrous connective tissue (dark red arrows) which also filled the void left by the polymer degradation (dark red brackets). Osteoblast cells were lining the osteoid (green arrows) and some erythrocytes (red blood cells) were seen in a medullary cavity of the calvaria (orange arrows). A) Implant area is devoid of significant new bone growth (orange circle). B) Fat cells filling the pericranial region of the defect (purple arrow). C) Fibrous tissue encapsulating island of cancellous bone (dark red arrow) and second island of new cancellous bone formation in early stage of development (blue arrow). D) Defect area pervaded by fibrous connective tissue (dark red arrows). E) Fibrous connective tissue filling the void left by the polymer degradation (dark red brackets). F) Plump osteoblast cells lining the osteoid (green arrows) and erythrocytes (orange arrows) within the host calvaria.

APPENDIX 2

"Osteogenic Differentiation of Pre-Osteoblasts on Biomimetic Tyrosine-Derived Polycarbonate Scaffolds"

Preface

"Reprinted with permission from J. Kim, M. H. R. Magno, P. Alvarez, A. Darr, J. Kohn and J. O. Hollinger. Osteogenic differentiation of pre-osteoblasts on biomimetic tyrosine-derived polycarbonate scaffolds. *Biomacromolecules*, 2011, **12** (10), 3520 – 3527. Copyright 2011 American Chemical Society"

Abstract

The osteogenic potential of biomimetic tyrosine-derived polycarbonate (TyrPC) scaffolds containing either an ethyl ester or methyl ester group combined with recombinant human bone morphogenetic protein-2 (rhBMP-2) was assessed using the pre-osteoblast cell line MC3T3-E1. Each composition of TyrPC was fabricated into three dimensional (3D) porous scaffolds with a bimodal pore distribution of micropores less than 20 μm and macropores between 200 - 400 μm. Scanning electron microscopy (SEM) characterization suggested MC3T3.E1 cell attachment on the TyrPC scaffold surface. Moreover, the 3D TyrPC-containing ethyl ester side chains supported osteogenic lineage progression, alkaline phosphatase (ALP) and osteocalcin (OCN) expression as well as an increase in calcium content compared to the scaffolds containing the methyl ester group. The release profiles of rhBMP-2 from the 3D TyrPC scaffolds by 15 days suggested a bi-phasic rhBMP-2 release. There was no significant difference in bioactivity between rhBMP-2 releasate from the scaffolds and exogenous rhBMP-2. Lastly, the TyrPC containing rhBMP-2 promoted more ALP activity and mineralization of MC3T3-E1 cells compared to TyrPC without rhBMP-2. Consequently, the data strongly suggest TyrPC chemistry will provide a highly useful platform for bone tissue engineering.

Key words: tyrosine-derived polycarbonates, biomimetic, three-dimensional scaffold, osteogenic differentiation, rhBMP-2

Introduction

Tissue engineering for bone regeneration exploiting biodegradable polymeric biomaterials, biologicals and osteoprogenitor cells offers potential alternatives to autografts and allografts. Consequently, numerous biomaterials have been developed as bone substitutes, ranging from naturally-derived materials to synthetic biopolymers.[1-3] Among synthetic biopolymers, the tyrosine-derived polycarbonates (TyrPCs) are a versatile polymer platform that can be tuned to different 'end-products' to promote tissue regeneration.[4] We define 'end-product' versatility as the capacity for the composition to be modified chemically and physically to produce a clinically relevant product with biological and mechanical properties that match the needs of selected clinical indications, for example: the delivery of rhBMP-2 to promote bone regeneration.[5]

The Kohn laboratory has developed an extensive, highly characterized library of TyrPCs derived from desaminotyrosyl tyrosine alkyl ester (DTR), that is, poly(DTR carbonate)s.[4] Physical and biological properties of poly(DTR carbonate) may be modulated through either desaminotyrosyl-tyrosine (DT) or poly(ethylene glycol) (PEG) incorporation, yielding poly(DTR-co-DT carbonate) or poly(DTR-co-PEG carbonate).[6-8] TyrPCs possess mechanical strength commensurate with biocompatible polymers such as poly(lactide-*co*-glycolide) (PLGA) and therefore are highly suitable for orthopedic applications.[9] Moreover, DTR, DT, and poly(ethylene glycol) (PEG) were combined to synthesize a new class of terpolymers for tissue engineering scaffolds.[10] This work verified that TyrPC terpolymers with DT content of 15-25 mol % and PEG content of 1 to

2 mol % had a minimal inflammatory response in vivo; however, the resorption rate was not sufficiently matched with bone formation. Consequently, an inadequate quantity of new bone formed.

Furthermore, our previous work suggested the polymer favored bone apposition rather than an undesirable fibrous encapsulation response. We posit this response is due to alkyl chain length. Consequently, TyrPC with ethyl groups (i.e., desaminotyrosyl-tyrosine ethyl: DTE) may favor bone apposition compared to butyl or octyl groups.[11] If this trend continues, methyl groups (i.e., desaminotyrosyl-tyrosine methyl: DTM) may be superior to DTE for bone tissue engineering applications.

Therefore, the current study is focused on in vitro investigation of two new TyrPC terpolymer compositions that have been designed to resorb more slowly than the original TyrPC at a rate in register with bone formation. The slower, controlled biodegradation rate is predominantly due to a lower DT content than previously investigated TyrPC terpolymer compositions. We consequently asked the question: Will the DTE and DTM-based TyrPC scaffolds, chosen based on the expected degradation rate, provide a suitable attachment substratum forMC3T3-E1 cells, reliably deliver rhBMP-2, and induce subsequent osteogenic differentiation? To answer these questions, we have completed a series of in vitro assays. MC3T3-E1 cells were used in three sets of experiments with the TyrPC scaffolds with and without rhBMP-2 to determine proliferation, alkaline phosphatase (ALP), and OCN expression as well as calcium content (Figure A2.1). The overall purpose of the current study was to determine the feasibility of modified TyrPC as a candidate for bone tissue engineering scaffolds that would be osteoconductive, biodegradable, and locally deliver rhBMP-2.

Materials and Methods

Polymer synthesis and characterization

Tyrosine-derived polycarbonates composed of DTE (desaminotyrosyl tyrosine ethyl ester) or DTM (desaminotyrosyl tyrosine methyl ester), DT (desaminotyrosyl tyrosine), and PEG (poly(ethylene glycol)) were synthesized using previously published procedures.[10] The generalized chemical structure is shown in Figure A2.2. The resulting polymers were characterized by ^{1}H-NMR (Proton Nuclear Magnetic Resonance Spectroscopy), and GPC (Gel Permeation Chromatography). By integration of the ^{1}H NMR peaks, the molar ratios of DTR, DT, and PEG were calculated. Molecular weights (number-average, M_n) and polydispersity index (PDI) were determined using GPC relative to polystyrene standards. The GPC system consisted of a 515 HPLC pump, 717plus autosampler, a 2414 RI detector, and Empower Pro Software (Waters Corporation, Milford,MA).

Scaffold fabrication, physical characterization

Cylindrical scaffolds (10 mm diameter by 5 mm in height) were fabricated from TyrPCs using a combination of solvent casting, particulate leaching, and phase separation.[10] Pore architecture of sputter-coated scaffolds (SCD 004, 30 milliAmps for 120 s with gold/palladium (Au/Pd)) was determined using a scanning electron microscope (SEM, Amray 1830I, acceleration potential of 20 kV). A 75x magnification was used to determine the gross structure, and a 250x magnification was used to measure the microporous structure of the scaffolds.

Thin films were prepared by compression molding at 50 ^{o}C + T_g (glass-transition temperature) for each polymer. To minimize polymer adhesion to the metal plates of the

mold, two Kapton films (American Durafilm, Holliston, MA) were added to line the metal plates. Samples were cut into 5 mm in diameter for the studies. Scaffolds and films were sterilized by ethylene oxide (EtO) sterilization (AN74i, Andersen Products, Haw River, NC) for 12 h at room temperature. Sterility was verified using a Steritest (AN-80, Andersen Products, Haw River, NC). After EtO sterilization, the scaffolds and films were degassed in a vacuum oven at room temperature for 7 days.

Cell culture and characterization

Mouse pre-osteoblasts, MC3T3-E1 (American Type Culture Collection: ATCC, Manassas, VA) were used to determine attachment on polymer compositions fabricated as 3D scaffolds and 2D films. We chose mouse preosteoblast MC3T3-E1 cell line because of its rich history and the advantage of reproducibility when compared with primary cell cultures.[12] Before cell seeding, the sterile 3D scaffolds and 2D films were fixed in a well of a 48-well plate with a clone ring (10 mm diameter, Fisher, Pittsburgh, PA) and incubated in the cell culture media (α-MEM medium, Invitrogen, Carlsbad, CA) supplemented with 10% fetal bovine serum, 100U/mL penicillin, and 100 μg/mL streptomycin at 37 $^{\circ}$C for 1 h to hydrate the scaffolds fully.[10] The media was fully removed from each well, and 200 μL of cell suspension (1 million/mL of media) was then added to the well at a density of 2 x 10^5 cells/scaffold. An additional 300 μL of media was added to the cells after 2 h of incubation at 37 $^{\circ}$C in a 5% CO_2 atmosphere and further cultured for 24 h in the media. For 2D surfaces, 0.5mL of cell suspension containing 20 000 cells was seeded on the surfaces. After 24 h of incubation, the media in each well was replaced with the osteogenic media (i.e., the culture media supplemented with 10 mM β-glycerophosphate and 50 μg/mL of ascorbic acid). The media was

changed every 2 days, and the cells were further cultured up to 21 days. At days 1, 4 and 14, MC3T3-E1 viability and attachment were determined using a live/dead staining method (Invitrogen, Eugene, OR) and SEM, respectively, as previously described.[10] For live/dead staining, the scaffold was washed with PBS and incubated in 0.5 mL of the live/dead dye solution (5 μL of Calcein AM and 20 μL of ethidium homodimer dye in 10 mL of PBS) for 30 min.

Proliferation

The MC3T3-E1 cells on the scaffolds were rinsed with phosphate buffered saline (PBS) three times and 0.5 mL of 1X cell lysis buffer (Cell signaling technology, Danvers, MA) was added to each scaffold to rupture the cell membranes. The cell lysates were subjected to a thaw/freeze cycle for three times (30 min thawing at 37 °C and freezing at -80 °C for 20 min) to extract DNA and proteins. The determination of the quantity of cells associated with the scaffolds was accomplished by measuring DNA content using a fluorometric Picogreen DNA quantification kit (Molecular Probes, Eugene, OR) and fluorescence absorbance was determined by a microplate reader (Tecan, Mannedorf, Austria) equipped with a 485/535 nm (excitation/emission) filter set.

Alkaline phosphatase (ALP) activity and total protein

ALP activity was measured using a previously established protocol.[10] Briefly, 20 µL of alkaline working buffer solution (Sigma), 80 µL of the lysate solution and 100 µL of substrate solution (5 mM p-nitrophenyl phosphate) were added to a 96 well plate. The plate was incubated at 37 °C for 1 h and the reaction was stopped by adding 100 µL of 0.3 N sodium hydroxide (NaOH) solution to each well. The absorbance of each well was measured at 405 nm and the value of ALP activity was normalized to the amount of DNA in the sample. Total protein in the cell lysate solution was quantified by the Bradford protein assay (Bio-Rad, Hercules, CA). In brief, 200 µL of the assay reagent was added to 10 µL of the sample and the absorbance of a differential color change was measured at 570 nm.

Osteocalcin (OCN) assay

The amount of OCN in the cell lysates was measured using a mouse OCN enzyme immunoassay (EIA) kit (Biomedical Technologies Inc, Stoughton, MA). The OCN concentration was measured at 450 nm in a microplate reader and normalized to the DNA content.

Mineralization assay

The calcium content in the extracellular matrix (ECM) was determined by a published method with a calcium assay kit (Teco Diagnostics, Anaheim, CA).[13] After 21 days of culture, each cell-scaffold construct was washed twice with PBS and incubated

overnight in 0.6 N hydrochloric acid (HCl). Calcium extracts (10 μg) were pipetted into a well of 96 well-plate, and 200 μL of a reagent mixture was added to the well. The mixture was composed of 100 μL of reagent A (0.14 mM o-cresolphthalein complexone and 13 mM 8-hydroxyquinoline) and 100 μL of reagent B (363 mM diethylamide and 2 mM potassium cyanide). The calcium content in each solution was measured at 570 nm by a microplate reader. Actual calcium content secreted by the cells was calculated by normalizing calcium content to DNA.

rhBMP-2 incorporation and release kinetics

The scaffolds were conditioned for one hour with PBS to reduce hydrophobicity. The rhBMP-2 (Wyeth, Cambridge, MA) was dissolved in deionized water (1 mg/mL) and added to each scaffold (5 μg/scaffold). Scaffolds were air-dried overnight and samples were placed into tissue culture media consisting of alpha-MEM supplemented with 100 U/mL penicillin, 100 μg/mL streptomycin and 1% bovine serum albumin (BSA) and incubated at 37 °C and 5% CO_2. The releasate was collected each day, stored at -80 °C and replaced with fresh media. The rhBMP-2 released from the scaffolds was measured using an ELISA kit (R&D Systems, Minneapolis, MN).

Bioactivity of the releasate

MC3T3-E1 cells were plated at a density of 20,000 cells/cm^2 on 24-well tissue culture plates. After 24 h of incubation at 37 °C, the media in each well was replaced with the osteogenic media (10 mM β-glycerophosphate and 50 μg/mL of ascorbic acid) supplemented with 10 ng/mL of either exogenous rhBMP-2 or rhBMP-2 releasate from

TyrPC scaffolds. Proliferation and ALP activity of the cells either in the absence or presence of exogenous rhBMP-2 or releasate were determined at 7, 14 and 21 days as described earlier in this section.

In a separate experiment, dried 3D TyrPC scaffolds with or without rhBMP-2 (5 µg/scaffold), as previously described, were placed in a well of 48-well plate, and a clone ring was used to secure the scaffold. The cell suspension (200 µL) was directly seeded on the 3D TyrPC scaffolds. Proliferation, ALP, and calcium content of the ECM of MC3T3-E1 cells cultured on 3D TyrPC scaffolds with or without rhBMP-2 were measured at days 7, 14, 21, as previously described.

Statistical analysis

All datawere reported as the mean and standard deviation. Statistical analyses were performed using single factor analysis of variance (ANOVA) with a posthoc multicomparison test (Tukey-Kramer method) with a significance level established as $p \leq$ 0.05.

Results

Polymer and sample characterization

GPC characterization following polymer synthesis resulted in molecular weights of 271 and 262 kDa and polydispersity of 1.3 and 1.2 for E1001(1K) and M1002(1K), respectively. ^{1}H NMR confirmed the expected chemical composition of the terpolymers. SEM images of the pore architecture of the 3D scaffolds revealed a bimodal pore distribution of micropores (<20 μm) and macropores (200 – 400 μm) in addition to an open pore architecture with high pore interconnectivity. Furthermore, there were oriented micropores surrounding the macropores, as previously described.[10] After 6 weeks of incubation in PBS at 37 ^{o}C, retention of molecular weight (M_n) of DTE-containing, E1001(1K), and DTM-containing, M1002(1K), scaffolds was 15.6 and 8.0%, respectively, and the E1001(1K) scaffolds degraded more slowly than the M1002(1K) scaffolds (Figure A2.3). Molecular weight retention was greater for E1001(1K) and M1002(1K) than for the previously investigated TyrPC terpolymers.[10] Additionally, no mass loss was observed for either of the current polymer scaffolds over the 6-week test period, whereas mass loss was measured in the previous terpolymer scaffolds after 1 week.[10] Compression molded films were transparent and were ~100 μm in thickness.

MC3T3-E1 Cell viability and attachment

Fluorescence microscopic images suggested 97% cell viability after 1 and 4 days of culture. Each scaffold possessed a bimodal pore distribution, micropores (<20μm), and macropores (200 – 400 μm). After cell seeding, the cells were well attached and spread throughout the scaffold surfaces and appeared to migrate into the pores. There were no macroscopic differences in cell morphology between the two scaffolds (Figure A2.4A).

After 24 h of culture, the cells fully covered the polymer surfaces. There was no macroscopic difference in cell attachment between days 1 and 4. To assess cell infiltration into the 3D tyrosine-derived polycarbonate scaffold, cell distribution on and throughout the scaffolds was were no significant differences in cell density by a proliferation assay

(Figure A2.5A) and no macroscopic difference in cell density was detected on the surface at days 4 and 14, the cells, however, appeared to have penetrated more deeply into the scaffolds at day 14 than at day 4 (Figure A2.4B).

Proliferation

On the 2D surfaces (i.e., tissue culture polystyrene: TCPS and 2D TyrPC film), the cell proliferation reached a plateau after 7 days and remained at a similar level thereafter (Figure A2.5A). On 2D TCPS surfaces, the cell density was significantly greater than 2D TyrPC film. At day 1, the cell density on 3D tyrosine-derived polycarbonate scaffolds was significantly greater than on the 2D surfaces. However, unlike the increase seen with 2D controls, cell proliferation on 3D TyrPC scaffolds remained constant over 21 days. There was no significant difference in DNA concentration between E1001(1K) and M1002(1K) scaffolds except at day 21, when DNA concentration on M1002(1K) was significantly greater than that on E1001(1K) scaffolds.

Osteogenic differentiation

ALP activity on each scaffold monotonically increased throughout 21 days of culture, regardless of scaffold polymer composition (Figure A2.5B). At all time periods, the cells on 3D TyrPC scaffolds produced significantly greater ALP activity compared with the 2D surfaces (i.e., 2D TCPS and 2D TyrPC film). ALP activity on 3D E1001(1K) scaffolds was greater than on 3D M1002(1K) scaffolds, except at day 21, when no significant differences were determined. There were no significant differences in ALP activity on 2D surfaces, except at day 21, when the protein activity on 2D TCPS was significantly lower than 2D TyrPC film.

Significant differences in OCN expression were detected on 2D and 3D scaffolds (Figure A2.5C) where the phenotypic expression on 2D was significantly less than the 3D scaffolds. There was also a significant difference in OCN for 3D TyrPC scaffolds at days 14 and 21, with the cells cultured on 3D E1001(1K) producing more OCN, compared to 3D M1002(1K) scaffolds.

There was a significant difference in calcium content between 3D E1001(1K) and M1002(1K) scaffolds (Figure A2.5D). The calcium deposition on 3D TyrPC scaffolds was significantly higher than the 2D surfaces.

rhBMP-2 release profiles

The release profiles from the scaffolds showed an initial burst release up to day 5 followed by little release up to day 15 (Figure A2.6A). There were no statistical differences in the cumulative rhBMP-2 release between the 3D TyrPC scaffolds at each

time period except day 2, suggesting that either E1001(1K) or M1002(1K) did not alter the rhBMP-2 release profile.

Bioactivity of rhBMP-2 releasates

The MC3T3-E1 cell density (Figure A2.6B) was similar among scaffold treatment groups at each time period, except at day 7, where the cell densities were significantly greater in the presence of rhBMP-2 releasates compared with the control (no releasates). The ALP activity (Figure A2.6C) in the presence of rhBMP-2 releasate at each time period was significantly greater than when cells were not exposed to rhBMP-2. There was no significant difference in ALP activity between exogenous rhBMP-2 and rhBMP-2 releasate from 3D TyrPCs at all time periods, except at day 4, indicating that the rhBMP-2 released from TyrPC scaffolds was biologically active.

Osteogenic differentiation on TyrPC containing rhBMP-2

The MC3T3.E1 cell densities (Figure A2.7A) cultured on the scaffolds with or without rhBMP-2 were similar throughout the time periods. It is noteworthy that rhBMP-2 containing scaffolds showed a decrease in DNA amount between days 14 and 21. Cell detachment may have occurred from the surface at day 21 possibly because of overconfluent cells.

ALP activity (Figure A2.7B) of the cells on the scaffolds with rhBMP-2 was significantly greater than that on the scaffolds without rhBMP-2 at day 14. There was also significant difference in calcium deposition between 3D TyrPC scaffolds with and without rhBMP-2 at day 21 (Figure A2.7C).

Discussion

The purpose of the study was to determine the osteogenic properties of E1001(1K)- and M1002(1K)-based scaffolds as a substratum forMC3T3-E1 cells as well as the delivery of rhBMP-2 and the promotion of osteogenic differentiation. Antecedent to in vivo applications, in vitro data provide a valuable guide for the fine-tuning of potential substratum mimetics for tissue engineering. Valuable outcome data were obtained in this study with the goal of progressing to in vivo work.

The degradation data (Figure A2.3) suggested that the properties of TyrPC were easily tuned by altering alkyl groups in the DTR building block, DT, and PEG content. Molecular weight retention was successfully increased over previous TyrPC terpolymers,[10] primarily through a reduction in DT content from15 to 10mol %. M1002(1K) degraded more quickly than E1001(1K) because of the increase in PEG content and presence of a less hydrophobic pendent chain.

More importantly, TyrPC scaffolds containing an ethyl ester pendent chain and 1 mol % PEG promoted greater expression of ALP and OCN as well as mineralization when compared with the scaffolds with a methyl ester pendent chain and 2 mol % PEG. The data also suggest that changes in chemical composition of the TyrPC scaffolds could make a significant difference in cellular response and physical properties such as scaffold degradation.

The observations may be due to the difference of hydrophobicity/hydrophilicity, surface properties of the polymers, or both.[14] Therefore, the more hydrophobic (i.e., E1001(1K)) terpolymer backbone may provide a more permissive substrate for cell adhesion proteins such as fibronectin and vitronectin. This response is encouraging in light of the fact that fibronectin is reported to induce cell attachment.[15] Extracellular

matrix (ECM) proteins, especially fibronectin and vitronectin, mediate osteoblastic – ECM interactions via integrin receptors $\alpha_5\beta_1$ or $\alpha_v\beta_3$.[16, 17] Hence, it is reasonable to deduce the outcome we measured may be a consequence of the hydrophobic segments of the polymer backbone initially recruiting cell adhesion proteins from the serum. The proteins may preferentially attach to the more hydrophobic TyrPC scaffolds (i.e., E1001(1K) vs M1002(1K)) and induce cell attachment to the scaffolds. Purportedly, the cells attached on the scaffolds may secrete significantly more ECM proteins, including osteogenic proteins, which initiate a differentiation cascade for the preosteoblasts.[13] Although the DNA data (Figure A2.5A) showed no significant differences between E1001(1K) and M1002(1K) scaffolds after 24 h of postculture, the attached cells on E1001(1K) scaffolds may produce more ECM proteins than M1002(1K) scaffolds through the hydrophobic interaction between the surface and the cells attached. This outcome may initiate osteogenic progression of the cell.

Moreover, surface properties of the TyrPC scaffolds could play an important role to promote desired biological outcomes. Supporting this speculation is the observation that surface roughness and microtopography are powerful stimulants of osteogenic differentiation and mineralization for osteoblasts.[18, 19] Furthermore, differences in the rate of hydrolysis of the pendent side chain[11] and the products formed as a result of this hydrolysis (e.g., ethanol for DTE-containing polymers vs. methanol for DTM-based polymers) may result in variation in the biological outcome. Finally, PEG-containing polymers will induce exogenous and intracellular reactive oxygen species (ROS) production and may cause changes in cell signal transduction pathways.[20] Therefore, the difference in the PEG content of the polymers used in this study may have contributed to the reported findings.

Although 3D scaffolds are more relevant for the in vivo environment, cellular responses have not necessarily been favorable on 3D porous substrates such as PLGA.[21, 22] The initial cell seeding densities on 3D TyrPC scaffolds were similar in magnitude as those reported for other 3D cultures such as collagen or PLGA.[19, 23] The cell seeding efficiency on the 3D TyrPC scaffolds was lower at 24 h of postculture than that on 2D surfaces considering the difference in the initial cell seeding densities (Figure A2.5A). The observed differences, therefore, may be due to the limited surface area of 3D scaffolds available for cell seeding as well as nonhomogeneity of cell distribution on the 3D scaffolds.[19, 22]

Absence of vascularity and interconnected pores in 3D scaffold may either significantly hinder or delay osteogenic differentiation and mineralization because of mass transit limitation of nutrients and oxygen throughout the scaffolds.[24] In this study, however, 3D TyrPC scaffolds supported cell ingrowth and subsequent osteogenic differentiation of MC3T3-E1 cells rivaling the 2D TyrPC film and TCPS. We deduce that this outcome is likely a result of the 3D TyrPC scaffolds having a pore structure that is similar to bone.[10] Consequently, this "bone-mimetic" pore architecture may provide topographical and physical cues as well as proper mass transfer of nutrients and oxygen, which are crucial for osteoblast lineage progression. The 3D topographical and physical cues cannot be replicated with 2D surfaces, and thus this distinction may offer a compelling feature for the superiority in outcome with the 3D TyrPC scaffolds. In addition, when TyrPC scaffolds were supplemented with rhBMP-2, ALP activity and calcium deposition increased as compared with TyrPC without rhBMP-2 (Figure A2.7). This is not an unexpected outcome. However, it is highly noteworthy to underscore that controlled release of a biomolecule from a delivery scaffold does not ensure biological

activity, for example, changes in the conformation of the protein biological may mitigate against receptor_ligand binding and subsequent internalization and cell up-regulation. In fact, rhBMP-2 releasate was equivalent in biological activity to the rhBMP-2 administered exogenously. Furthermore, in terms of rhBMP-2 release kinetics, there was an initial burst release of rhBMP-2 up to 5 days, followed by a little release over 15 days. This kinetic profile suggests diffusion dependence from the TyrPC polymeric network as well as concomitant polymer degradation.[13] The total rhBMP-2 release after 15 days was <40% of the initial amount, suggesting possible rhBMP-2 aggregation or denaturation of the protein on the scaffold.[25, 26] The findings in this study emphasize the need for a precise calibration of the important parameters of scaffolding materials such as porosity and hydrophobicity/hydrophilicity, which may be either overlooked or neglected by tissue engineers. Moreover, on the basis of the highly favorable in vitro outcome and the physical and chemical versatility of the TyrPC platform, it is anticipated that there will be a positive outcome when the TyrPC platform is exploited for bone tissue engineering applications in vivo.

Conclusions

Biomimetic tyrosine-derived polycarbonates were synthesized and fabricated into 3D porous scaffolds as candidate prototypes for bone tissue engineering scaffolds. The chemical structures of the TyrPC scaffolds designed and tested for the study promoted different biological outcomes. Specifically, the MC3T3-E1 preosteoblastic cells cultured on E1001(1K) scaffolds produced more ALP, OCN, and mineralized calcium compared with M1002(1K) scaffolds. Furthermore, 3D TyrPC scaffolds promoted osteogenic differentiation and mineralization as compared with 2D conventional tissue culture plates or 2D film. The MC3T3-E1 cellular responses were further stimulated when TyrPC scaffolds were treated with rhBMP-2. The release kinetics of rhBMP-2 from the TyrPC was biphasic, with an initial burst release, followed by slow release. The bioactivity of the rhBMP-2 releasate was equivalent to exogenous rhBMP-2 in promoting ALP activity and calcium deposition. The data from this study suggest that the terpolymer is biocompatible, is biodegradable, effectively delivers rhBMP-2, enables MC3T3-E1 attachment, and promotes osteoblast marker expression. Consequently, it is anticipated that the versatile TyrPC platform can be designed to address an array of tissue engineering clinical criteria for bone regeneration.

Acknowledgement

REFERENCES

1.   Ratner, B. D.; Bryant, S. J., Biomaterials: Where we have been and where we are going. *Annual Review of Biomedical Engineering* **2004,** 6, 41-75.

2.   Khan, Y.; Yaszemski, M. J.; Mikos, A. G.; Laurencin, C. T., Tissue Engineering of Bone: Material and Matrix Considerations

J Bone Joint Surg Am **2008,** 90 (Suppl 1), 36 -42.

3.   Mikos, A. G.; Herring, S. W.; Ochareon, P.; Elisseeff, J.; Lu, H. H.; Kandel, R.; Schoen, F. J.; Toner, M.; Mooney, D.; Atala, A.; Van Dyke, M. E.; Kaplan, D.; Vunjak-Novakovic, G., Engineering complex tissues. *Tissue Engineering* **2006,** 12, (12), 3307-39.

4.   Bourke, S. L.; Kohn, J., Polymers derived from the amino acid L-tyrosine: polycarbonates, polyarylates and copolymers with poly(ethylene glycol). *Advanced Drug Delivery Reviews* **2003,** 55, (4), 447-466.

5.   Zegzula, H. D.; Buck, D. C.; Brekke, J.; Wozney, J. M.; Hollinger, J. O., Bone formation with use of rhBMP-2 - (Recombinant human bone morphogenetic protein-2). *Journal of Bone and Joint Surgery-American Volume* **1997,** 79A, (12), 1778-1790.

6.   Tziampazis, E.; Kohn, J.; Moghe, P. V., PEG-variant biomaterials as selectively adhesive protein templates: model surfaces for controlled cell adhesion and migration. *Biomaterials* **2000,** 21, (5), 511-520.

7.   Sharma, R. I.; Kohn, J.; Moghe, P. V., Poly(ethylene glycol) enhances cell motility on protein-based poly(ethylene glycol)-polycarbonate substrates: A mechanism for cell-guided ligand remodeling. *Journal of Biomedical Materials Research Part A* **2004,** 69A, (1), 114-123.

8.   Briggs, T.; Treiser, M. D.; Holmes, P. F.; Kohn, J.; Moghe, P. V.; Arinzeh, T. L., Osteogenic differentiation of human mesenchymal stem cells on poly(ethylene glycol)-variant biomaterials. *Journal of Biomedical Materials Research Part A* **2009,** 91A, (4), 975-984.

9.   Engelberg, I.; Kohn, J., Physico-mechanical properties of degradable polymers used in medical applications: a comparative study. *Biomater* **1991,** 12, 292-304.

10.   Magno, M. H. R.; Kim, J.; Srinivasan, A.; McBride, S.; Bolikal, D.; Darr, A.; Hollinger, J. O.; Kohn, J., Synthesis, degradation and biocompatibility of tyrosine-

derived polycarbonate scaffolds. *Journal of Materials Chemistry* **2010,** 20, (40), 8885-8893.

11.   James, K.; Levene, H.; Parsons, J. R.; Kohn, J., Small changes in polymer chemistry have a large effect on the bone-implant interface: evaluation of a series of degradable tyrosine-derived polycarbonates in bone defects. *Biomaterials* **1999,** 20, (23-24), 2203-12.

12.   Wang, D.; Christensen, K.; Chawla, K.; Xiao, G. Z.; Krebsbach, P. H.; Franceschi, R. T., Isolation and characterization of MC3T3-E1 preosteoblast subclones with distinct in vitro and in vivo differentiation mineralization potential. *Journal of Bone and Mineral Research* **1999,** 14, (6), 893-903.

13.   Kim, J.; Hefferan, T. E.; Yaszemski, M. J.; Lu, L., Potential of Hydrogels Based on Poly(ethylene glycol) and Sebacic Acid as Orthopedic Tissue Engineering Scaffolds. *Tissue Engineering* **2009,** 15, (8), 2299-2307.

14.   Ertel, S. I.; Kohn, J., Evaluation of a Series of Tyrosine-Derived Polycarbonates as Degradable Biomaterials. *Journal of Biomedical Materials Research* **1994,** 28, (8), 919-930.

15.   Hynes, R. O., Integrins - a Family of Cell-Surface Receptors. *Cell* **1987,** 48, (4), 549-554.

16.   Wilson, C. J.; Clegg, R. E.; Leavesley, D. I.; Pearcy, M. J., Mediation of biomaterial-cell interactions by adsorbed proteins: A review. *Tissue Engineering* **2005,** 11, (1-2), 1-18.

17.   Garcia, A. J.; Vega, M. D.; Boettiger, D., Modulation of cell proliferation and differentiation through substrate-dependent changes in fibronectin conformation. *Molecular Biology of the Cell* **1999,** 10, (3), 785-798.

18.   Lincks, J.; Boyan, B. D.; Blanchard, C. R.; Lohmann, C. H.; Liu, Y.; Cochran, D. L.; Dean, D. D.; Schwartz, Z., Response of MG63 osteoblast-like cells to titanium and titanium alloy is dependent on surface roughness and composition. *Biomaterials* **1998,** 19, (23), 2219-2232.

19.   St-Pierre, J. P.; Gauthier, M.; Lefebvre, L. P.; Tabrizian, M., Three-dimensional growth of differentiating MC3T3-E1 pre-osteoblasts on porous titanium scaffolds. *Biomaterials* **2005,** 26, (35), 7319-7328.

20.   Sung, H. J.; Chandra, P.; Treiser, M. D.; Liu, E.; Iovine, C. P.; Moghe, P. V.; Kohn, J., Synthetic polymeric substrates as potent pro-oxidant versus anti-oxidant

regulators of cytoskeletal remodeling and cell apoptosis. *J Cell Physiol* **2009,** 218, (3), 549-57.

21.   Huang, W. B.; Carlsen, B.; Wulur, I.; Rudkin, G.; Ishida, K.; Wu, B.; Yamaguchi, D. T.; Miller, T. A., BMP-2 exerts differential effects on differentiation of rabbit bone marrow stromal cells grown in two-dimensional and three-dimensional systems and is required for in vitro bone formation in a PLGA scaffold. *Experimental Cell Research* **2004,** 299, (2), 325-334.

22.   Ishaug, S. L.; Crane, G. M.; Miller, M. J.; Yasko, A. W.; Yaszemski, M. J.; Mikos, A. G., Bone formation by three-dimensional stromal osteoblast culture in biodegradable polymer scaffolds. *Journal of Biomedical Materials Research* **1997,** 36, (1), 17-28.

23.   Schoeters, G.; Leppens, H.; Van Gorp, U.; Van Den Heuvel, R., Haemopoietic long-term bone marrow cultures from adult mice show osteogenic capacity in vitro on 3-dimensional collagen sponges. *Cell proliferation* **1992,** 25, (6), 587-603.

24.   Karageorgiou, V.; Kaplan, D., Porosity of 3D biornaterial scaffolds and osteogenesis. *Biomaterials* **2005,** 26, (27), 5474-5491.

25.   Yeo, Y.; Park, K., Control of encapsulation efficiency and initial burst in polymeric microparticle systems. *Arch Pharm Res* **2004,** 27, (1), 1-12.

26.   Zhu, G. Z.; Mallery, S. R.; Schwendeman, S. P., Stabilization of proteins encapsulated in injectable poly (lactide-co-glycolide). *Nature Biotechnology* **2000,** 18, (1), 52-57.
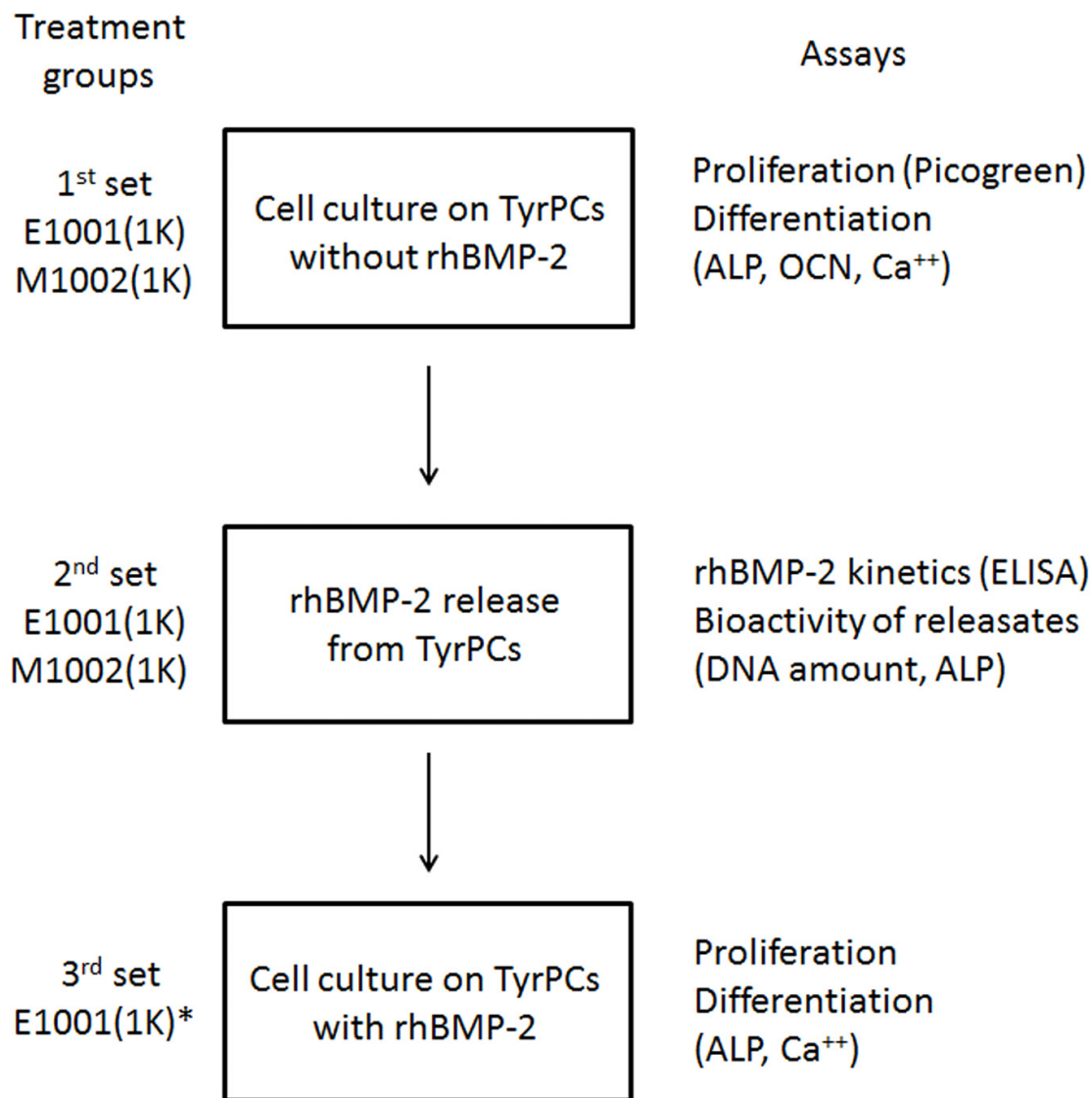
Figure A2.1. Flow diagram of the experimental design. The first set of experiments was designed to determine if 3D TyrPC scaffolds supported osteogenesis of MC3T3-E1 cells cultured on the scaffolds. The second set was to determine the bioactivity of rhBMP-2 releasates from 3D TyrPC scaffolds compared to the exogenous rhBMP-2. The third set was to determine if osteogenesis of MC3T3-E1 cells were further enhanced when the cells were cultured on the scaffolds containing rhBMP-2. *: E1001(1K) scaffolds were down-selected based on the data from 1st and 2nd sets of experiments.
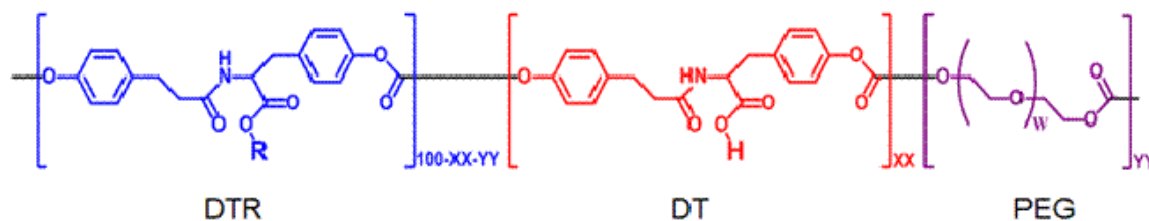
Figure A2.**2** Chemical structure of poly(DTR-co-xx%DT-co-yy%PEG$_{MW}$ carbonate), where *x* and *y* are mole fractions of DT and PEG, respectively, and where *z*, mole fraction of DTR, equals 1- xx-yy and w is the number of ethylene glycol repeat units in PEG. E1001(1K) polymer represent poly(DTE-co-R=ethyl ester for DTE and R=methyl ester for M1002(1K).
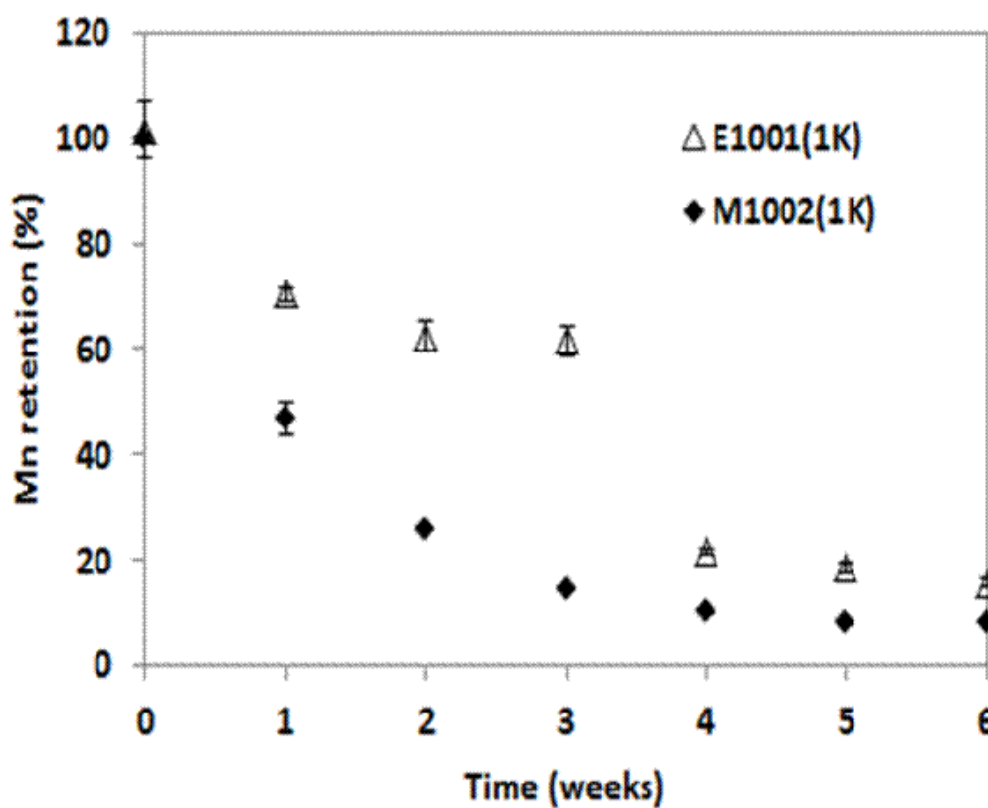

Figure A2.3. *In vitro* degradation profiles of tyrosine-derived polycarbonate scaffolds at specific time periods in PBS at 37 °C. Error bars represent means ± standard deviation for n=3.
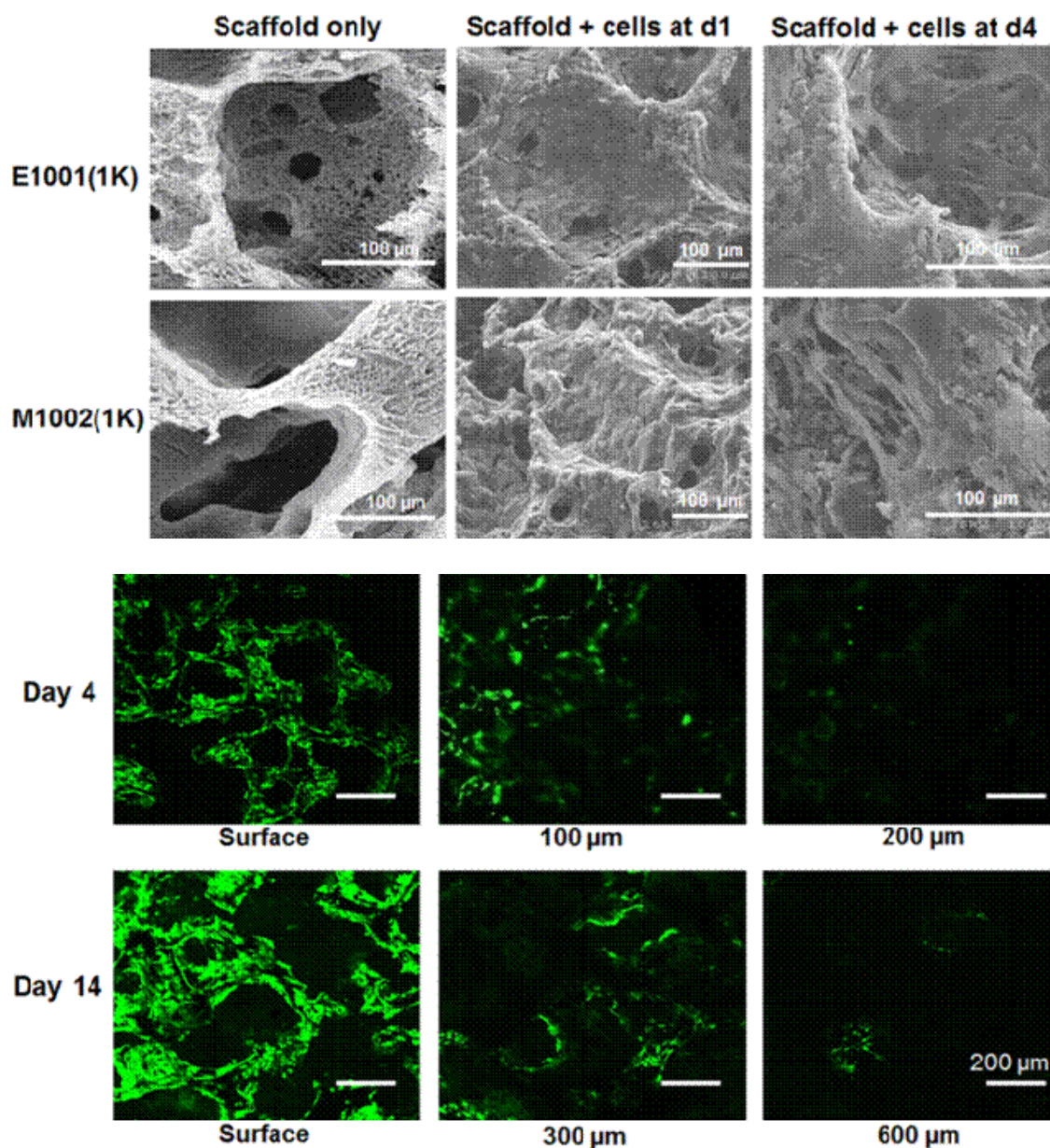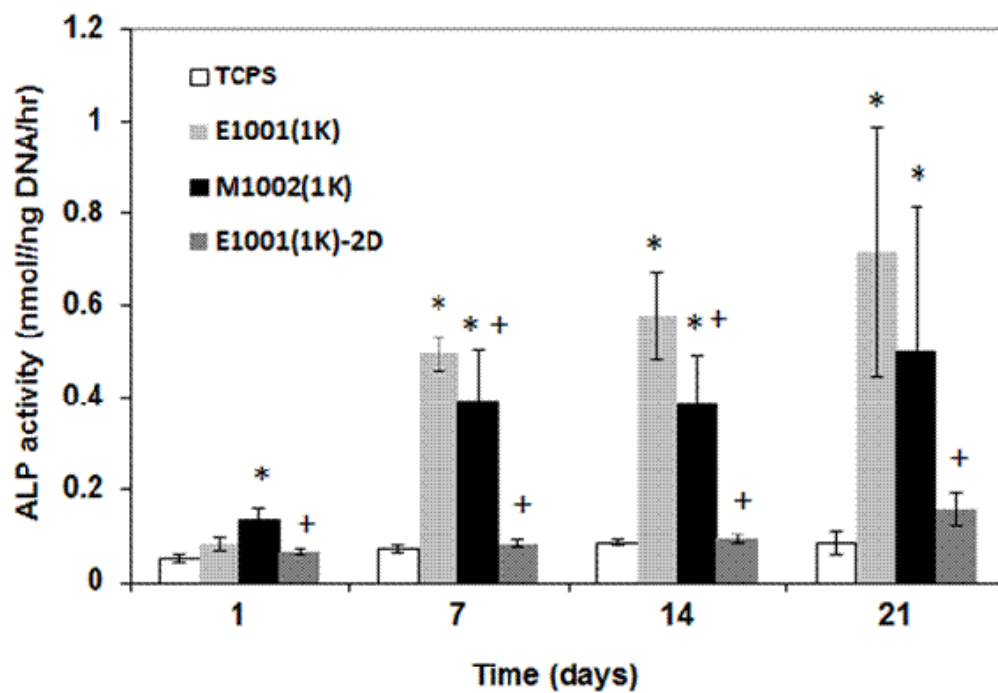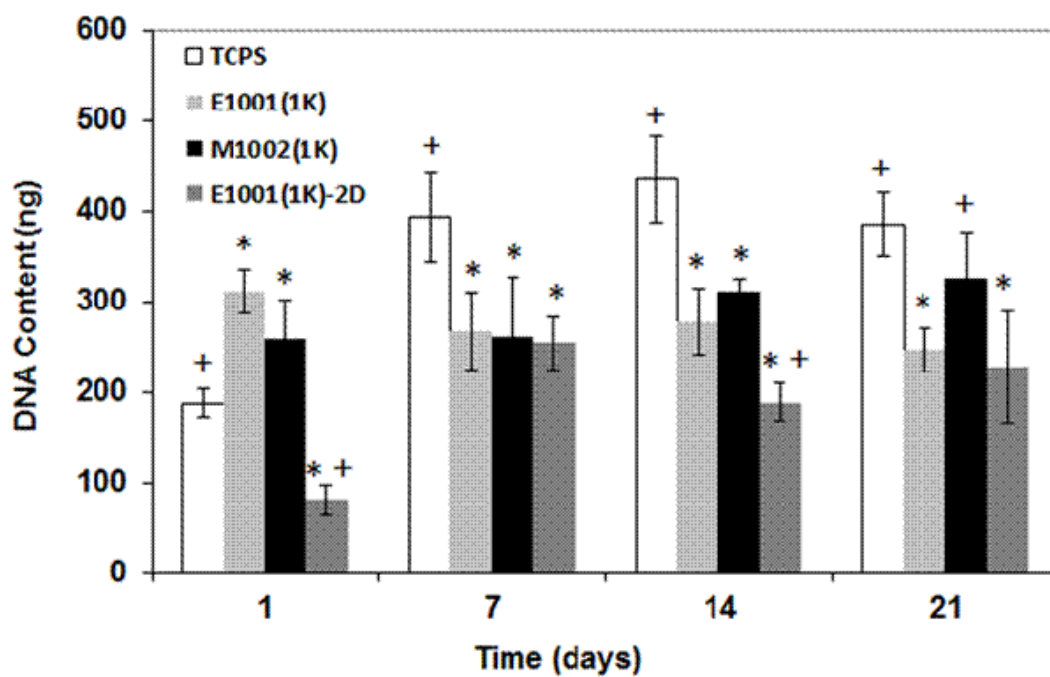
Figure A2.4. (A) SEM images of TyrPC scaffolds and MC3T3-E1 cells cultured on TyrPC scaffolds up to 4 days. (B) Confocal microscopic images of MC3T3-E1 cells inside the scaffold (E1001(1K)) up to day 14. The cell infiltration can be seen up to 600 μm deep in the scaffold.

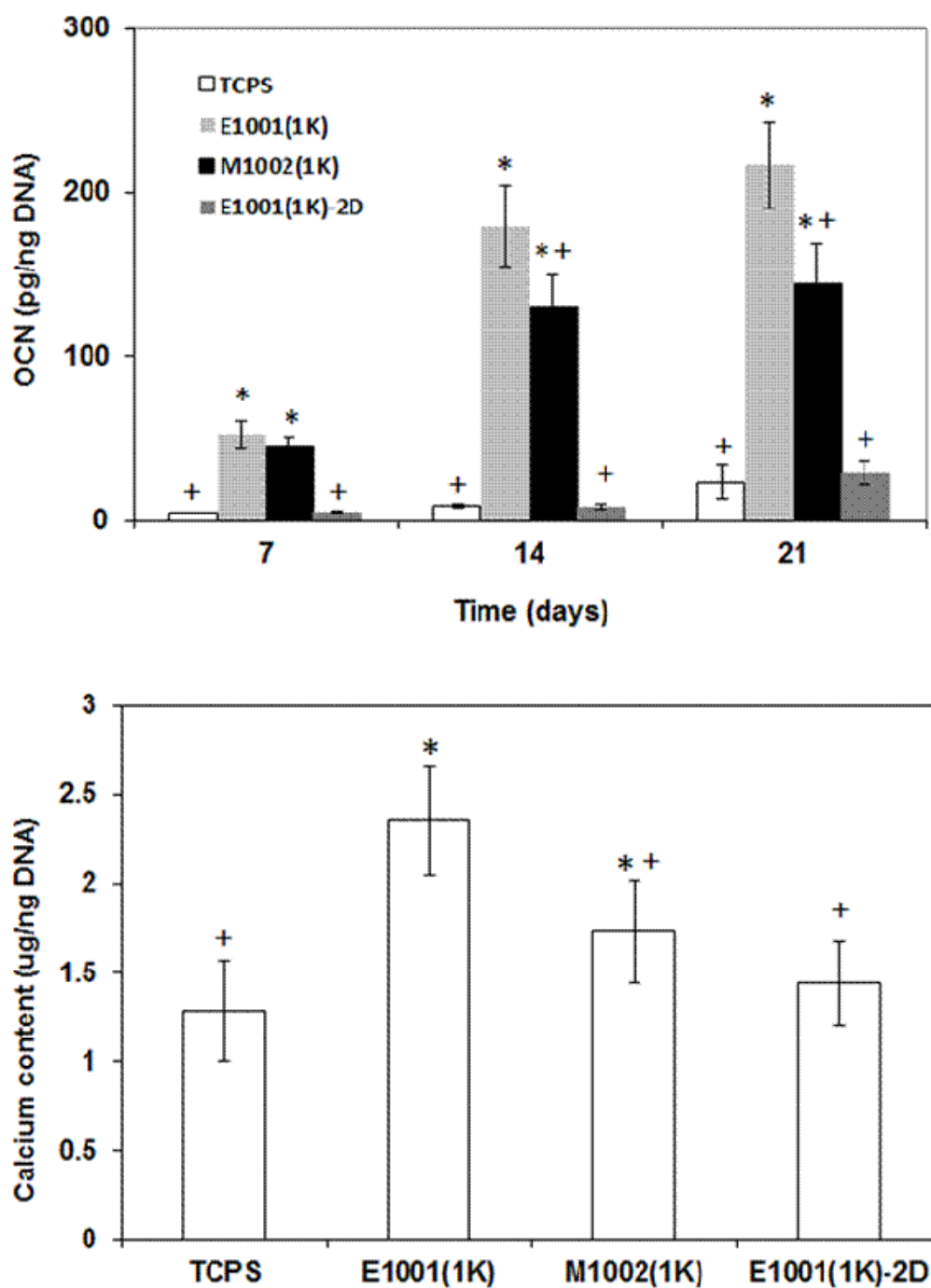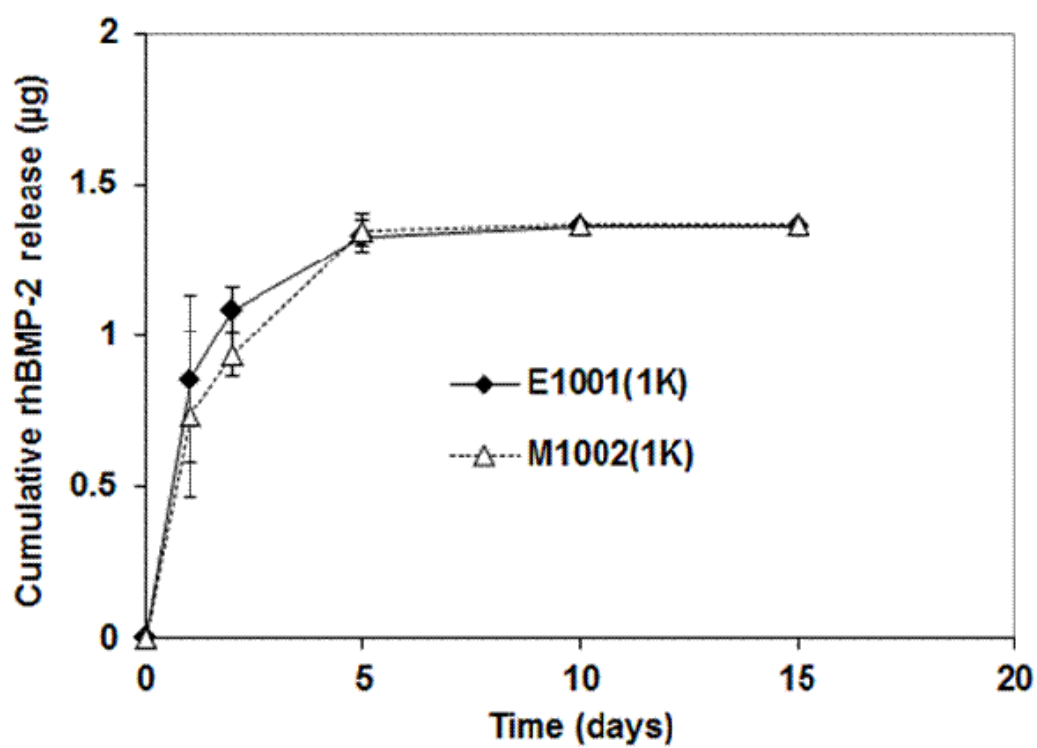**Figure A2.5**. (A) DNA content, (B) Normalized ALP activity, and (C) OCN content and produced by pre-osteoblasts (MC3T3-E1) cultured on different substrates at various time periods. (D) Mineralized calcium deposition of the ECM at day 21. Error bars are the mean ± standard deviation for n=3 and * and + represents significant difference (p < 0.05) compared to the control (TCPS) and 3D E1001(1K) scaffolds, respectively.
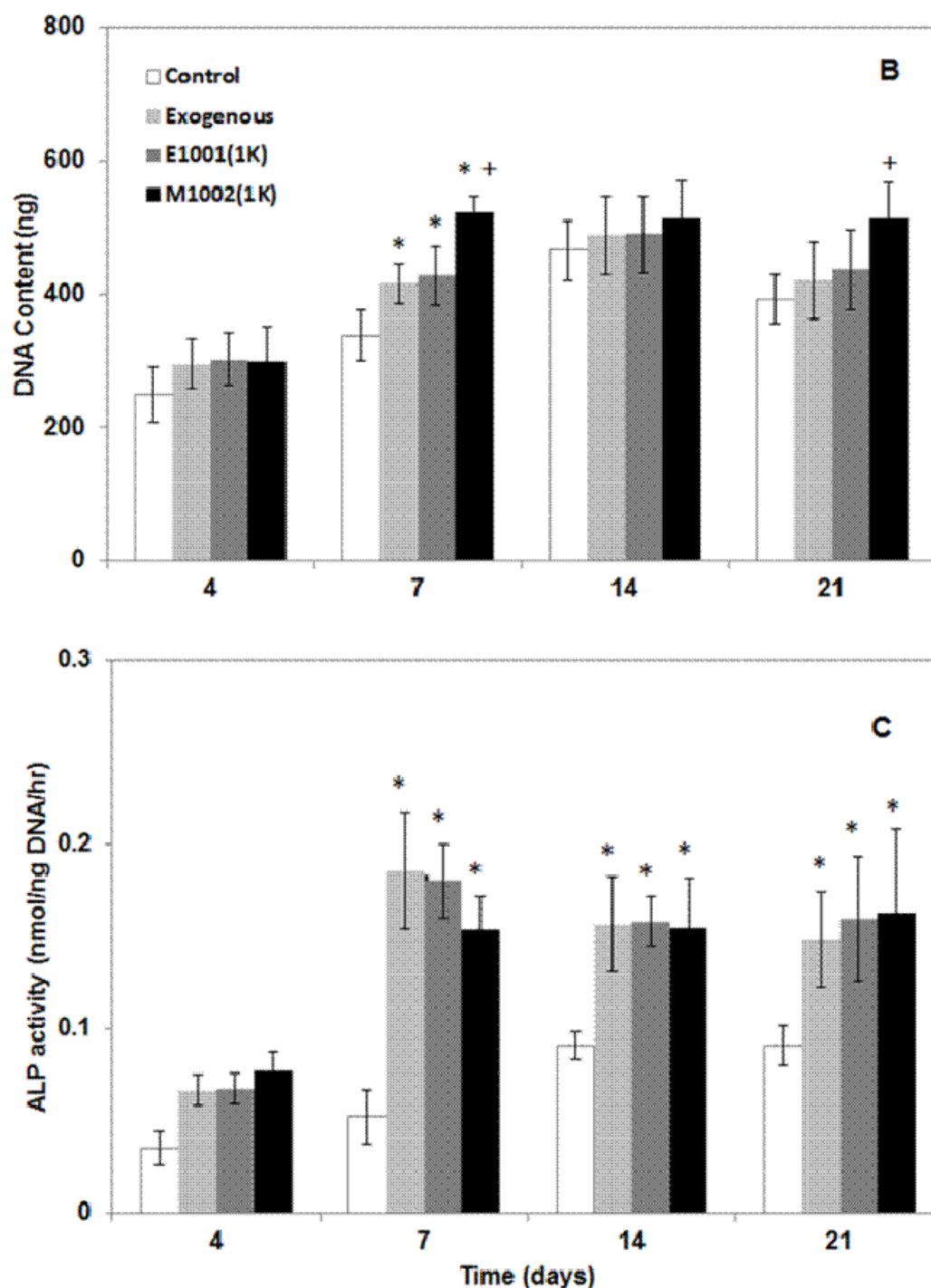
Figure A2.6. (A) Release profiles of rhBMP-2 from tyrosine-derived polycarbonates and bioactivity of MC3T3-E1 cells in the presence of rhBMP-2 releasates; (B) DNA content and (C) normalized ALP activity of the cells at selected time periods. Error bars are the mean ± standard deviation for n=4. The * and + represent significant differences ($p < 0.05$) from the controls, negative control (i.e., without rhBMP-2) and positive control (i.e., in the presence of exogenous rhBMP-2), respectively.
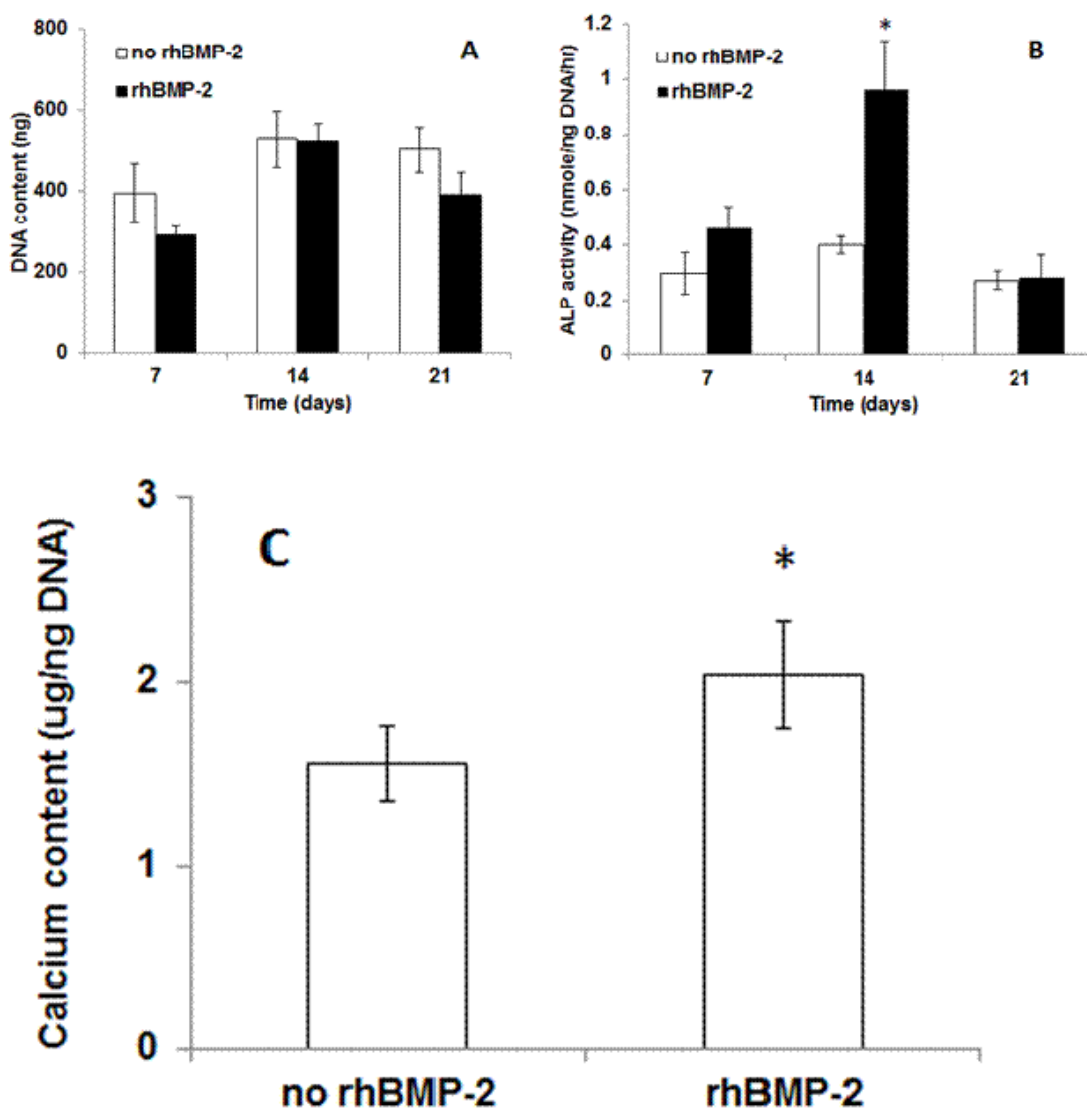
Figure A2.7 (A) DNA content and (B) Normalized ALP activity at designated time periods produced by pre-osteoblasts cultured on tyrosine-derived polycarbonate scaffolds with (rhBMP-2) or without rhBMP-2 (no rhBMP-2). (C) Mineralized calcium deposition of the ECM at day 21 produced by pre-osteoblasts cultured on the scaffolds containing rhBMP-2. Error bars are the mean ± standard deviation for n=3 and * represents significant difference (p < 0.05) compared to the control (i.e., no rhBMP-2).

APPENDIX 3

In vivo **biocompatibility assessment in rabbit critical-sized calvarial defect (performed by colleagues at Carnegie Mellon University and Cleveland Clinic)**

A-3.1 Rabbit critical-sized calvarial defect (as described in the methods section, Chapter 2)

A-3.2 Histology/Histomorphometry

The specimens were dehydrated in ascending grades of ethanol, cleared in xylene at 4 °C to minimize implant solvation during the processing and embedded in poly(methyl methacrylate). The specimens were cut and ground to 30 μm thick sections with an Exakt diamond band saw and MicroGrinder (Exakt Technologies, Oklahoma City, OK). The slides were prepared and stained with Sanderson's Rapid Bone Stain and counterstained with van Gieson's picrofuchsin, which resulted in soft tissue staining blue and bone staining pink/red.

New bone formation within the defect was measured histomorphometrically using an image analysis program (Optimas version 6.5, Media Cybernetics, Bethesda, MD). Briefly, the defect area (region of interest, ROI) including new bone area on each histology section was determined on each histology section at 1.5x. The areas of new bone, remaining implant and connective soft tissues in the defect area were determined by capturing each region based on predetermined color thresholds. The percentage of new bone area was obtained by dividing the bone area by whole defect area.

A-3.3 Micro-computed tomography (μ-CT or micro-CT)

Each specimen was placed on the scanning platform of a GE eXplore Locus micro-CT (GE Healthcare, Piscataway, NJ) and 360 X-ray projections were collected (80 kVp; 500 mA; 26 min total scan time). Projection images were preprocessed and reconstructed into 3D volumes (20 μm resolution) on a 4PC reconstruction cluster using a modified tent-FDK cone beam algorithm (GE reconstruction software). 3D data was processed and rendered (isosurface/maximum intensity projections) using MicroView (GE Healthcare). Each volume was scaled to Hounsfield Units (HU) using a calibration phantom containing air and water (phantom plastic); a plug within the phantom containing hydroxyapatite was used as a bone mimic for bone mineral/density calculations. Volumes were imported into Matlab (R2009b, Mathworks) for automated batch analysis. Briefly, a fixed cylindrical volume of interest (VOI, 14 mm diameter, 5 mm height) was applied to each volume. Since each volume was calibrated using a fixed standard, calcium phosphate, cortical bone, trabecular/woven bone, and scaffold content was determined using predefined Hounsfield Unit thresholds (>3000, 2000-3000,750-2000, and 300-750 respectively). To account for partial volume and beam hardening artifacts around calcium phosphate granules, calcium phosphate regions were morphologically "dilated" by 5 voxels and subtracted from the trabecular/woven bone mask. For calculation of percent bone coverage, calcium phosphate (when present), cortical bone, and trabecular/woven bone masks were "added" together, a 2D maximum intensity projection was generated, and non-zero pixels were summed and divided by the initial cylindrical cross-sectional area (14 mm diameter circle).

A-3.4 Statistical analysis

All data are represented as means ± standard deviations. Statistical analysis was performed using single factor analysis of variance (ANOVA) with Tukey–Kramer's *post hoc* test at a significance level of $p \leq 0.05$.

CURRICULUM VITAE

Maria Hanshella C. Resurreccion-Magno

Education

Ph.D. in Chemistry   *January 2012*
Department of Chemistry and Chemical Biology
Rutgers, The State University of New Jersey
Piscataway, NJ 08854

M.S. in Chemistry   *April 2002*
Institute of Chemistry
University of the Philippines, Diliman
Quezon City, Philippines 1101

B.S. in Chemistry   *April 1993*
Institute of Chemistry
University of the Philippines, Diliman
Quezon City, Philippines 1101

Professional Experience and Scientific Skills

Laboratory Safety Officer   *2009 – present*
New Jersey Center for Biomaterials
Department of Chemistry and Chemical Biology
Rutgers, The State University of New Jersey, Piscataway, NJ 08854

Graduate research assistant   *2008 - present*
New Jersey Center for Biomaterials
Department of Chemistry and Chemical Biology
Rutgers, The State University of New Jersey, Piscataway, NJ 08854

Teaching assistant   *2006 – 2008*
Department of Chemistry and Chemical Biology
Rutgers, The State University of New Jersey, Piscataway, NJ 08854

Instructor   *1995 - 2003*
Institute of Chemistry
University of the Philippines, Diliman, Quezon City, Philippines 1101

Science Research Specialist I   *1994 - 1995*
Institute of Chemistry
University of the Philippines, Diliman, Quezon City, Philippines 1101

Laboratory Technician   *1994*
United Laboratories, Inc., Mandaluyong City, Philippines

Safety and Environmental Affairs Consultant   *1993*
Johnson & Johnson (Phils.) Inc., Parañaque City, Philippines

Publications

Magno, MHR, Kim J, Srinivasan A, McBride S, Bolikal, D, Darr A, Hollinger JO, Kohn, J., "Synthesis, degradation and biocompatibility of tyrosine- derived polycarbonate scaffolds", *J. Mater. Chem*, **20**, 8885 – 8893, 2010

J. Kim, **Magno, MHR**, Alvarez, P, Darr, A, Kohn, J and Hollinger, JO. Osteogenic differentiation of pre-osteoblasts on biomimetic tyrosine-derived polycarbonate scaffolds. *Biomacromolecules*, 2011, **12** (10), 3520 – 3527.

Kim, J, **Magno MHR**, Waters, H, Doll BA, McBride S, Alvarez P, Darr A, Vasanji A, Kohn J, Hollinger JO, "Bone regeneration in a rabbit critical size calvarial model using tyrosine-derived polycarbonate scaffolds" *accepted, Tissue Engineering*, 2012

Resurreccion-Magno, MHC, Villaseñor, IM, Harada, N, Monde, K, "Antihyperglycaemic flavonoids from *Syzygium samarangense* (Blume) Merr. and Perry" *Phytother. Res.* **19**, 246 – 251, 2005

Villaseñor, I, **Resurreccion, H,** Peczon, B, "Ipil-Ipil Seed Gum: Part III. Bulk Extraction and Mutagenicity/Antimutagenicity Studies", Philippine Journal of Science, 126 (4), 1997